Dissecting the molecular mechanisms of RIF1 in maintaining DNA replication-associated genome stability

Inaugural-Dissertation

to obtain the academic degree

Doctor rerum naturalium (Dr. rer. nat.)

submitted to the Department of Biology, Chemistry, Pharmacy

of Freie Universität Berlin

by

Sandhya Balasubramanian

2021

This study was performed from February 2016 to May 2021 under the supervision of Prof. Dr. Michela Di Virgilio at “Max Delbrück-Center for Molecular Medicine” in the Helmholtz Association, in Berlin.

1st Reviewer: Prof. Dr. Michela Di Virgilio

Max Delbrück Center for Molecular Medicine

2nd Reviewer: Prof. Dr. Oliver Daumke

Freie University - Max Delbrück Center for Molecular Medicine

Date of Doctoral Thesis Defense: 5th November, 2021

Abstract

Timely and accurate genome duplication is essential to maintain genome integrity and cell survival. DNA replication-associated damage is one of the leading causes of genome instability and a precursor for carcinogenesis. The DNA replication fork (RF), the site for assembly of replication proteins, encounters a variety of obstacles, which slow or stall its progression, a process termed replication stress. Cells have evolved a number of mechanisms to stabilize stalled forks and to ensure replication restart and timely completion. However, during chronic stress, forks can no longer be stabilized and collapse, creating toxic DNA double-strand breaks (DSB). These DSBs, when left unrepaired, can lead to chromosomal rearrangements and promote genomic instability. RIF1, a multifunctional protein, is critical not only to promote fork stability and to ensure that replication is completed, but also to repair DSBs in the event of prolonged replication stress. While modulation of DSB repair pathways represents one of the resistance mechanisms to chemotherapeutic drugs, maintenance of fork stability is critical to prevent carcinogenesis from developing in the first place. Here, we have identified novel post translational modifications of RIF1 that are critical for its role in the maintenance of genome stability. Specifically, phosphorylation of a conserved cluster of SQ sites in RIF1 modulates its role in fork stabilization while being dispensable for its function in DSB repair.

Zusammenfassung

Eine rechtzeitige und akkurate Genomduplikation ist für die Aufrechterhaltung der Genomintegrität und das Überleben der Zelle unerlässlich. Replikationsassoziierte Schäden sind eine der Hauptursachen für Genominstabilität, eine Vorstufe zur Karzinogenese. Die Replikationsgabel (RF), der Ort für den Zusammenbau der Replikationsproteine, stößt auf eine Vielzahl von Hindernissen, die ihre Progression verlangsamen oder aufhalten, ein Prozess, der als Replikationsstress bezeichnet wird. Die Zellen haben eine Reihe von Mechanismen entwickelt, um blockierte Gabeln zu stabilisieren, sowie den Neustart und den rechtzeitigen Abschluss der Replikation sicherzustellen. Bei chronischem Stress können die Gabeln jedoch nicht mehr stabilisiert werden und kollabieren, wodurch toxische DNA-Doppelstrangbrüche (DSB) entstehen. Diese DSBs können, wenn sie nicht repariert werden, zu chromosomalen Rearrangements führen und genomische Instabilität fördern. RIF1, ein multifunktionales Protein, ist nicht nur entscheidend für die Stabilität der Gabel und den Abschluss der Replikation, sondern auch für die Reparatur von DSBs im Falle von anhaltendem Replikationsstress. Während die Modulation der DSB-Reparaturwege einen der Resistenzmechanismen gegenüber Chemotherapeutika darstellt, ist die Aufrechterhaltung der Gabelstabilität entscheidend, um die Entstehung von Karzinogenese von vornherein zu verhindern. Die Ergebnisse dieser Studie identifizieren neue posttranslationale Modifikationen auf RIF1, die für seine Rolle bei der Aufrechterhaltung der Genomstabilität entscheidend sind. Hier haben wir festgestellt, dass die Phosphorylierung von konservierten Stellen auf RIF1 seine Rolle bei der Gabelstabilisierung moduliert, aber für seine Rolle bei der DSB-Reparatur entbehrlich ist.

Table of Contents

1. INTRODUCTION

1.1. The basics of eukaryotic replication

Genome instability is a driver for carcinogenesis and DNA replication is the most vulnerable cellular process that can lead to it. Every time a mammalian cell divides, billions of nucleotides must be accurately replicated in coordination with the cell cycle. Faulty DNA replication can result in replication blockage or mutations, that can lead to chromosomal rearrangements, mis-segregation and or breakage of chromosomes all of which lead to genome instability[1]. Replication initiates within special sequences in the duplex DNA called origins. In yeast the origin sequences are extremely A-T rich and they have a 11bp consensus sequence [5/(A/T)TTTA(T/C)(A/G)TTT(A/T)-3]. However in multicellular organisms the exact sequence is unknown, although a preference for CpG islands and GC rich sequences is identified[2,3]. Replication initiation begins with origin licensing that marks which origin to start replication from. This is determined during the late M and G1 phase by the loading of the eukaryotic core helicase complex MCM2-7 (minichromosome maintenance 2-7). The MCM2-7 is loaded with the help of 6 subunit origin recognition complex (ORC) which is the eukaryotic initiator and cell division cycle 6 (CDC6) ATPase and the chromatin licensing and DNA replication factor 1 (CDT1) which are cofactors. This complex together is called the pre-RC (pre-replication complex) and marks the origins that are licensed to. Origin activation happens in the S-phase by Cyclin Dependent Kinases (CDK) and Dbf4-dependent kinase (DDK) which promote MCM2-7 activation. This MCM2-7 double hexamer is converted into two distinct active CDC45-MCM2-7-GINS (CMG) helicases where Cdc45 and GINS are other components of the helicase complex[4,5]. Simultaneously the origin DNA is melted and replication factors are recruited to establish bidirectional replication forks where multiprotein complexes assemble to synthesize the new DNA strand (Fig. 1). The MCM2-7 complex binds to the DNA in several regions however, only few are activated in the S phase by the CDK and DDK enzymes. The rest are dormant origins ready to be fired if some activated origins fail to start or as a backup origin when replication forks starting from one origin stall[6].

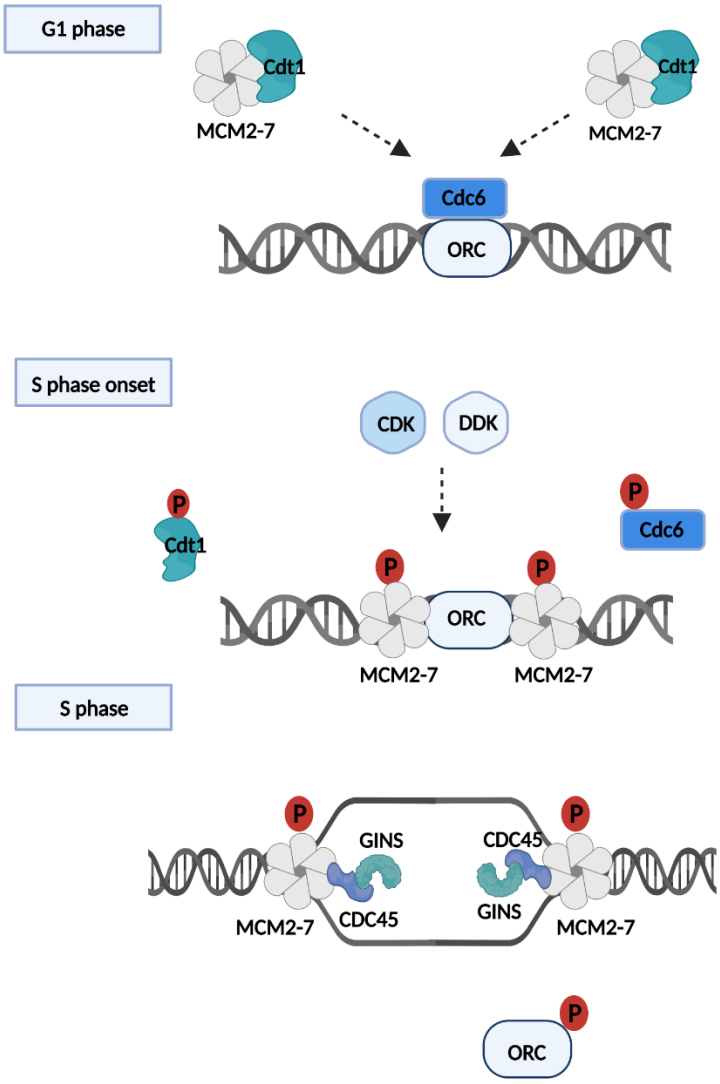

Figure 1. MCM2-7 loads onto DNA at replication origins during G1 and unwinds DNA ahead of replicative polymerases. During G1 phase of the cell cyle the combined activities of Cdc6 and Cdt1 bring MCM complexes to replication origins. The onset of S phase is marked by CDK/DDK-dependent phosphorylation of pre-RC components which leads to replisome assembly and origin firing. Cdc6 and Cdt1 are no longer required and are removed from the nucleus or degraded. During S phase MCMs and associated proteins (GINS and Cdc45 are shown) unwind DNA to expose template DNA.

Once the origin is fired and the DNA is melted, it generates single strand DNA (ssDNA) which is the template for replication. Replication of the leading and lagging strands is coordinated with helicase unwinding in a large protein complex called the replisome; together, the replicating DNA and replisome constitute the replication fork[7]. The RF has 2 main activities: DNA unwinding with the help of helicases

and DNA synthesis by polymerases (Fig 1). Polymerases Pol ε and Polδ synthesize the leading and lagging strand respectively. Both polymerases synthesize DNA in a 5' to 3' direction. Processive DNA synthesis requires binding of co-factor Proliferating cell nuclear antigen (PCNA) to the polymerases which form a ring structure that tethers the polymerases securely to the DNA. Binding of PCNA to the polymerases enhances the replicative processivity by up to 1000 fold[7].

1.2 Replication stress and fork stability

1.2.1. Causes and consequences of replication stress

Once replication forks are established, there are numerous challenges they face before the genome is fully duplicated. This causes the progressing RF to slow down or stall which affects DNA synthesis. This is termed as replication stress (RS)[8]. Lesions in the DNA like gaps, nicks and DSB are a common source of RS which form a physical barrier to replication fork progression[8]. Gaps are also caused by aberrantly processed misincorporated nucleotides. Although Pol ε and Pol δ have high fidelity, they still incorporate wrong nucleotides at a strikingly high rate[9]. Collisions between transcription and replication machinery are also an important source of replication stress. This is evidenced by the elevated spontaneous mutations and recombination events in high transcribed regions which are stimulated by replication[10,11]. Additionally, the dNTP and histone supply must be coordinated with fork elongation for proper S-phase progression and fork stability[12,13]. Nucleotide depletion is one of the earliest drivers of tumorigenesis[14,15]. It has been shown that disruption of the origin activation timing program leads to dNTP depletion, causing slowed fork elongation, fork stalling, and checkpoint activation and in cases of low origin firing leads to under replicated DNA and loss of genetic information[14,13,16].

It has been widely observed that specific regions of the genome called fragile sites are particularly prone to damage in the presence of replication stress, demonstrating that also endogenous characteristics of the DNA sequence and/or chromatin structure is problematic for fork progression[17]. The structure of dsDNA also poses a threat to progressing replication fork specifically in the case of G-Quadraplexes. G-quadraplexes are highly stable secondary structure that forms at G-rich DNA and present a physical barrier to replication forks[18,19]. Finally, overexpression or constitutive activation of oncogenes like MYC, HRAS and cyclin E lead to aberrant origin firing and activation leading to depletion of dNTP pools and/or increased activation with transcription complexes which are sources of RS[20,21].

In most cases replication stress leads to only a transient slowing or stalling of the replisome. Although stalled forks can resume replication once the stress has been alleviated, it leads to the uncoupling of the helicase-polymerase machinery leading to the production of large stretches of ssDNA. This activates the intra-S checkpoint that stops the firing of new origins and stop S phase progression until the damage is repaired[22,23,24,25]. Lagging strand lesions are overcome more easily than leading strand lesions due to their discontinuous nature which allows the polymerase to simply bypass the lesion to start the synthesis again and the lesion is repaired post replicatively. Leading strand template lesions cause helicase and polymerase uncoupling that activates the checkpoint response. In this case repriming can occur to allow for continued fork movement[23].

However, some types of damage can lead to more persistent fork stalling. In this event the forks cannot stabilize and hence they collapse[26]. This means that the replication factors disassociate and DSBs are generated and most importantly collapsed forks no longer have the ability to perform DNA synthesis[26,27]. Replication forks upon collision with inter-strand crosslinks and single strand breaks can collapse to form DSB[27] (Fig. 2a). Forks also collapse when they encounter the transcription machinery or regions in the genome with multiple clustered lesions[28]. Refiring of a single origin twice in the same S phase leads to the formation of DSB through head-to-tail collision of the replication fork. Converging replication forks also collide leading to the formation of DSB[24].

1.3 Fork collapse and DSB

DSBs are extremely toxic lesions which when left unrepaired can lead to large scale chromosomal rearrangements including deletions, chromosomal fusions and translocations that lead to loss of genetic information[29,30]. In fact, germline mutations in DSB repair genes cause genomic instability in numerous hereditary human diseases, especially those associated with cancer predisposition, developmental disorders and premature ageing[31]. This is why cells have evolved a sophisticated and extensive network of signaling called the DNA damage response (DDR) to detect the DSBs, signal their presence and repair them accurately[32].

1.3.1. DSB recognition and signaling

DDR is driven by protein phosphorylation mediated by two protein kinases mainly ATM (Ataxia-Telangiectasia mutated) and ATR (ATM- and Rad3-related) members of a family of phosphoinositide 3-kinase (PI3K)-related kinases (PIKKs)[33]. While ATM is mainly activated in response to DSB, ATR is the

activated upon replication stress. Although it is not completely clear how DSBs are detected, recent studies have shown that they are identified by poly ADP-ribose polymerase-1 (PARP1), the MRN complex (MRE11, RAD50, NBS1) and Ku70/80 complex[34,35,36,37]. PARP1 is an abundant and ubiquitous nuclear protein that is involved in single strand break repair, DNA replication and transcription. PARP-1 catalyses the production of PAR chains which promotes local chromatin relaxation and histone displacement, as well as facilitating the recruitment of repair factors such as MRE11 and NBS1, subunits of the MRN complex[35]. Ku70/80 bind to broken DNA ends with very high affinity and recruit DNA-PKcs (DNA-dependent protein kinase catalytic subunit) another DDR response kinase, which in turn recruits the master kinase ATM[37,38]. ATM phosphorylates several substrates to mediate repair, checkpoint activation, senescence, or apoptosis depending upon the levels of DNA damage. ATM phosphorylates histone variant H2AX(S139) termed γH2AX: the main DNA damage histone mark which is detected for several kilobases away from DSB[39,40]. The kinase activity of ATM is enhanced upon PARP1 and NBS1 interaction, collectively leading to the autophosphorylation of ATM[33,41]. Collectively PARP1, MRN, ATM and γH2AX form a positive feedback loop amplifying the signal and modulating chromatin accessibility to facilitate recruitment of other DNA repair factors.

1.3.2. Modes of repair

Replication-associated DSBs are repaired by 2 major pathways: non-homologous end joining (NHEJ) and homologous recombination (HR). Both of these multi-step processes have been object of intense investigation for more than two decades but continue to be studied, as new factors involved in their regulation and execution are identified. These pathways are regulated at different steps and when both are active and competing in S/G2 phase, the coordination of factors and enzymes allows one or the other to prevail.

a)

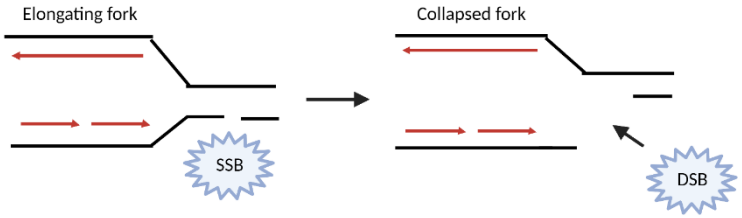

b)

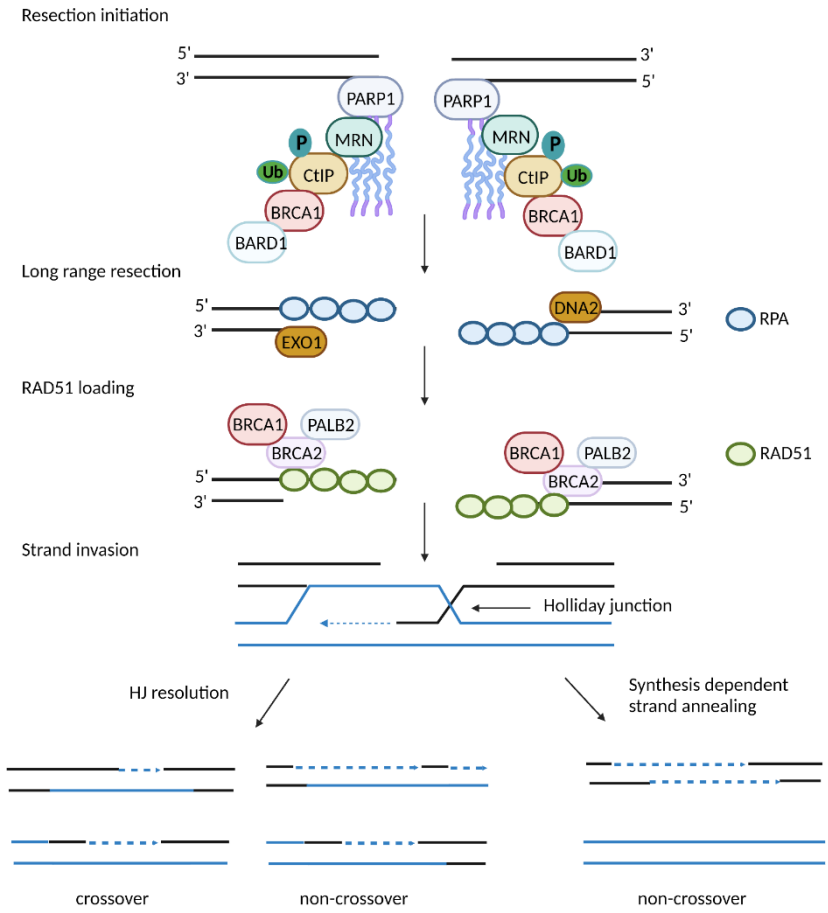

Figure 2. DSB formation and mechanism of homology-dependent repair. a) Persistent replication stress leads to fork collapse resulting in DSB formation. For example, elongating forks can collapse upon encountering an unrepaired SSB. b) DSBs are recognized by PARP1 which autoparylates itself upon DSB recognition to get activated and also creates long PAR chains which serves as a platform for loading of early resection mediators like MRN. CDK phosphorylated CtIP is recruited by MRN to begin end processing. Additionally, CtIP is also ubiquitinated by BRCA1-BARD1 complex to continue MRN recruitment. Long range resection is mediated by nucleases EXO1 and DNA2 which are also targets of CDK phosphorylation. ssDNA generated upon resection is rapidly bound by RPA. BRCA1 recruits BRCA2-PALB2 to facilitate

loading of RAD51 to resected DNA. RAD51 forms a protein-nucleofilament assembly which is an essential intermediate for strand invasion. A Holliday junction is formed which is resolved to generate either cross over or non crossover products. Somatic cells mostly undergo non-crossover reactions using the synthesis dependent strand annealing (SDSA) pathway.

1.3.2.1. HR

HR is a homology-dependent repair pathway that is restricted to the S/G2 phase due to the requirement of sister chromatid as a template. This pathway is error-free and is intimately linked to cancer risk due to the involvement of BRCA1 and BRCA2 that are two major hereditary breast and ovarian cancer predisposition genes[42]. Due to its fidelity, HR is used as the predominant pathway to repair replication-associated DSBs. HR begins with nucleolytic degradation of the broken ends to produce long 3' overhangs. This process is called resection and is required to mediate strand invasion into the sister chromatid which is used as the template, leading to error-free repair. Short range resection is mediated by nucleases MRE11 from the MRN complex and exonuclease CtIP in concert with BLM helicase (Bloom syndrome RecQ like helicase) which generate short stretches up to 50-100 bp of 3' overhangs[43,44]. Here BLM unwinds the duplex DNA to provide substrate for the nucleases. The overhangs are extended by other nucleases mainly EXO1 and DNA2 (DNA replication helicase/nuclease 2) that mediate long range resection of more than 100bp on both DNA ends[44]. BRCA1 promotes DSB repair towards HR by forming a heterodimer with its cofactor BARD1 which possess a RING domain: together they ubiquitinate CtIP which recruits MRN to begin resection[45]. BRCA1 also promotes HR by inhibiting factors involved in the competitive NHEJ pathway which will be discussed in later section.

The ssDNA formed after resection is immediately bound and stabilized by ssDNA binding protein RPA which prevents it from pairing with similar intermediates from other nuclear processes. Thus, RPA opens up secondary structures and limits spurious interactions. This phase is called pre-synaptic phase. RPA must be displaced by recombination mediator proteins to allow for nucleoprotein filament formation which is required for strand invasion into the sister chromatid. Breast cancer type 2 susceptibility protein (BRCA2) is the major recombination mediator in mammalian cells, acting in concert with partner and localizer of BRCA2 (PALB2) to displace RPA from the ssDNA and load RAD51[46,47,48]. RAD51 is a multifunctional protein that binds to resected DNA and forms the nucleoprotein filament. This intermediate is essential to begin the search for homologous sequence in the sister chromatid. Consequently, defects in RAD51 loading are correlated with impaired HR[49]. The homology search and

DNA strand invasion are collectively called synapsis. This process generates regions of heteroduplex DNA comprising DNA strands from different sister chromatids. This recombination intermediate is referred to as the D-loops or displacement loops. The conservative, non- crossover synthesis- dependent strand annealing (SDSA) pathway is the predominant repair pathway in somatic cells[50,51]. SDSA occurs by disruption of the extended D-loop and annealing the newly synthesized DNA with the second end of the broken molecule[52]. DSB repair by HDR can also involve the formation two Holliday junctions (HJ), which are cross-shaped structures that occur when two double-stranded DNA molecules become separated into four strands to exchange segments of genetic information. HJ is resolved without crossover in somatic cells, restoring the DNA to its original condition without sequence abnormalities (Fig. 2b).

1.3.2.2. NHEJ

NHEJ is active in all stages of the cell cycle and is the pathway of choice when the DSB ends are protected from nucleolytic digestion. This process is termed as end protection and is critical to mediate repair by NHEJ[53]. This pathway is proficient in ligating DSBs with widely different end structures and in general repairs breaks without regard to homology. Since NHEJ can introduce small insertions or deletion at the DSB site, it is considered error-prone as opposed to HR.

This pathway begins with the Ku proteins binding to the DSB ends with high affinity and recruiting DNA-dependent protein kinase catalytic subunit (DNA-PKcs), DNA ligase IV (LIG4) and the associated scaffolding factors XRCC4, XRCC4-like factor (XLF) and paralogue of XRCC4 and XLF (PAXX)[54]. XRCC4 is essential for LIG4 stability and function, whereas XLF and PAXX have partially redundant scaffolding roles. There are three enzymatic activities required for repair of DSBs by the NHEJ pathway: (a) nucleases to remove damaged DNA, (b) polymerases to aid in the repair, and (c) a ligase to restore the phosphodiester backbone. DNA-PKcs has multiple roles, with its major one being bringing the two DSB ends together[55]. Autophosphorylation of DNA-PKcs recruits the nuclease Artemis to process the DNA ends for ligation. Once the 2 ends have been brought together by Ku-DNA-PKcs then non-ligatable termini must be filled in by polymerases μ and λ[56]. Finally, ligase IV/XRCC4 catalyses the ligation of the broken ends. This activity is enhanced by the scaffolding protein XLF[55]. It is in the above two steps that NHEJ is considered error-prone due to the loss or insertion of nucleotides. This is termed resection-dependent NHEJ.

In case of breaks with complementary overhangs re-joining occurs via the restoration of the phosphodiester bond between the free 5’ phosphate and 3’ hydroxyl groups by the XRCC4-DNA ligase IV

(LIG4) complex with no loss of genetic material. Since this type of repair does not require DSB end processing, it is called resection-independent NHEJ[57].

1.3.3. Regulation of pathway choice

Although NHEJ is active throughout the cell cycle, HR is restricted to S to G2 phases. This means that pathway choice between the two competing process happens during S Phase when both are active. As discussed before, the decision of which pathway to choose depends on the structure of the broken ends[58]. Fork collapse leading to the formation of replication- associated DSB needs to be repaired by the high-fidelity pathway HR. Since NHEJ does not require sequence homology, it aberrantly ligates DSBs present in different chromosomes when HR is impaired causing extensive rearrangements, mutations at the break site and translocations[29,59]. Thus, its critical for cells to choose the correct pathway to prevent accumulation of genome instability which is a hallmark of carcinogenesis. End processing of DSBs by nucleases generates long 3' overhangs that are essential intermediates for strand invasion into the homologous sister chromatid. Thus, end resection promotes HR. On the other hand, when DSBs are protected from nuclease mediated digestion, they are substrates for repair by NHEJ. In the following paragraphs I will explain the factors that mediate pathway choice also in the context of cell cycle phase for better understanding.

Immediately following DSB induction, the KU70/80 protein binds to broken ends with very high affinity and recruits DNA-PKcs. Together they form the DNA-dependent protein kinase complex (DNA-PK) that protects breaks from digestion during G1 phase[33]. The transition from G1 to S activates the CDK1/2 kinases that sets into motion the factors involved in end processing. Resection is initiated upon phosphorylation of CtIP by CDK1/2 which is required for its association to MRN complex[60]. CDK1/2 also phosphorylates DNA2 which promotes long range resection in conjunction with DNA unwinding by BLM helicase[61]. On the other hand, ATM mediated phosphorylation of CtIP is required for recruitment of EXO1[62]. Together the nucleases CtIP-MRN initiate resection which is continued by DNA2 and EXO1 at the breaks. This produces long 3' overhangs that evicts the KU70/80 heterodimer from the DSB due to its reduced affinity for ssDNA (Fig. 3a)[63].

Another critical resection promoting factor acting in concert with CtIP is BRCA1. BRCA1 possesses multiple cellular functions including checkpoint control, transcription regulation, ubiquitination, apoptosis, however its role in DSB repair is perhaps the most critical mechanism to maintain genome stability[64]. As a

result, Individuals carrying germ line mutations in BRCA1 have an extremely high risk of developing breast, ovarian, prostrate and pancreatic cancer[58]. CtIP phoshorylated by CDK in the late G1 phase recruits MRN to form a complex with BRCA1[60]. The BRCA1-CtIP complex promotes resection at DSBs leading to the displacement of competing end protection factors 53BP1-RIF1 which are recruited to the broken ends[65].

53BP1 (TP53BP1, tumor suppressor p53 binding protein 1) is a large multi-functional protein regulating DSB repair, synapsis of DNA ends, mobility of damaged chromatin and repair in heterochromatic regions. In the context of a conventional DSB, 53BP1 suppresses DNA end resection which promotes cNHEJ, although it is not a 'core' cNHEJ factor[66]. 53BP1 effectors include RIF1, PTIP, REV7 and DYNLL1. Recent studies identified the shieldin complex (SHLD1/2/3 and REV7) also as 53BP1 effectors which are critical to mediate end protection[66–69].

53BP1 is recruited to chromatin surrounding DSB by binding histone H4 monomethylated at Lys20 (H4K20me1) or H4K20me2 and histone H2A monoubiquitylated at Lys15 by RNF168 ubiquitin ligase which is recruited following DSB induction. 53BP1 binds through its Tudor and UDR domain to the methylated and ubiquitinated histone marks respectively[70]. In parallel, another damage-dependent ubiquitin ligase RNF8 catalyses Lys63 (K63)-linked polyubiquitylation of histone H2A, which is required for recruiting BRCA1. Hence, distinct histone post translational modifications recruit distinct repair proteins supporting the presence of 'histone code' in DSB repair[71].

Following 53BP1 recruitment to the DSB, it undergoes ATM mediated phosphorylation at 28 different sites through which different protein-protein interactions are mediated. Phosphorylated 53BP1 recruits downstream effectors RIF1 and PTIP through distinct phosphodependent interactions[72]. Due to the absence of catalytic activity of 53BP1, RIF1, PTIP the search for downstream effectors continued in order to understand how end protection is mediated at the molecular level. Recently the Shieldin complex containing REV7 and SHLD1/2/3 was identified. SHLD2 contains OB fold domains that are ssDNA binding domains similar to those present in RPA[67,68]. This suggests that Shieldin competes with RPA for the binding to ssDNA generated by the short-range 3'-5' exonuclease activity of MRE11, thus preventing further long-range resection mediated by EXO1 and DNA2 and HR repair. Eventually, this roadblock would then promote the conversion of resected DSB ends into appropriate NHEJ substrates. Shieldin in turn contacts a complex made up of CST complex (CTC1, STN1, and TEN1) together with DNA polymerase Pol-α. CST-Pol-α is critical to fill in the resected DNA ends so that 53BP1 and its effectors may not only block resection but also reverse it[68]. Therefore, 53BP1-RIF1-Shieldin-CST not only protects the break ends but remodels it to be repaired by the action of XRCC4/XLF and LIG4 to mediate proficient NHEJ reactions (Fig. 3b)[54].

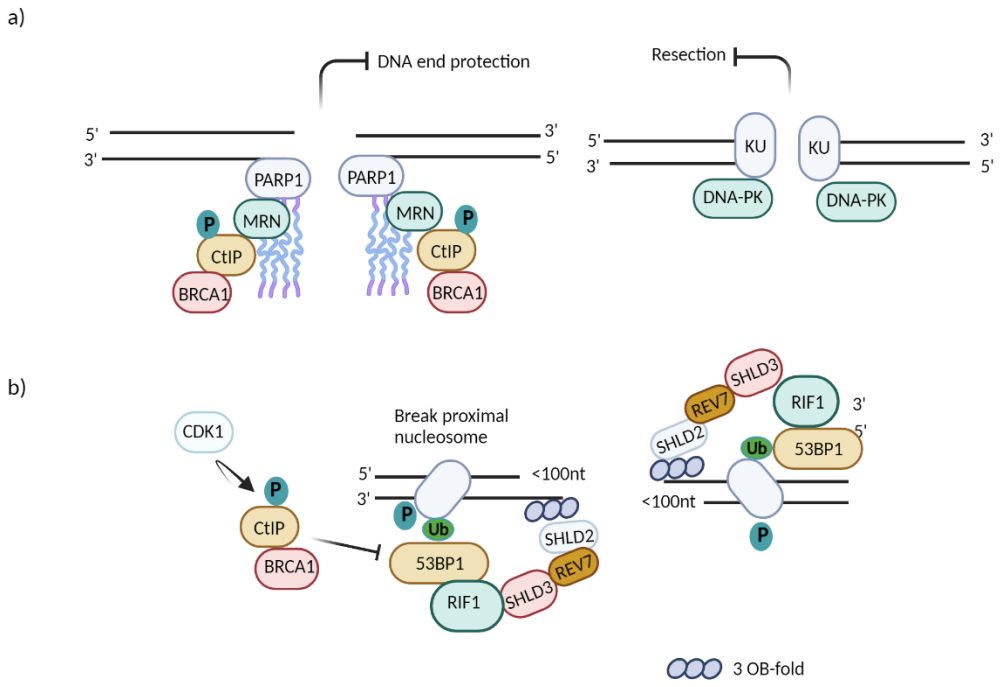

Figure 3. Interplay between pathway choice mediators during S phase. a) When DSBs are formed, one of the first responders is the Ku complex comprising of the Ku70/80 heterodimer. Ku recruits DNA-PKc, which is required for ATM activation. DNA-PKcs also recruits the nuclease Artemis for end processing promoting the pathway choice to NHEJ. On the other hand, the G1-S phase transition activates CDK1 which phosphorylates CtIP. This is critical to recruit MRN. CtIP and MRN mediated resection initiation displaces the Ku complex and promotes HR during S phase. b) In the next step, 53BP1-RIF1 and BRCA1-CtIP compete for the DSB ends where BRCA1-CtIP prevents the focal accumulation of the RIF1 during S phase. ATM mediated phosphorylation of 53BP1 recruits RIF1 and the Shieldin complex (REV7, SHLD1, SHLD2 and SHLD3) to the DSB. SHLD2 contains OB-fold domains similar to RPA which binds to the minimally processed ends (<100nt). The 53BP1-RIF1-Sheildin complex are critical to protect the DSB ends thereby promoting NHEJ.

The importance of correct pathway choice is highlighted in the case of BRCA1-deficient cancers which are HR impaired. Due to its critical role in repair of HR repair of DSB, conventional knockout of BRCA1 is lethal in mice. Cells from conditional BRCA1 knockout mice accumulate high number of aberrations specially radials upon treatment with DSB-inducing agents[53,73]. Radials are toxic structures produced by aberrant end joining of distal chromosomes and are classical structures found in HR deficiency. Seminal studies found that deletion of 53BP1 in BRCA1-deficient mice rescued the embryonic lethality and significantly reduced levels of genome instability[73,74]. Not only 53BP1, deletion of other end protection effectors like

RIF1 and Shieldin complex also produced similar results in BRCA1-deficient models in both mouse and human[46,69,75]. This is due to the fact that in HR impaired cells, the DSBs formed upon fork collapse can only be repaired by NHEJ which in this context is extremely deleterious for the cells. Hence, the choice of which repair pathway to use needs to be carefully controlled.

1.3.4. Exploitation of DSB repair pathway choice for chemotherapy and resistance

Exploiting the DSB repair pathway choice formed the basis of action of PARP inhibitors (PARPi), a relatively recent chemotherapeutic strategy for treating BRCA1/2-deficient cancers. PARPi is a single molecule inhibitor against PARP1 which is involved in Single Strand Break repair (SSBR)[76]. As explained before, PARP1 mediates PARylation: a post translational modification that orchestrates several DNA repair processes mainly DNA DSB repair, stabilization of replication forks, and for the accurate detection and repair of single strand breaks (SSB)[64]. Upon DNA damage PARP1 is rapidly recruited to nicks and catalayses the formation of branched PAR structures which serves as a platform for recruiting several downstream repair effectors. Once the DNA damage is removed, effective removal of DNA repair factors and PARP1 is critical. PARPi block the catalytic activity of PARP1 and trap it to the DNA[77]. Persisting PARP1-DNA complexes are a source of chronic replication stress and eventually lead to fork collapse and formation of DSB upon encounter with a progressing replication fork[65]. In BRCA1-deficient cells these are repaired by NHEJ that causes extensive chromosomal aberrations leading to genome instability and subsequent apoptosis. Thus, it was found PARP1 and BRCA1 share a synthetic lethal interaction. This means inactivation of either of two genes is tolerated, but the combined inactivation of both genes is lethal in this case PARP1 and BRCA1. Following their high anti-tumor efficacy during clinical trials several PARPi have been approved in the clinic for treatment of BRCA1/2 breast and ovarian cancers[77,78].

Since PARPi targets only BRCA-deficient cells and not the surrounding healthy tissues, it is highly effective and has low side effects. However, resistance to PARPi has been observed in several patients. Some of the common mechanisms of drug resistance are increased drug efflux by overexpression of drug transporters, downregulation of PARP1 expression, partial restoration of PARylation and also rewiring of the DDR response[79,80]. Rewiring DDR response refers to restoration of HR either by reactivation of BRCA1/2 or by modulating end protection factors like 53BP1, RIF1 and shieldin. Keeping in mind the discovery that 53BP1 deletion rescued the HR defect in BRCA1-deficient cells, mouse model of PARPi resistant mouse models contained *de novo* protein truncating mutations in the *Trp53bp1* gene [80,81]. Follow up studies revealed that deletion of RIF1 in BRCA1 deficient mouse mammary tumors and cell lines also restored resection

and HR, contributing to PARPi resistance. Recent genetic screens to identify more effectors of therapy resistance revealed the Shieldin complex as a top hit. Consequently, deletion of Sheildin rescued viability of cells from BRCA1-defecient mouse following PARPi treatment[69]. In conclusion, by relieving the end protection block on DSB ends, resection is restored in a BRCA1-independent manner which rescues HR and alleviates genome instability.

1.3.5. RIF1 in CSR

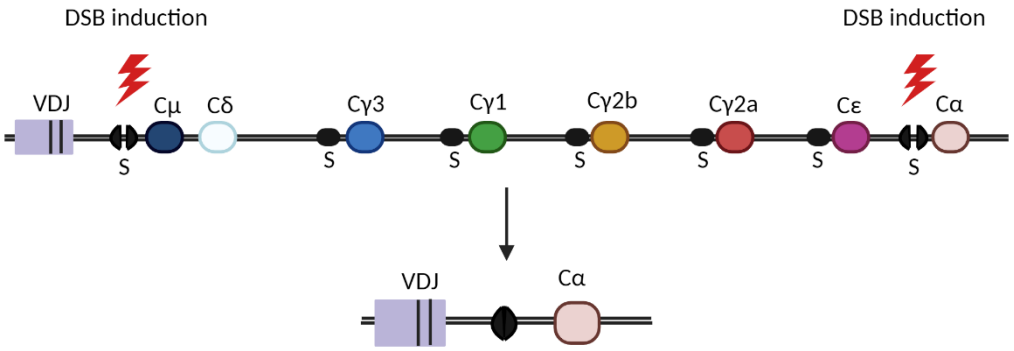

Figure 4. Schematic representation of the murine *Igh* locus. The Igh locus in mouse consists of VDJ region followed by the constant regions. The constant regions are interspersed with long repetitive regions (1-10kb) called the switch regions where the programmed DSB are introduced.

RIF1 is also required for the repair of programmed DSBs in the immunoglobulin (Ig) heavy chain (*Igh*) locus[46,65,75]. The *Igh* locus encodes for the heavy chain of antibodies and consists of the VDJ (Variable, Diversity and Joining genes), the switch regions (S) and the Constant regions (C). VDJ encodes the antibody portion that specifically recognizes and bind antigens whereas the constant region determines the antibody isotype (IgM/IgG3/IgG1/IgG2b/IgG2A/IgE and IgA). Programmed DSBs are introduced in the switch regions and repair of these breaks by NHEJ replaces the constant region of the IgM with one of the alternative isotypes (Fig. 4). This process is called class switch recombination (CSR) which happens in the G1 phase of the cell cycle[82–84].

Similar to stochastic DSBs, programmed breaks in the *Igh* locus is also recognized by Ku70/80 and MRN, which initiate the DDR signaling cascade involving ATM-mediated phosphorylation of H2AX and other downstream factors (Section 1.3.1)[37,38,85,86]. Eventually, the NHEJ pathway ligates the S-region DSBs which leads to productive antibody isotype switching[82,83]. DNA end-protection function of 53BP1-RIF1-Shieldin (Section 1.3.2.2) is required for productive CSR[67,75,87,88]. As a result, deficiency in the 53BP1-dependent

pathway causes uncontrolled resection of S-region DSBs ensuing in unproductive internal switch deletions. As a result, resection is deleterious and BRCA1 does not function in CSR by mediating end processing[89,90]. Since end protection mediated by 53BP1-RIF1 is essential to mediate productive antibody switching, CSR is often used as a functional readout for DSB repair by NHEJ during G1 phase.

1.4 Fork stalling and stabilization

Another major cause of genome instability during replication arises when moving replication forks encounter an obstacle which leads to its slowing down or stalling of the replication fork which needs to be stabilized and then the forks restarted to complete replication (Fig. 5). Stabilization of stalled forks is critical to prevent the fork from collapsing into poisonous DSB[91]. Repair of such breaks was addressed in the previous sections. In this section I will address the mechanism of fork stabilization which is used by the cells as a first aid mechanism when encountering damage during replication.

1.4.1. RPA activation and ATR signaling

As the replication fork stalls, the polymerase stops to synthesize new DNA but the helicase continues to unwind generating long stretches of ssDNA. ssDNA are immediately bound by the ssDNA binding protein RPA that protects them from degradation and prevents the formation of secondary structures that hinder its processing[8,76]. The RPA bound sssDNA adjacent to the newly replicated DNA forms the signal for activation: a primer-template junction which forms a platform for recruitment of ATR, the central replication stress response kinase. ATR phosphorylates several downstream effectors that have local and global effects in the cell[8,25]. Locally ATR helps stabilize the fork, restart replication and prevents aberrant recombination events leading to genome instability. Globally ATR suppresses late origin firing and halts cell cycle progression until the damage is repaired[28]. ATR phosphorylation of RPA at S33 signals the switch from replicative DNA synthesis to reparative DNA synthesis[92]. One of the main substrates of ATR is cell cycle checkpoint kinase CHK1. ATR phosphorylates CHK1 which in turn phosphorylates several substrates amplifying the original signal and mediating cell cycle arrest, replisome stability and unscheduled origin firing thereby activating the S-phase checkpoint[93]. ATR/CHK1 also maintains the cellular levels of RPA to enable optimal ssDNA protection (Fig. 5). Since intracellular RPA pool is finite, its critical to prevent unscheduled origin firing that produces long stretches of ssDNA to which RPA binds[94]. ATR inhibition is catastrophic to the cells in that it depletes the RPA cellular pool leading to deprotection of ssDNA and global replication fork collapse[94,95]. RPA mediated protection of ssDNA is a pre-requisite for fork

stabilization but is not enough to rescue stalled forks and enable fork restart. RPA-ssDNA structure is highly dynamic and does not persist for long before being replaced by RAD51 that mediates the next step fork reversal[96].

1.4.2. Fork reversal

Fork reversal is evolutionarily conserved and protective mechanism that bridges fork stabilization with fork restart and prevents the degradation of newly replicated strands. Here the three-way junction typical of a replication fork is converted into a four-way junction during replication blockade. When the progressing RF senses an obstacle in front of it, it stalls and moves "behind" i.e. moves in the direction opposite to replication fork progression and simultaneously the newly replicated "nascent" leading and lagging strands detach from the parental strand and pair to form a new arm[97,98]. This forms the four-way junction is called the reversed fork or chicken foot structure resembling Holliday junctions (Fig. 5). The regression of the replication fork is critical to prevent it from colliding with the damage in front of it. Fork reversal allows for the formation of a stable structure that allows more time to repair the DNA damage, prevent the accumulation of dangerous ssDNA and potentially deleterious fork progression[99,100]. Since the nascent strands are prone to nucleolytic digestion, reannealing prevents aberrant degradation by nucleases like MRE11, EXO1 and DNA2[101]. Fork reversal is a protective mechanism since the generation of one ended DSB provides an entry point to nucleases that perform controlled resection of nascent DNA to promote repair by HR (Fig. 5).

Several enzymes promote replication fork reversal: mutation of which increases predisposition to cancer. ZRANB3 and SMARCAL1 are two translocases that remodel the fork following replication stress. SMARCAL1 binds to RPA and promotes remodeling of forks with persistent ssDNA gaps at the fork junction[102]. ZRANB3 interacts with polyubiquitinated PCNA to promote fork remodelling and removing recombination intermediates[103]. The reduction in the levels of SMARCAL1 or ZRANB3 leads to increased sister chromatid exchanges and DNA damage sensitivity following replication stress.

The central recombinase factor RAD51 is another factor critical for fork reversal although its function here is independent from its role in HR. Unlike DSB repair where RAD51 is loaded onto ssDNA by mediator protein BRCA2, at stalled forks MMS22L-TONSL replace RPA with RAD51 to promote fork reversal[104,105]. siRNA depletion of RAD51 displayed significantly reduced fork reversal events as observed by EM analysis in replication stress conditions. Although it is known that RAD51 is required, the exact mechanism of how it promotes fork reversal is still yet to be discovered. This is complicated by its other functions at the

replication fork mainly protection of nascent forks from nuclease mediated degradation[106]. Further studies are required to uncouple the various function of RAD51.

Fork reversal although considered protective can also have deleterious consequences when not appropriately regulated. Reversed forks are one of the frequent recombination intermediates observed upon oncogene induced replication stress presumably due to deregulated origin firing which results in nucleotide shortage[107]. They are also substrates for structure-specific endonucleases like MUS81 that cleave them to generate toxic DSB. This happens particularly in checkpoint-deficient cancer cells[108]. Since reversed forks are also substrates for nucleolytic digestion, deletion of SMARCAL1 in BRCA2-deficient cells reduces the number of reversed forks formed which are substrates for MRE11. This rescues fork degradation effect and restores genome stability[109].

1.4.3. Nascent fork protection

The newly replicated DNA is under constant threat following replication stress. This is because fork reversal generates a one ended DSB that are substrates for resection[29,101]. Similar to DSB repair, in the context of stalled forks as well it is necessary to maintain strict control of initial resection by MRN-CtIP and long-range resection by DNA2 and EXO1[101,110]. Uncontrolled degradation destabilizes reversed forks forcing them to collapse. This generates toxic DSBs and also leaves large portions of DNA unreplicated (Fig. 5). Several factors are involved in fork protection with the BRCA/FA pathway being the classical pathways.

BRCA1/2

An emerging function of the BRCA proteins is their role in nascent fork protection following replication stress. It is important to note that this function is independent of their role during HR repair of DSB. Deficiency of either of these proteins leads to uncontrolled degradation by the nuclease MRE11[111,112]. This leads to chromosomal instability and high sensitivity to replication stress inducing agents[113]. BRCA1/2 protect stalled replication forks in a HR independent but RAD51 dependent manner[114,115]. Briefly, RAD51 coats the nascent strands and forms stable nucleoprotein filaments which are required for strand invasion but are not compatible substrates for the nucleases[116]. BRCA1/2-deficient cells can no longer load RAD51 on reversed forks thereby leading to aberrant degradation of nascent DNA leading to chromosomal instability[117]. Once again, its important to note that RAD51 is required for both mediating fork reversal and fork protection.

Another mechanism of fork protection mediated by the BRCA proteins involves the fork reversal SMARCAL1, ZRANB3 and HTLF. In studying how cells respond to replication stress to maintain genome integrity, hydroxyurea (HU) has been used extensively as a model drug[13]. HU acts by inhibiting ribonucleotide reductase leading to depletion of cellular deoxyribonucleotide triphosphate (dNTP) pools, slowing down the progression of active replication forks in the cell. BRCA-deficient cells upon treatment with hydroxyurea accumulate DSBs which can be alleviated by loss of SMARCAL1, ZRANB3 and HTLF[103]. Here, SMARCAL1, ZRANB3 and HTLF loss reduces the number of reversed forks formed thereby reducing the amount of substrate available for nuclease mediated digestion[109].

FA proteins

Fanconi Aneamia (FA) is a rare autosomal disorder characterized by increased spontaneous and mutagen-induced chromosome instability, congenital malformations and cancer susceptibility[118]. The FA pathway mainly functions in resolving mutagenic interstrand cross links (ICL). FANCD2 introduces a DSB to repair ICL by HR which requires BRCA2[119]. Thus, FA and HR proteins together suppress cellular sensitivity to DNA replication poisons that induce DNA ICL. Independent from its ICL repair roles, depletion of FANCD2 leads to degradation of stalled forks by MRE11. FANCD2 also stabilizes RAD51 filament formation on newly replicated DNA which protects it from MRE11 dependent degradation[119].

RIF1

RIF1 was recently found to mediate fork stabilization following HU. *Rif1*$^{-/-}$ MEFs, HAP-1 and primary B cells following RS, displayed a severe fork degradation phenotype with no effect in reversed fork formation. To understand how RIF1 protected nascent forks if it does not affect fork reversal, the function of different nucleases was tested. It was identified that at stalled replication forks RIF1 inhibits the activity of DNA2 nuclease. DNA2 in both DSB and at stalled forks mediates long range resection. Fork degradation following RIF1 depletion have detrimental effects leading to delayed fork restart and increased levels of ssDNA which leads to the cells accumulating at S/G2. Following chronic replication stress, RIF1-deficient cells are significantly less viable due to the formation of chromosomal aberrations from fork collapse events. It is important to mention that this function of RIF1 is not dependent on 53BP1 so it functions in a completely independent mechanism at stalled forks as opposed to DSB end protection[42,120,121].

Apart from the mentioned factors, several others are continuously being discovered that promote regulate fork protection following replication stress. XRCC1 another DSB repair factor also promotes

nascent fork degradation in BRCA2-deficient cells by MRE11[122]. MRNIP an MRE11 binding protein prevents fork degradation by inhibiting the activity of MRE11[123]. BRCA2 prevents long range degradation in by EXO1 following initial degradation by MRE11. CST complex also involved in end protection also prevents the activity of MRE11 at stalled forks[124]. The continuous discovery of new factors reveals the importance of nascent fork protection. Given the various sources of replication stress (discussed in 1.2.1.1), and the fact that faulty replication always has detrimental outcomes, cells have evolved a complex network of effectors to ensure that stalled forks are continuously stabilized and replication can be completed.

Recently, fork protection was also discovered as another mechanism contributing to PARPi resistance. Deletion of PTIP in BRCA2-deficient cells *protected* from nascent DNA degradation by MRE11. As explained before BRCA1-deficient cells following replication stress or in this case PARPi undergo MRE11 dependent degradation of stalled forks which eventually leads to cell death under chronic stress conditions[111]. Alarmingly, primary splenocytes from *Brca2*$^{F/F}$ *Ptip*$^{-/-}$ mice rescued the fork protection defect observed by preventing the access of MRE11 to stalled forks. This rendered them resistant to PARPi[42].

In summary, this highlights how fork protection is not just required to maintain the integrity of the genome but also modulating it could have harmful effects on chemotherapeutic sensitivity.

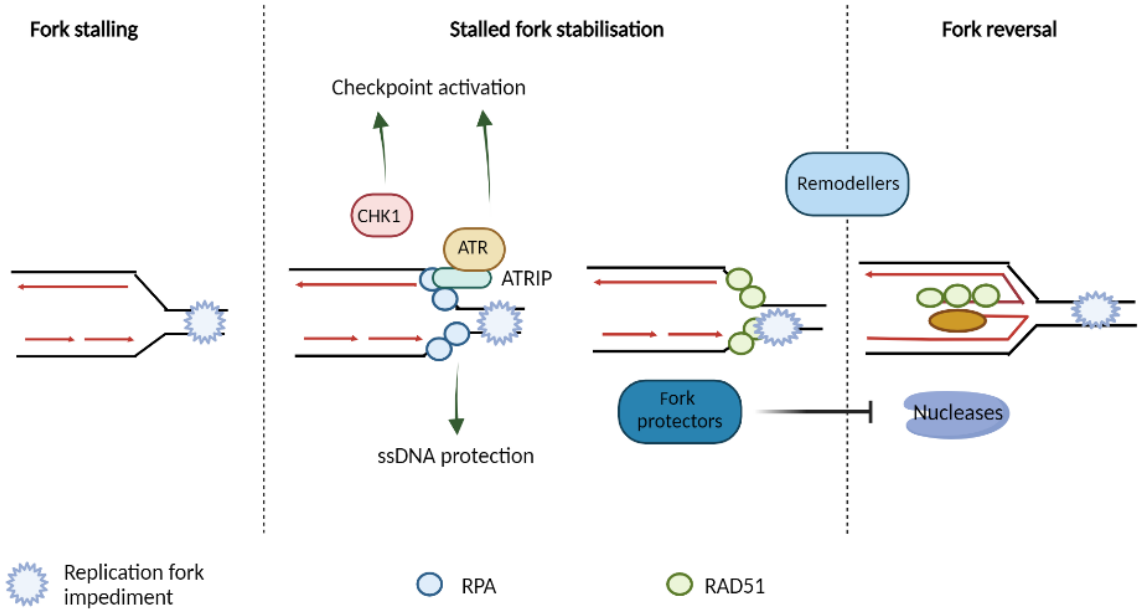

Figure 5. A simplified model for the rescue of stalled replication forks. After fork stalling, ssDNA generated by polymerase–helicase uncoupling is coated by RPA to prevent secondary structure formation.

The ssDNA–RPA complex then induces activation of the replication checkpoint, which will regulate a wide range of cellular events to promote fork recovery. RAD51 soon replaces RPA and mediates replication fork reversal to facilitate fork repair. This process also involves many other replication fork remodelers such as SMARCAL1. The reversed forks are protected by various fork protectors from deleterious fork degradation that can destabilize stalled forks like BRCA1/2, RIF1, FANCD2 to name a few.

1.4.4. Fork restart

A stalled replication fork is arrested but is capable of resuming replication (replication fork restart) once the inhibition is removed, whereas a collapsed fork has become inactivated through dissociation of the replication machinery or the generation of DNA double-strand breaks. After the removal of replication inhibitors such as aphidicolin and hydroxyurea, replication resumes by mechanisms that have been poorly understood in mammalian cells[125]. More is known about replication restart in *Escherichia coli*, in which stalled or collapsed forks are reactivated by recombination-dependent or recombination independent pathways, depending on their structure. The proteins involved in these pathways are not conserved in eukaryotes. Eukaryotic chromosomes contain more replication origins than are activated during each round of replication and these can serve as backups for completion of replication if progression of nearby forks is impaired[126]. It has therefore been unclear whether eukaryotes use specialized mechanisms for replication restart after the removal of replication inhibitors similar to what is observed in bacteria. Broadly, 2 fork restart pathways can be postulated[127].

Holliday junction mediated restart

The reversed fork resembles a Holliday junction and can perform strand invasion due to the presence of RAD51. RAD51 loading onto DNA requires a lagging-strand gap or a 3'-overhang and therefore involves end processing. These structures may be generated by MRE11-dependent DNA resection which promotes HR repair. RAD51 is loaded onto ssDNA to form protein–DNA filaments, which then catalyse homology search and strand exchange. This promotes strand invasion and D-loop formation during Holliday junction-mediated restart[128].

DSB-mediated restart

If mammalian replication forks are stalled for many hours, fork-associated DSBs are generated by structure specific endonuclease MUS81. This suggests that DSB formation may play a part in replication fork restart, especially after long periods of stress. This leads to repair by a form of homology-dependent repair called Break Induced replication (BIR)[129]. BIR also starts with RAD51 nucleofilament formation and strand invasion but results in conservative synthesis of DNA as opposed to semi conservative way in normal replication. As a result, BIR is highly mutagenic and subjected to template switching, leading to complex chromosomal rearrangements and loss of genetic information[130]. Due to the high mutagenicity it is the last-resort pathway for repair of replication-associated DSB.

1.5 RIF1

RIF1 is a multi-functional protein which is conserved from budding yeast to humans and is critical for maintaining genome integrity at several steps of the chromosome cycle. It was originally identified as a negative regulator of telomere length in budding yeast *Saccharomyces cerevisiae*[131]. While its telomere length regulation function appears to be specific to yeast, RIF1 in higher eukaryotes protects DSB ends from nuclease mediated resection. This promotes repair by NHEJ while inhibiting HR[46,65,75]. RIF1-mediated DSB end protection is toxic in BRCA1-deficient background as it leads to inappropriate end joining reactions leading to gross chromosomal rearrangements and genome instability. Subsequently, RIF1 deletion leads to substantial rescue of BRCA1-deficient cells rendering them resistant to PARPi.

RIF1 also exerts its end protection function in the repair of programmed DSB occurring in the *Igh* locus during CSR. In this case though, repair by NHEJ leads to productive CSR events leading to the formation of requisite antibodies[46,75]. Another conserved function of RIF1 is control of DNA replication initiation and timing. RIF1 not only prevented unscheduled origin firing in yeast but also regulated higher order chromatin structure in humans through which it controlled replication timing in S phase. Deletion of RIF1 here leads to delayed replication of normal sequences and advanced initiation of late-replicating sequences[132,133]. It was also recently demonstrated that mammalian RIF1 protects nascent DNA at replication forks that are challenged by replication inhibitors[120,121]. Human RIF1 was shown to protect the nascent DNA in a function that depends on RIF1 interaction with PP1. The structural requirements for the various functions of RIF1 are described below (Fig. 6).

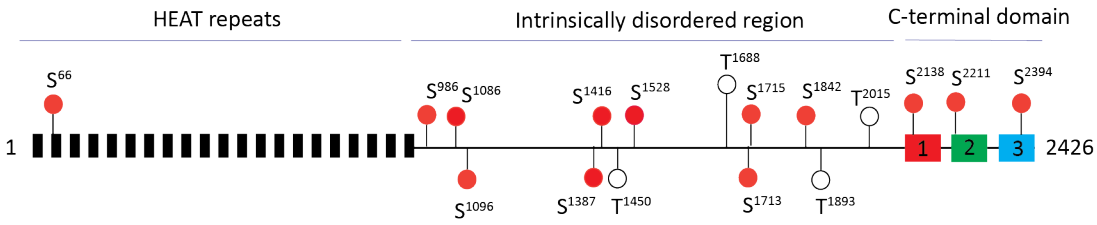

Figure 6. Structure of murine RIF1. Schematic representation of RIF1 protein (NP_780447.4). Predicted domains are indicated with boxes: 21 N-terminal HEAT repeats domain (black box); C-terminal CTD-I (RVxF/SILK motif, red), CTD-II (DNA binding domain, green) and CTD-III (BLM interaction domain, blue). Red balloons indicate serine (S) and white balloons indicate threonine (T) residues within putative ATM/ATR phosphorylation sites (SQ/TQ).

1.5.1. Domains of RIF1 and its functions

Mammalian RIF1 is a large protein of 270kDa and 2426 amino acids. RIF1 contains HEAT ((Huntingtin, Elongation factor 3, protein phosphatase 2A, Tor1)-like repeats in the N-terminal followed by an intrinsically disordered region and a C-terminal domain encoding specific RvSF-SILK motifs which are consensus sequence for PP1.

The N-terminal HEAT repeat shares the highest sequence homology to the yeast ortholog. HEAT repeats usually mediate protein-protein interactions in several different processes including the DDR[131]. The 21 repeats in NTD of RIF1 were indispensable for its accumulation to IR-induced foci[134]. Recently it was identified that the HEAT repeats also mediated RIF1 recruitment to phosphorylated 53BP1. The HEAT domain and CTD also promote Rif1 binding to G-quadruplexes secondary structures in yeast (Fig. 7).

The CTD is divided into 3 parts-CTD1, CTDII and CTDIII. CTD-I contains the mammalian RVxF-SILK motif required for PP1 binding. One of the conserved functions of RIF1 is in regulating replication timing. It was identified that RIF1-PP1 suppress premature activation of the MCM2-7 complex: RIF1 targets PP1 to dephosphorylate the MCM complex and counteracting its phosphorylation by DDK. This function is essential to restrain the activity of MCM complex and prevent unscheduled origin firing[72,135].

RIF1-PP1 binding is also essential for stabilization of stalled replication fork following replication stress. RIF1-deficient MEFs showed significant nascent fork degradation and this led to accumulation of chromosomal abnormalities causing genomic instability[120]. RIF1 recruits PP1 through its C-terminal

domain which dephosphorylates DNA2. This restrains DNA2 activity and prevents it from aberrantly degrading stalled replication forks.

CTD-II was shown to have DNA-binding properties in vitro[131]. CTD-III contains a BLM helicase-interaction domain. BLM interaction is essential for stalled replication forks restart and resolution of anaphase ultrafine bridges, two roles of RIF1 that are independent of its interaction with 53BP1[136] (Fig. 6).

The IDR of RIF1 constitutes more than half of its length. These regions do not adopt any stable and defined secondary or tertiary structure. This allows disordered proteins to switch between different confirmational states which ultimately affects the functions and interactions with other proteins[137]. Additionally, PTM in the IDR in known to affect protein folding and mediate protein-protein interactions in several DDR factors[137,138]. In fact, the largely unstructured NTD of 53BP1 contains 28 S/T Q sites which are phosphorylated by ATM upon IR. This step is key to recruiting all of its binding partners namely RIF1, PTIP and the Shieldin complex albeit through independent phosphoresidues. Together the 53BP1-RIF1-Shieldin complex mediate DSB end protection thereby promoting repair by NHEJ.

Interestingly, RIF1 also contains several S/T Q sites which are consensus sites for ATM/ATR and in fact three S/T Q clusters are present in the IDR (Fig. 6). MS-based identification of ATM/ATR target proteins revealed RIF1 to be phosphorylated at the human ortholog of S1528 following irradiation[139]. A recent report found that abrogation of consensus Mec1/Tel1 (ATR/ATM) phosphorylation sites in yeast Rif1 role in nascent fork protection[140]. Phosphorylation in a different cluster of Rif1 was also shown to regulate telomere length in yeast[141].

Both human and yeast RIF1 do not posses any catalytic activity. The presence of HEAT repeats and a large IDR both that mediate protein-protein interactions, indicated RIF1 was likely to function as a bridging factor recruiting key proteins to maintain genome stability. In the start of this study, very few effectors of RIF1 were identified and the exact function of RIF1 in several crucial process like DSB repair and replication fork stabilization was still undiscovered. Recent research identified several key mediators of end protection namely the Shieldin complex (SHLD 1,2,3 and REV7) that were recruited in a 53BP1-RIF1 dependent manner. SHLD2 was discovered to bind directly to minimally resected DSB ends through its OB-fold domains. These domains are crucial for ssDNA binding and are present in several ssDNA binding proteins namely RPA. 53BP1-RIF1 mediated recruitment of the shieldin complex protected the DSB ends from resection due to ssDNA binding activity of SHLD2. This would evict the competing resection promoting factors and promote repair by NHEJ. Even though shieldin was identified, several questions

remain. Knockdown of RIF1 disrupts Shieldin recruitment by 53BP1 in human cell lines. However, the exact function of RIF1 in this process is still yet to be discovered. Moreover, its exact molecular mechanism in DNA DSB repair and replication fork protection is yet to be discovered. As seen from the previous sections, accurate regulation of these processes are critical to maintain genome stability. Dissecting the molecular mechanism of RIF1 function by identifying its effectors and PTM specifically phosphorylation will shed light on its functions in maintaining genome stability.

2. Aims of the study

RIF1 mediates two critical functions to maintain genome stability during replication: stabilization of stalled replication forks and repair of DSBs following fork collapse. Fork stabilisation enables replication to proceed and no under replicated DNA is formed. During DSB, repair RIF1 protects broken ends from nucleolytic resection and promotes repair by NHEJ. However, in the context of BRCA1-deficient cancers treated with PARPi the pro-NHEJ function of RIF1 is toxic. Hence, deletion of RIF1 in this context promotes PARPi resistance as the HR defect is restored. To understand how RIF1 functions in these 2 independent processes I would like to understand both its interactome and PTMs specifically phosphorylation. Identifying the molecular mechanism of RIF1 function not only sheds lights on how it maintains genome stability but also gives clues on how it promotes PARPi resistance.

Aim 1. To identify novel RIF1 interactors promoting PARPi resistance.

Our lab has recently defined RIF1 interactome in actively proliferating primary B cells using Isotopic-Differentiation of Interactions as Random or Targeted (I-DIRT) proteomics-based approach (ref). In order to identify potential RIF1 partners required for DSB repair pathway choice, I have screened for RIF1 I-DIRT candidates that promote genome instability in the absence of BRCA1. To do so, I have first generated BRCA1-deficient murine B cell lines that fully recapitulate the genomic instability observed in BRCA1-deficient mice. Second, I have applied a functional rescue-of-proliferation assay following CRISPR-Cas9-mediated somatic targeting of each individual I-DIRT candidate in a BRCA1-deficient murine B cell line.

Aim 2. To characterize the role of RIF1 phosphorylation in DSB repair and replication fork protection.

The I-DIRT list also identified several residues on RIF1 that were phosphorylated in irradiated cultures of highly proliferating primary B cells. To understand the role of these phosphorylation events in DSB pathway choice in BRCA1 deficiency, I have created BRCA1-deficient cell lines harboring alanine or aspartate substitutions at these sites by CRISPR-Cas9 mediated knock-in editing. Furthermore, I have analyzed the levels of genome instability and lethality exhibited by these cell lines in response to treatment with PARPi. To understand if abrogation of phosphorylation mediates nascent fork protection, I created cell lines harboring alanine substitutions at these sites on a wild-type background by CRISPR-Cas9 mediated knock-in editing, and have analyzed the levels of nascent fork degradation following replication stress.

3. Materials and Methods

3.1 Materials

Table 1: Oligonucleotides used in the study

Name	Sequence (5'-3')	Application
Brca1-1	CCGATGTTCCTTGGATAACA	Generation of *Brca1*^{mut} CH12 clones
Brca1-2	GCGTTCAGAAAGTTAATGAG	
Brca1-3	GCAAAGTCTGTGCCCTGAGA	Generation of *Brca1*^{mut} CH12 clones
Brca1-4	GAGCTACCACCGATGTTCCT	
Rif1-1	GGAAGACCCCTCGGTGCCTC	Generation of *Rif1*$^{-/-}$ CH12 clones
Rif1-2	AAGTCTCCAGAAGCGGCTCC	
Zranb2-1	GAATTTCCGAGTCAGTGACG	Generation of *Zranb2*$^{-/-}$ CH12 clones
Zranb2-2	GTCACTGACTCGGAAATTC	
Zranb2-3	TCCGAGTCAGTGACGGGGAC	Generation of *Zranb2*$^{-/-}$ CH12 clones
Zranb2-4	GTCCCCGTCACTGACTCGGA	

Table 2: Reagents used

Name	**Source**	**Cat. #**
Plasmids		
pX458G (pSpCas9(BB)-2A-GFP)	Addgene	48138
pX330G (pX330-T2A-GFP)	V.T. Chu (K. Rajewsky's lab)	N/A
pX330Gn (Cas9D10A)	M. Andreani	N/A
pMA-PhoMim	M. Andreani (GeneArt)	N/A
pMA-PhoNull	M. Andreani (GeneArt)	N/A
Recombinant proteins and chemicals		
LPS	Sigma-Aldrich	L2630
IL-4 (mouse recombinant)	Sigma-Aldrich	I1020
TGFβ-1 (mouse recombinant)	R&D Systems	7666-MB-00
FBS	Sigma-Aldrich	F7524
RPMI 1640	Thermo Fisher Scientific	21875091
HEPES	Thermo Fisher Scientific	15630056

Sodium Pyruvate	Thermo Fisher Scientific	11360039
Antibiotic Antimycotic	Thermo Fisher Scientific	15240062
L-Glutamine	Thermo Fisher Scientific	25030024
2-Mercaptoethanol	Thermo Fisher Scientific	21985023
NuPage LDS Sample buffer	Thermo Fisher Scientific	NP0008
Proteinase K	Peqlab	3375501
Phenol:Chloroform:Isoamyl alcohol	Roth	A156.3
PARPi Olaparib/AZD2281, Ku-0059436	Selleckchem	S1060
Colcemid	Sigma-Aldrich	1029589200
KaryoMAX Giemsa Stain Solution	Gibco	10092013
Gurr Buffer Tablets	Gibco	10582013
Kits, enzymes and other reagents		
PureLink HiPure Plasmid Filter Midiprep Kit	Thermo Fisher Scientific	K2100-15
PureLink HiPure Plasmid Filter Maxiprep Kit	Thermo Fisher Scientific	K210017
Stbl2 Competent E. coli	Thermo Fisher Scientific	10268019
Stbl3 Competent E. coli	Thermo Fisher Scientific	C737303
TOP10 Competent E. coli	Thermo Fisher Scientific	C404003
Neon Transfection System, 100 mL Kit	Thermo Fisher Scientific	MPK10025
TOPO TA Cloning Kit	Thermo Fisher Scientific	450641
NucleoSpin DNA Purification Kit	Macherey-Nagel	740499
Gibson assembly cloning kit	NEB	E5510S
QuickExtract Solution	Epicentre	QE09050
HotStarTaq DNA Polymerase	Qiagen	203205
Phusion High-Fidelity DNA Polymerase	Thermo Scientific	F530L
Taq DNA Polymerase with ThermoPol Buffer	NEB	M0267
T4 DNA Ligase	NEB	M0202
T7 DNA Ligase	NEB	M0318
Phase Lock Gel tubes	VWR	2302820
IdU	Sigma Aldrich	I0050000
CldU	Sigma Aldrich	C6891-100MG
Superfrost slides	VWR	631-0909
Mounting media	Thermo Fischer Scientific	P10144
Software		
FACS Diva	BD	N/A
FlowJo v.10	Treestar	N/A
MacVector v15.0	MacVector, Inc.	N/A
Prism v.6	GraphPad	N/A
ImageJ	GitHub	N/A

Table 1. List of antibodies used

Antibody	Company	Catalog number	Dilution	Preparation
Mouse αRIF1	In house (# 2034)		1:2500	3% BSA in PBST
Mouse αZRANB2	Novus Biologicals,	H00009406-M02	1:1000	3% BSA in PBST
HRP Goat αRabbit	Jackson immunoresearch	111-035-008	1:10000	3% BSA in PBST
HRP Goat αMouse Lc	Jackson immunoresearch	115-035-174	1:10000	3% BSA in PBST
Mouse αIdU	BD Biosciences (Clone B44)	347580	1:50	5% BSA in 1X PBS
Rat αCldU	Abcam	ab6326	1:500	5% BSA in 1X PBS
Goat anti-Rat IgG (H+L), Alexa Fluor 488	Invitrogen	A-11006	1:500	5% BSA in 1X PBS
Goat anti-Mouse IgG (H+L), Alexa Fluor 546	Invitrogen	A-11030	1:500	5% BSA in 1X PBS

Table 2. List of primers used

Name	5'-3' sequence	Purpose
MDV_149	ATTACAGCCTGAGACCAGC	Amplification of Cas9 targeted region in *Brca1* exon 11
MDV_150	CCTCTACTGGTTTGGAGAAG	Amplification of Cas9 targeted region in *Brca1* exon 11
MDV_p124	GAGTAAATAAGCGCGAGCCG	Amplification of Cas9 targeted region in *Rif1* Exon 2
MDV_p131	AACCCACTAACTCCGGATCG	Amplification of Cas9 targeted region in *Rif1* Exon 2
MDV_288	AAGCGAAGCAGAGCCTCAG	Amplification of Cas9 targeted region in *Zranb2* Exon 1
MDV_289	TGAGCTCACGGTTCAGTG	Amplification of Cas9 targeted region in *Zranb2* Exon 1
MDV_282	GCGGTGCTTGAACTTCAGGG	Amplification of Cas9 targeted region in *Rif1* Exon 30 (For KI clones)
MDV_286	GCTGCGTGCTCAGTCTCAAC	Amplification of Cas9 targeted region in *Rif1* Exon 30 (For KI clones)

Table 3: List of gRNAs used in the gain-of-viability screen

gRNA	Protospacer sequence
CD36 #1	TCAATAAGCATGTCTCCGAC (-)
CD36 #2	CGGAACTGTGGGCTCATTGC (+)
CD36 #3	CTGTTCTTTGCCACGTCATC (-)
MGA #1	AGGAATAGCTCCGATCAAGA (+)
MGA #2	GTAAGACGAACACGATGAGC (-)
MGA #3	ACCACGCCGACGCCGCTCAT (-)
LYD #1	CACGTGACATCGAAGTGCCC (-)
LYD #2	TGACCAGCCTCTCGTTGCAT (+)
LYD #3	CCATGTCAGCAGTGGTTCCG (+)
BACH2 #1	CTGTGACGTGACGCTGATCG (+)
BACH2 #2	TCCGTTGGTCATTGAGGCCC (-)
BACH2 #3	ACCAATTCCAGTGACGAGTC (+)
PLD4 #1	CATGATCCACATAGCGGACT (+)
PLD4 #2	TCATGGGCACTTGTCGTATC (-)
PLD4 #3	CGTGCTGGACAATGCGCTAC (+)
EIF5 #1	ACGTTGCAAAGGCGCTTAAT (+)
EIF5 #2	GTATGATGCCGACCTGTTAG (+)
EIF5 #3	GACCTCCTCCTCTAACAGGT (-)
CHMP5 #1	TGACAAAAAGATTTCCCGGC (+)
CHMP5 #2	TGAGCAACAGCGAGACAACC (+)
CHMP5 #3	TCCGCTCCTGCAATTCCGGA (+)
RNF31 #1	GCCCGCAGCGGCCCCGGTAT (+)
RNF31 #2	GTCTCGGGTTCGGTTGCACA (-)
RNF31 #3	TGGGCACGAGACTTGGTTAC (-)
ANHAK #1	AACTCCCCTGCGGCCCGCAC (+)
ANHAK #2	ACCACCCCAGTGCGGGCCGC (-)
ANHAK #3	CTGGGCAATGGTCAGCCCGT (-)
TIMELESS #1	CCACAAGGAGCCGGATTGCC (+)
TIMELESS #2	CTAGCCACGTGTAGCGCCCT (+)
TIMELESS #3	AGGATTTGATCCGATACCTG (+)
POLE #1	ACTTACGGTTTGGTTTCGAA (+)
POLE #2	GTGATATCCCCTGCCGGTTT (+)
POLE #3	GATGCTGAGACCTACGTCGG (+)
TLK2 #1	CAGTTAGCGCCACGGGGAGC (+)

gRNA	Protospacer sequence
TLK2 #2	TAAAGTGGCCTAATCGCAAT (+)
TLK2 #3	TAAAGTGGCCTAATCGCAAT (-)
NAA50 #1	CTTGCACCTTACCGAAGACT (-)
NAA50 #2	CTAGTCTTCGGTAAGGTGCA (+)
NAA50 #3	ATTCTACAAGGATGTGCTAG (-)
RNF2 #1	GTGTTTACATCGGTTTTGCG (+)
RNF2 #2	AGTGCATCAAAGTTCGGGTC (-)
RNF2 #3	TGATGAGTATGAAGCGCATC (+)
TEX10 #1	AATGTGTTCAGTTCGTATTT (+)
TEX10 #2	TGAGAAGTGACTCTCCGATT (+)
TEX10 #3	TGAGAAGTGACTCTCCGATT (+)
LAS1L #1	TGGATCGCGTGTGGCGTGCG (+)
LAS1L #2	CCAAGAGACGACGATACCCC (-)
LAS1L #3	CGCTGAACCGAATTACAGTA (+)
PYHIN1 #1	ATACTGCTGGACGGTCTTTT (-)
PYHIN1 #2	AAGACCGTCCAGCAGTATTC (+)
PYHIN1 #3	CTAGAGGAACTCCTAGTGCC (-)
CD55 # 1	CGAAAACAACCTCCACTCCC (+)
CD55 # 2	TCAAGGCAAGTTGCTTTTCC (-)
CD55 # 3	CACAGGAAATACTGTTGATT (+)
SPCS2 #1	TCCCACTTATCAATTTTTAC (-)
SPCS2 #2	GCCAAAACTGGCTTGGACTC (-)
SPCS2 #3	GAATGGATCCTGATGATATT (+)
CPM #1	CCCCATGGAGATTCGCAGAG (-)
CPM #2	GTGCTGTAAATATCCTCGCG (+)
CPM #3	TCCACGATTACATTCGGTAA (-)
COXB5 #1	TAGCCTGCTCCTCATCAGTG (-)
COXB5 #2	TGTCCCCACTGATGAGGAGC (+)
COXB5 #3	GTGCCTGAAGCTGCCTTTGG (-)
MS4A4A #1	TATATGTGAATTCGCATTCA (+)
MS4A4A #2	ATAATTGCCACTGTGTCGAC (+)
MS4A4A #3	GCTGATTACGATCCCCGAGA (-)
PDLIM2 #1	TGGGGCTTCCGAATTAGCGG (+)
PDLIM2 #2	AGAGAACATGCTACACGCGG (+)
PDLIM2 #3	GCCTTGGGGCGGCCCGTCCC (-)

EXOSC8 #1	TGGAGCCGCTGGAGTATTAC (+)
EXOSC8 #2	AAGGAAAACTGCCGTCCTGA (+)
EXOSC8 #3	AGCGGTGGTAGATCCACATT (-)
SYK #1	AATTGCGGCTCTGGCGTAGC (-)
SYK #2	TACTCCCGGGGGCCGGTTGA (-)
SYK #3	CCGGCCCAAAGAGGTCTACC (+)
GBAS #1	CGGGTGTTGCTCGCGCGAGG (+)
GBAS #2	TTGTCAGAAAGGTCGATCCA (+)
GBAS #3	GCTTGTGCCAGGCCGCGTTC (-)
PSMD4 #1	AGCAACCCTGAGAATAACGT (+)
PSMD4 #2	CTTCTGCACTGGCATCCGCG (+)
PSMD4 #3	AGCAGGAGTTTGGCCGTCCT (+)
IFIH1 #1	TTGACATAGCGCGCGGCTAG (-)
IFIH1 #2	TGCCGCGCTGGTGTTACCAC (-)
IFIH1 #3	CAGAGAAGTGTTATTAACGA (-)
DPP4 #1	AACTATTGGCACGGTGATGA (-)
DPP4 #2	TAGTACTCCCACCGTGACAC (-)
DPP4 #3	CTGCCGTTCCATGAATAAGG (-)
APRT #1	CGCGCCACCAGTTTCAACTC (-)
APRT #2	GTCGATCTTGCCGCTGTGCG (-)
APRT #3	CTGTGTGCTCATCCGGAAAC (+)
ARPC1A #1	GACGAAAGCGCACGAGCTGA (+)
ARPC1A #2	CAGACCGCAACGCCTATGTC (+)
ARPC1A #3	TGGCTGCACGGTTAATCCTC (-)
SLC2A1 #1	GGTGACGGGCCGCCTCATGT (+)
SLC2A1 #2	GGATGGGCTCTCCGTAGCGG (-)
SLC2A1 #3	GTTGACGATACCGGAGCCGA (-)
TCEB1 #1	AGGGCCTTCACAGCCACCAT (-)
TCEB1 #2	GGAGAGGAGAAGACCTATGG (+)
TCEB1 #3	ACAATAAAGGCTATGTTGAG (+)
NDUFB7 #1	CCCGCCGGACCTCGGCTTTC (+)
NDUFB7 #2	CCCACAGATAGCGCCGGGTC (-)
NDUFB7 #3	CAAGCACGAGCAGCACGACT (+)
IGLV2 #1	AGAGAGTATAAGTGAAGTCC (-)
IGLV2 #2	GTGAGTATGACTGTTCCACC (-)
IGLV2 #3	AACACCTGGAGCTCGGTTGC (-)
PAG #1	GTGGGGAAGTCTGGCTGCCG (+)
PAG #2	TGGTCCCCGCTATGCTGCCG (-)
PAG #3	GATCCCGCCTGAGAACGCCG (+)
ZRANB2 #1	TCCGAGTCAGTGACGGGGAC (+)
ZRANB2 #2	CATTGGCACTAAATAAGCCC (-)
ZRANB2 #3	TGGCCCTGCATCTATATTAA (+)
BMP2K #1	GTTCGCCGTCGGCCGCTACC (+)
BMP2K #2	TCCCACTGTGAGTCCGCACC (-)
BMP2K #3	CAAAAATATTGTCGGTTATT (+)
GBP3 #1	ATTGTTGGTTTATATCGTAC (+)
GBP3 #2	AATCCGAAACCAAGGGTATC (+)
GBP3 #3	CATGAGCACCATCAACCAGC (+)
EIF2B5 #1	CGAACAACGTTGGGGGACGT (+)
EIF2B5 #2	ACTCGAGATGATTTTGTACG (+)
EIF2B5 #3	AAAGCGTGCAGCTGACCACT (+)
CISD1 #1	GCACAGCGGAGTTGGAGCTG (-)
CISD1 #2	GGTGCATGCCTTCGACATGG (+)
CISD1 #3	GAAGAGACTGGCGACAACGT (+)

3.2 Methods

3.2.1. Cell culture

In the present study, the following CH12 cell lines were used: wild-type CH12, *BRCA1*^{mut} CH12, *BRCA1*^{mut}*Rif1*$^{-/-}$ CH12 *Rif1*$^{-/-}$ CH12, *Rif1*$^{S>A}$ CH12, *Rif1*$^{S>D}$ CH12, *ZRANB2*$^{-/-}$ CH12. Cells were grown in RPMI 1640 medium supplemented with 10% fetal bovine serum (FBS), 10 mM HEPES, 1 mM Sodium Pyruvate, 1X Antibiotic Antimycotic, 2 mM L-Glutamine, and 1X 2 Mercaptoethanol at 37°C and 5% CO2 levels.

3.2.2. Generation of clonal derivatives by CRISPR-Cas9 mediated genome editing

2-4 guide RNAs against the targeting region was designed using the CRISPRdesign software developed by the Zhang's lab (www.crispr.mit.edu) and CRISPRGold. The guide RNAs were cloned into tandem U6 cassettes in pX330-GFP encoding for Cas9^{D10A} and electroporated into CH12 using the Neon Transfection System (Thermo Fisher Scientific). GFP-positive cells were single-cell sorted into 96 well plates, and allowed to grow for 10-12 days, following which they were split into 3 replica plates for freezing, DMSO and 1µM Olaparib treatment. 72h post treatment individual clones were analysed for viability in high throughput (HTS). Residual viability was calculated by normalizing the olaparib value to the corresponding DMSO treated one. 6 clones were selected and expanded based on low or high residual viability values for the generation of *Brca1*^{mut} and *Brca1*^{mut}*Rif1*$^{-/-}$ respectively. Further validation was done by genetic scar analysis and western blotting to check for protein levels. To determine the genetic scar, the targeted region was amplified by PCR (Table 2 for primers) and was cloned into the pCR 2.1 TOPO TA vector (Thermo Fischer) and transformed into TOP10 cells. Single colonies were inoculated and the plasmids were sent for Sanger sequencing. This was aligned to the wildtype genomic sequence to determine the insertions or deletions introduced. The scheme of Brca1 and Rif1 genomic locus was adapted from ENSMBL ENSMUST00000017290.11 and ENSMUST00000112693.10 respectively.

3.2.3. Western blotting

Cell pellets were prepared by centrifuging CH12 cells at 1200rpm for 5 minutes at 4°C. The pellets were washed with 1X PBS and then snap frozen. RIPA lysis buffer (Sigma) containing 1µM DTT and EDTA free protease inhibitor (Sigma) was used for cell lysis and incubated for 20 minutes at 4°C. The cells were centrifuged at 12000rpm for 20 minutes. Bradford reagent (Biorad) was used to determine protein concentration and the whole extracts were denatured using NuPage loading dye (Thermo fischer) at 72°C for 10 minutes. The samples were run on precast NuPage 3-8% Tris acetate or 4-12% Bis-Tris gels (Thermo

Fischer) at 120V and Proteins were transferred to a PVDF (polyvinylidene difluoride, Millipore) membrane using the Mini Trans-Blot Tank (ThermoFisher Scientific) containing transfer buffer (25nM Tris, 192 mM glycine, 20% methanol) at 220 mA for 1.5 – 2 h. The membrane was blocked using either 3% BSA in PBST (1X Phoshpate Buffer Saline, 0.1% Tween-20) or 2% skim milk in TBST (1X Tris-Buffered saline, 0.1% Tween-20) for 1 hour, followed by primary antibody (Table 1) incubation overnight. The membrane was washed 3 times with PBST/TBST for 10 minutes each and incubated for 1 hour with HRP-tagged secondary antibody at room temperature (RT). After washing thrice, the membrane was developed using membranes were activated with freshly prepared chemiluminescence solution (PerkinElmer) and exposed to films (Amersham hyperfilm ECL, VWR) that were developed using the OPTIMAX 2010 film developer.

3.2.4. Metaphase analysis

CH12 cells were seeded at 80,000 cells/ml and treated with 1µM Olaparib for 24 hours. To trap the cells in metaphase, 2.5µg of Colcemid (Roche) was added for 45 minutes. Cells were harvested by centrifugation at 1000rpm for 10 minutes. The supernatant was aspirated except for 1ml which was used to resuspend the pellet in 1ml hypotonic solution (0.075M KCl) with gentle mixing. It was then filled up with 40ml of hypotonic solution and placed at 37°C for exactly 15 minutes with gentle mixing every 5 minutes. 1ml of fixation solution (70%(v/v) Methanol, 30%(v/v) glacial acetic acid) was added on top, mixed gently and the sample was washed at 1000rpm for 10 minutes. The supernatant was aspirated except 1ml which was used to gently resuspend the pellet. The falcon was filled up with 40ml of fixative and then incubated at RT for 30 minutes with gentle mixing every 10 minutes. After washing, the falcon was filled once again with 40ml of fixative and centrifuged. This process was repeated once more and the samples were stored at 4°C overnight after tightly wrapping in parafilm. To obtain metaphase spreads, the samples were once again washed in fixative solution and then resuspended in a volume of fixation solution that gives a translucent solution. Using a Pasteur pipette, 2-3 drops of cells were dropped from a height of at least 30cm on a slightly angled, wet slide and allowed to disperse. The slides were immediately then placed on a humidifier and the fication solution was allowed to evaporate for 1-2 minutes. The excess humidity was removed and the slides were allowed to air dry. The slides were placed in a 42°C hybridization oven for 1 hour to ‘age’ them. Meanwhile to prepare the staining solution 1X GURR buffer is prepared by dissolving 1 tablet GURR in 1 litre of MilliQ water. 47ml of this was taken to which 3ml of GIEMSA stain was added and thoroughly mixed. The slides were placed in staining solution for 2 minutes, then placed in a jar containing 1X GURR buffer to wash off excess stain and then placed in water. The slides were air dried overnight at RT and metaphases were acquired using an Automated Metaphase

Finder System Metafer4 at 63X magnification. Chromatid breaks and radials were manually counted from at least 100 metaphases per sample.

3.2.5. Residual viability assay

CH12 cells were seeded at 30,000 cells/ml in 2ml and treated with either 1µM olaparib (Selleckchem.com) or the same volume of DMSO. 72h/96h later, 1ml of the cells was collected, washed with 1X PBS at 1200rpm at 4°C, resuspended in FACS buffer (1X PBS+3% FBS) and analysed for viability in the flow cytometer. The percentage residual viability was calculated by normalizing the viability of a sample on Olaparib treatment with the viability upon DMSO treatment and multiplied to 100.

3.2.6. Genomic DNA isolation

Genomic DNA was extracted using phenol/chloroform method. For this, cells were centrifuged at 1200rpm for 5 minutes following which they were washed in 1X PBS. The supernatant was removed and to the pellets were resuspended in 500µl of Proteinase K Buffer (100mM Tris-pH 8, 0,2% SDS, 200mM NaCl, 5mM EDTA) per 1 million cells. To this 5ul of Proteinase K enzyme (Peqlab) was added and incubated at 55°C overnight without shaking. The following day, PLG light tubes (VWR) were centrifuged at 12000g for 30 seconds after which the genomic DNA solution was added on top. To this, equal volumes of Phenol/Chloroform/Isoamyl alcohol (Roth) was added and thoroughly mixed to have a homogenous solution of the aqueous and organic phases. This was centrifuged at 12000-16000g at room temperature for 10 minutes. 470µl of the supernatant was taken and added to a new tube to which equal volumes of Phenol/Chloroform/Isoamyl alcohol was added. The sample was centrifuged at 12000-16000g again for 10 minutes at room temperature. 420µl of the supernatant was carefully transferred without disturbing the lower layer. To this, $1/10^{th}$ the volume of 3M sodium acetate, pH 5.2 was added. When trace amount of genomic DNA is present, 1µg/µl of glycogen was added. 2.5 times this final volume of 100% ethanol was added and gently inverted several times and placed at -20°C for 30 minutes. The solution was then centrifuged at maximum speed for 15 minutes at 4°C. The supernatant was carefully aspirated and to the pellet 1ml of 70% ethanol was added and centrifuged at maximum speed for 10 minutes. The washing step was repeated once more and then the pellet was air dried until its no longer visible to the naked eye. To this, pre warmed Tris-EDTA was added and allowed to dissolve for 1 hour at 65°C and at room temperature overnight. The concentration was measured using the nano drop.

3.2.7. Genomic scar analysis

The targeted region was amplified by PCR using Phusion polymerase (Thermo scientific) and cloned into pCR-TOPO 2.1 vector as per manufacturers instructions. This was transformed into TOP10 cells, the

colonies were inoculated and the plasmids were isolated using Plasmid isolation kit (Machery Nagel). The plasmids were sequenced by Sanger sequencing using the universal M13 forward/reverse primer. The obtained sequences were compared to the wild type genomic sequence from ENSMBL using the MacVector program and the indels was obtained. The new mRNA sequence containing the indels was translated using ExPasy translate program to understand if the targeting led to a premature termination codon or an internal deletion in the protein translated.

3.2.8. I-DIRT

I-DIRT was performed as previously described147. Briefly, splenocytes from Rif1FH/FH and WT mice were isolated and cultured in SILAC medium supplemented with either labeled (heavy medium, Rif1FH/FH culture) or unlabeled (light medium, WT culture) L-arginine and L-lysine.

Upon 96 h culture, cells were exposed to 20 Grays of IR and then frozen in liquid nitrogen, after 45 min. of recovery at 37°C. RIF1 immunocomplexes were isolated from a 1:1 mix of frozen Rif1FH/FH and WT cells, upon sub-stoichiometric treatment with glutaraldehyde to preserve labile interactions and without altering the native composition of protein complexes. RIF1 and co-precipitating proteins were pulled down using anti-FLAG conjugated magnetic beads. Immunocomplexes were purified and analyzed by LC-MS/MS. Peptide identification and quantification were performed using the MaxQuant software

3.2.9. Gain-of-viability assay screen

CH12 was electroporated with 3 plasmids encoding gRNAs against a single candidate. 40 hours later, the high GFP+ cells were single cell sorted and allowed to recover for 72 hours. At 72 hours, cells were counted and seeded at 30,000cells/ml. 1µM of PARPi was added and cells were kept for 72 hours. Vaibility was analysed by flow cytometry.

3.2.10. Screening for KI positive clones

Genomic DNA was extracted using the method mentioned above and targeted region was amplified with at least 1 primer annealing outside the homology arms. The PCR product was purified with a plasmid purification kit (Machery Nagel) and then digested with 10 units of Nhe1 enzyme overnight. The PCR products were run on a 1% gel for determining the positive clones.

3.2.11. DNA fiber assay

CH12 cells were seeded at 350,000 cells/ml the previous day of the experiment. On the day of the experiment, 40µM of IdU was added for 20 minutes. 400µM of CldU was added after for exactly 20 minutes. The labelled media was removed by washing the cells with 1X PBS for 5 minutes at 1200rpm. 4µM of hydroxyurea was added for 3 hours. A small aliquot was taken for counting and the remaining cells were washed at 1200 rpm for 5 minutes and resuspended in 1X PBS at a concentration of 0.35 x 10^5 cells/ml. 3µl of the suspension was added to superfrost slides (VWR) and 10µl of lysis buffer (200mM Tris-HCl, 0.5% SDS and 50mM EDTA) was added on top. On-slide digestion was performed for 2 minutes at room temperature and then the slide was tilted using a 10ml pipette to obtain DNA fibers. The slides were fixed using 3:1 methanol: acetic acid for 10 minutes and excess solution was removing by washing with water. The slides were then denatured using 12N HCl for 80 minutes. Excess denaturation solution was removed by washing twice with 1X PBS. Filter sterilized blocking solution (5% BSA in 1X PBS) was added directly on the slides and incubated for 45 minutes in a humidified chamber at 25°C. The primary antibody for IdU ad CldU was prepared in blocking buffer and was added directly on the slide and incubated for 1.5 hpurs in the humidified chamber. The slides were washed thrice using wash buffer (1X PBS+ 0.05% Tween-20) for 5 minutes. The secondary antibody was prepared also using blocking buffer and added directly on the slides and incubated for 45 minutes in the humidified chamber. The slides were washed thrice. Mounting media was added and the slides were frozen at -20C. The image acquisition was performed soon after using 40X objective of Zeiss LSM800 confocal microscope and images were analysed using ImageJ software.

3.2.12. CSR assay

For CSR assay, 30,000 cells/ml CH12 cells were cultured for 40 hours in RPMI 1640 supplemented with 5-15 mg/mL αCD40L (BioLegend), 5 ng/ml TGFβ and 5 ng/ml of mouse recombinant IL-4 to induce the expression of IgA antibodies. Cell suspensions were collected, washed once in PBS and incubated for 20 min. at 4°C on a rotator with fluorochrome-conjugated anti-IgA antibodies (Southern Biotech). Stained cells were again washed and resuspended in 200 µL PBS 3% FBS. Samples were acquired on an LSRFortessa cell analyzer (BD-Biosciences). For single cell and bulk sorting, cells were collected 24-48 h after transfection and the portion of cells with highest GFP expression (top 3-5 %) were sorted using a BD FACSAria cell sorter (BD-Biosciences, MDC FACS Core facility).

Table 4: List of PCR protocols used

Amplification of Cas9 targeted region in *Brca1* exon 11	
95°C 12 minutes	1X
95°C 2 minutes 55°C 30 seconds 72°C 3 minutes	32X
72°C 5 minutes	1X
Hot Start Polymerase	

Amplification of Cas9 targeted region in *Rif1* exon 2	
95°C 12 minutes	1X
95°C 2 minutes 56°C 30 seconds 72°C 3 minutes	32X
72°C 5 minutes	1X
Hot Start Polymerase, 3% DMSO	

Amplification of Cas9 targeted region in *Zranb2* exon 1	
95°C 15 minutes	1X
95°C 2 minutes 57°C 30 seconds 72°C 3 minutes	32X
72°C 5 minutes	1X
Hot Start Polymerase	

Amplification of Cas9 targeted region in *Rif1* exon 30	
98°C 30 seconds	1X
98°C 10 seconds 68°C 15 seconds 72°C 90 seconds	30X
72°C 5 minutes	1X
Phusion polymerase	

4. Results

4.1 Deletion of ZRANB2 modestly rescues viability following PARPi treatment of *Brca1*^{mut} CH12 cells

4.1.1. BRCA1-mutated CH12 cell lines recapitulate the genomic instability in BRCA1-deficient background

BRCA1-deficient tumor models display a severe HR defect, which is exploited for treatment in the clinic with PARPi therapy. In this context, tumor cells repair replication-associated DSBs using the competing NHEJ pathway instead. This is mediated by end protection factors 53BP1-RIF1 which persistently protect the breaks and channelize repair through toxic NHEJ reactions which is detrimental to the viability of BRCA1-deficient cells. Hence, deletion of end protection factors rescues the HR defect in BRCA1-deficient mouse models and human cell line and promotes cell survival. This is called HR rewiring[77,142]. Consequently, deletion of both 53BP1 and RIF1 promote PARPi resistance *in vivo*. To understand how RIF1 promotes resistance at the molecular level, I set out to screen for RIF1 effectors, whose deletion restores HR proficiency and viability of BRCA1-deficient cells.

1. To do so, I first created a BRCA1-deficient model system using the murine B lymphoma cell line CH12. Although several other BRCA1-deficient model systems were available, creating one in CH12 was imperative sinceCH12 is a suspension cell line with a very high doubling time which would make it a powerful model system for FACS based proliferative assays which form the basis of the screening method I will describe below.
2. A high proliferation rate in addition to a stable diploid genome enables to study events during replication and also to quantify genome instability events in the chromosomal level which are essential to understand RIF1 function in repair of replication-associated DSB.
3. CH12 is the only cell line that can perform CSR to IgA *in vitro*. As explained in section 1.3.5. RIF1-mediated DSB end protection leads to genome instability in some contexts but is also critical for antibody diversification through CSR that leads to the production of antibodies expressed on the surface of the B cell; quantification of which is a functional readout for DSB end protection during G1 phase of the cell cycle.

Hence CH12 is a unique model system to perform proliferation-based high throughput screens, and also provides a functional readout for several functions of RIF1 which made it a powerful model system for my study.

In order to generate and screen for potential BRCA1-deficient CH12, I set up a functional loss-of-viability assay where BRCA1-deficient clones upon treatment with PARPi show a substantial reduction in viability. Commercially available PARPi Olaparib was used which targeted PARP1/2 from the PARP family of proteins. As explained in section 1.3.4., PARP family of proteins whose main member is PARP1 is critical for SSB repair. PARP1 produces several branched PAR structures in a mechanism called PARYlation that helps recruit downstream factors involved in SSB repair. Once the repair of the break is completed, it is critical that PARP1 be removed from DNA so that protein-DNA adducts are not formed. Inhibiting PARP1 by PARPi reduces its enzymatic activity and prevents it from dissociating from DNA thereby trapping it. The increasing amounts of DNA-PARP1 complex is a source of chronic replication stress which eventually leads to fork collapse producing DSBs. DSBs in healthy S-phase cells are repaired by HR. However, in BRCA1-deficient cells are repaired by competing NHEJ pathway that causes toxic genomic rearrangements leading to cell death of specifically the BRCA1-deficient cells. I wanted to exploit this selective killing as a strategy to functionally identify BRCA1-deficient clones in a high-throughput format.

In order to create BRCA1-deficient CH12, CRISPR-Cas9 genome editing system with nickase Cas9 ($Cas9^{D10A}$) was employed in place of wildtype Cas9 to reduce the risk of off-target effects. The gRNAs pairs were specifically designed against exon 11 of the murine *Brca1* gene, which encodes for approximately 60% of the protein (Fig. 7a). Mouse models with targeted deletion of exon 11 ($Brca1^{\Delta 11/\Delta 11}$) express a truncated protein that can no longer support BRCA1 role(s) in DSB repair, thus resulting in increased genomic instability in the form of translocations, deletions and chromosome breaks in these mouse models and cell lines generated from them[143].

Two different nickase gRNA pairs against *Brca1* exon 11 were transfected into CH12 *via* electroporation of a single-plasmid system expressing also Cas9-T2A-GFP. GFP^{+} single cells were sorted 40 hours later into 96-well plates and let grow for 12 days. Individual clones were then analyzed in a high-throughput (HTS) format via a loss-of-viability screen following treatment with PARPi (Fig. 7b).

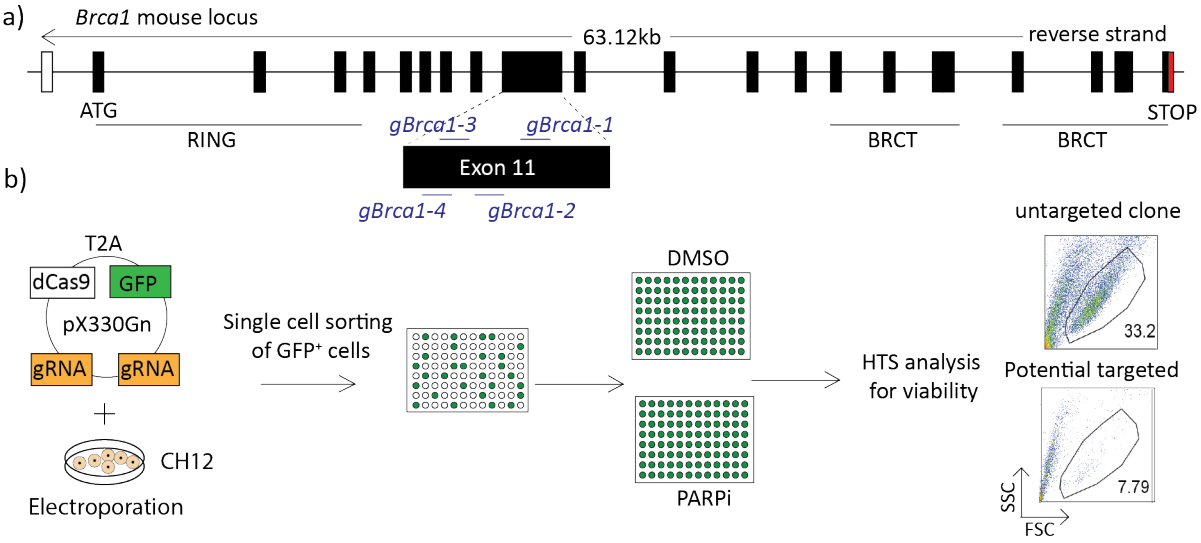

Figure 7. Somatic targeting of the *Brca1* gene in CH12 cells using CRISPR-Cas9 genome editing. a) Scheme of mouse *Brca1* genomic locus and location of gRNAs used in this study. b) Following electroporation of pX330Gn plasmid that encodes the gRNAs into CH12, GFP⁺ cells are single-cell sorted, allowed to recover and split into replica plates treated with either DMSO or 1µM PARPi for 72 hours and the viability was analysed using flow cytometry. HTS: High Throughput Screening.

Targeting of *Brca1* by both pairs of nickases led to a significant decrease in viability (Fig. 8a). I selected six derivatives per nickase gRNA pair for further expansion and large-scale repeat of the assay. All the selected clones exhibited more than 2-fold decrease in viability following treatment with PARPi in comparison to the control clones (Fig. 8b) (control clones were generated by targeting CH12 cells with gRNAs against sequences not present in the mouse genome), which confirmed the initial selection based on our HTS analysis.

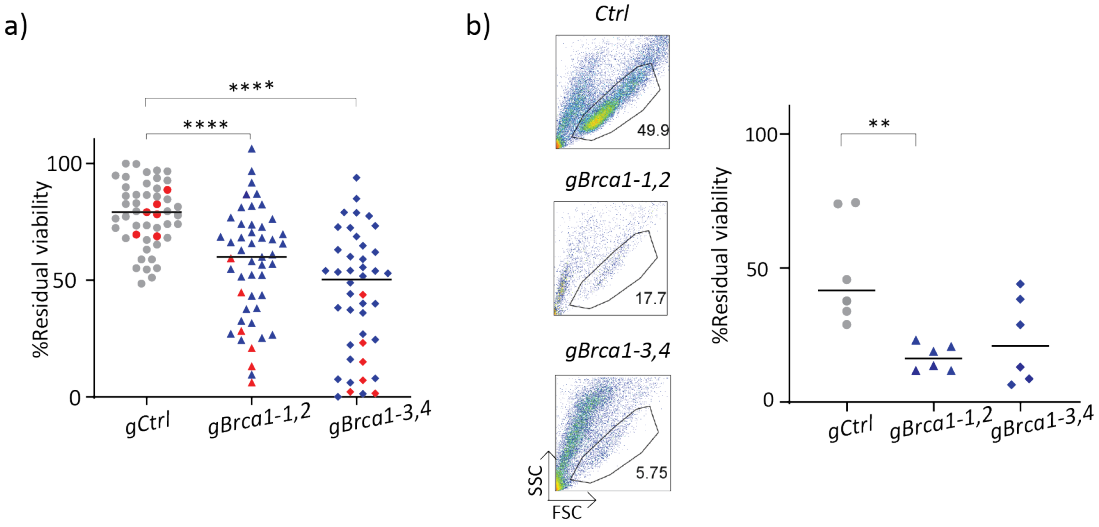

Figure 8. Screening for functionally null *Brca1*$^{-/-}$ clones. a) Graph showing distribution of residual viability of all clones obtained after treatment with PARPi for 72h. Each data point represents a single clone. The indicated clones in red were selected for large scale characterization. b) (Left) representative FACS plots showing percentage of live cells following PARPi treatment (right) summary dot plot indicating residual viability of the potential *Brca1*$^{-/-}$ CH12 clonal derivatives selected from (a). (a) and (b) line indicates median and statistics were plotted using Mann Whitney U test. ** p<0.01, ****p<0.0001

To confirm efficient targeting in both *Brca1* alleles, I analysed the nature of insertions/deletions (from now on referred to as genetic scars) induced by CRIPSR-Cas9 genome editing. For this, I amplified the targeted region of exon 11 in 3 selected clones from each nickase pair. All clones contained either a homozygous or a heterozygous genomic scar except for 1 that revealed three genomic scars indicating a possible amplification of chromosomes during CRISPR-Cas9 targeting (Fig. 9a). The genetic scars of all clones revealed putatively in-frame internal deletions of codons, thus indicating they are all likely express hypomorph mutant BRCA1 proteins (Fig. 9b). Because of the poor performance of commercially available antibodies against murine BRCA1, we could not confirm the expression of truncated mutants. However, our results are in line with previous research showing that conventional knockout of *Brca1* is lethal[74].

a)

Clone 1

Nickase 1

Brca1-2 *Brca1- 1*

WT GAGCTACCACCGATGTTCCTTGGATAACACTAAATAGCAGCGTTCAGAAAGTTAATGAGTGGTTTTCCAGAACTGGTGAAATG

Scar GAGCTACCA----------GAAATG

66bp deletion → 22aa deletion → Internal deletion

Clone	Scar 1	Scar 2	Scar 3
2	41bp deletion leads to PTC	43bp deletion leads to PTC	84bp deletion leads to 28aa deletion
3	4bp deletion leads to PTC	36bp deletion leads to 12aa deletion	not applicable

b)

Clone 1

Nickase 2

Brca1-3 *Brca1- 4*

WT TAGAGAGAAGTGGACTCACCCGCAAAGTCTGTGCCCTGAGAATTCTGGAGCTACCACCGATGTTCCTTGGATAACACTAAATAG

Scar TAGAG----------TAAATAG

72bp deletion → 24aa deletion → Internal deletion

Clone	Scar 1	Scar 2
2	9bp deletion leads to 3aa deletion	19bp deletion leads to PTC
3	30bp deletion leads to 6aa deletion	not applicable

Figure 9. Genetic scar analysis of 6 *Brca1*-functionally null CH12 reveals hypomorphic mutation. a) Representative genetic scar analysis of clone 1 targeted by *Brca1-1,2*. Tabular column below describes the genomic scar in 2 other clones targeted with same nickase pair. b) Representative genetic scar analysis of clone 1 targeted by *Brca1-3,4*. Tabular column below describes the genomic scar in 2 other clones targeted with same nickase pair. a) and b) sequence marked in red refers to indicated gRNA and sequence marked in green indicates the PAM. Bp is base pairs, aa is amino acids and PTC is Premature Termination Codon.

To enquire if the viability of *Brca1*-mutated (*Brca1*^{mut}) cells decreased due to accumulation of genomic instability, I set up and performed chromosomal aberration analysis on metaphase spreads following PARPi treatment for 24 hours (Fig. 10a). Since accumulation of genome instability precedes cell death, I collected samples at an earlier time point of 24 hours. This assay allowed to robustly quantify chromatid breaks and radials that are hallmarks of HR deficiency following PARPi. Radials are formed due to toxic NHEJ reactions of distal DSBs which are otherwise inhibited when BRCA1 is available. All clones showed negligible amount of aberrations following control DMSO treatment. However upon PARPi treatment, they accumulated high levels of chromosomal aberrations, both chromatid breaks and radials (Fig. 10b). Clone 2 targeted by *gBrca1-1,2* showed the highest accumulation of damage, however this was due to chromosomal amplification from 38-40 chromosomes in wild type CH12 to 58-60 chromosomes in this clone (Fig 10a). I selected clone 1 targeted by *Brca1-3,4* which had diploid chromosomes, a homozygous deletion in *Brca1* exon 11 that led to a putative in-frame internal deletion and displayed an increase in chromatid breaks and radials resulting in loss of viability following PARPi treatment (Fig 8b, 9b, 10b). I concluded that the *Brca1*^{mut} CH12 cell lines that I generated bear deletions of the *Brca1* gene and exhibit the typical phenotype of HR-deficiency, namely increased levels of genome instability and lethality following PARPi treatment.

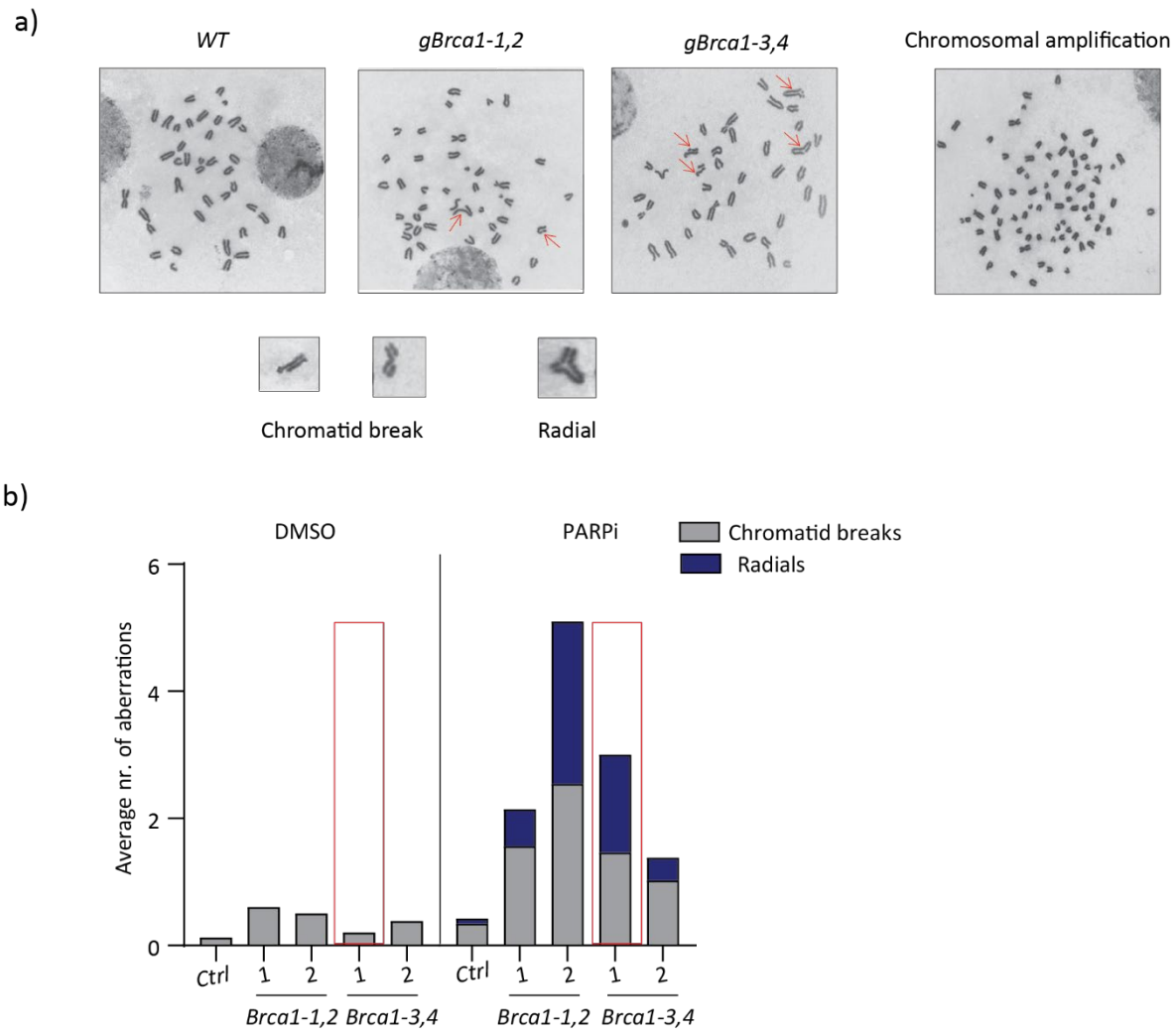

Figure 10. Chromosomal aberration analysis of selected *Brca1*^{mut} clones. (a) (Top) representative metaphase spreads of the indicated genotype following PARPi treatment for 24h. Red arrows indicate radials and chromatid breaks. (Bottom) representative images of chromatid breaks and radial. (b) Summary bar graph indicating average number of chromatid breaks and radials from the indicated genotype. 100 metaphases were analysed per genotype. Ctrl refers to wild type CH12 and red box indicates the clone selected for further analysis.

4.1.2. Deletion of RIF1 in BRCA1-mutated CH12 cell lines recapitulates the PARPi resistance phenotype

Deletion of RIF1 in the BRCA1-deficient background rescues HR defect upon treatment with PARPi in a resection independent pathway. This reduces aberrant repair of replication-associated DSB and promotes

cell survival[46,73,77]. To verify if this can be recapitulated in the newly generated *Brca1*^{mut} CH12 cell lines, I generated *Brca1*^{mut} *Rif1*$^{-/-}$ clonal derivatives through CRISPR-Cas9 genome editing using Cas9^{D10A} nickase. I used gRNAs targeting exon 2 of murine *Rif1* since it is very close to the start codon and targeting this exon abolished protein levels of RIF1 in other studies [131](Fig. 11a).

The same workflow for generation of clones was used as *Brca1*^{mut} (Fig. 7). However, I used the gain-of-viability assay as the functional readout since RIF1 deficient clones rescue the viability of *Brca1*^{mut} following PARPi treatment. Following single cell sorting of GFP^{+} cells, I observed a significant increase in the survival of *Brca1*^{mut}*Rif1*$^{-/-}$ clones after treatment with PARPi in both high throughput setting (Fig. 11b) and also in the 6 selected clones in a large scale confirmation (Fig. 11c).

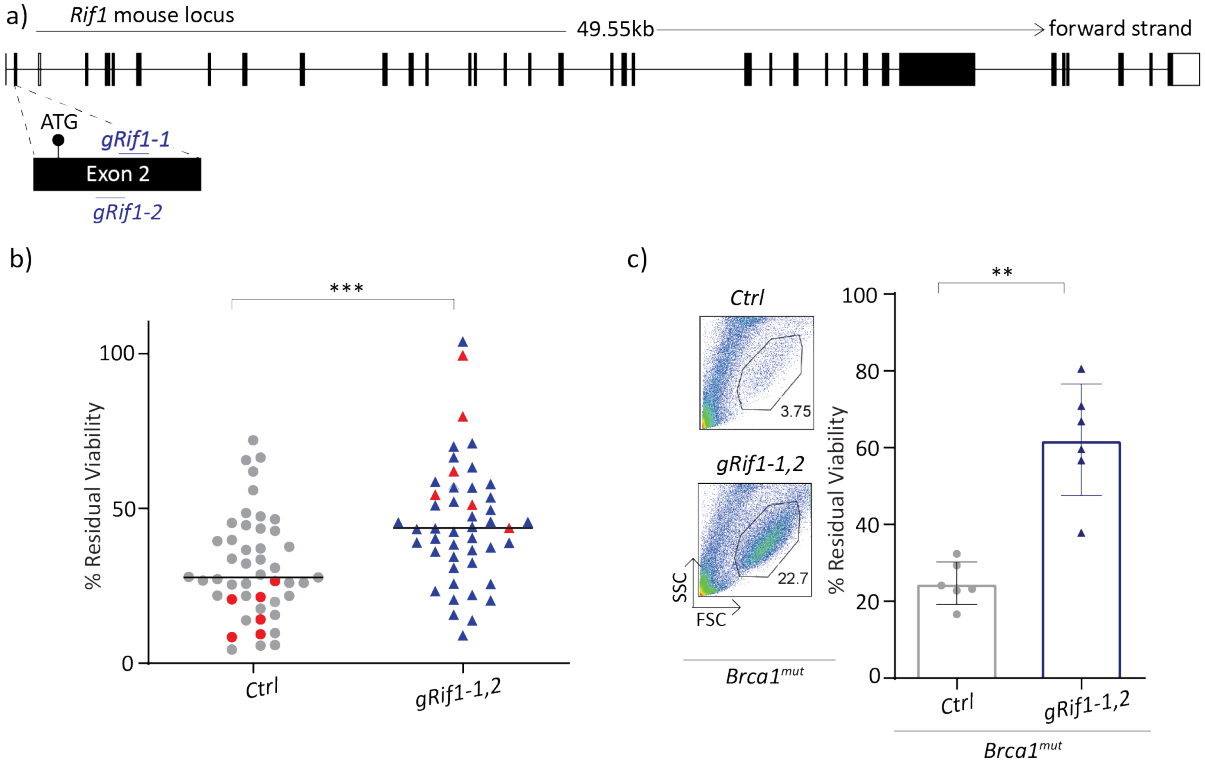

Figure 11. Generation of *Brca1*^{mut}*Rif1*$^{-/-}$ CH12. (a) Scheme showing murine *Rif1* genomic locus and the location of targeting gRNAs. (b) Graph showing distribution of percentage residual viability of all the clones following single cell sorting and treatment with 1µM PARPi for 72h. Each data point represents a single clone. Clones marked in red were considered for large scale expansion. (c) (Left) representative FACS plots showing percentage of live cells of indicated genotypes following PARPi treatment for 72h (right) bar graph showing percentage residual viability values. (b) line represents median and statistics were plotted

using Mann-Whitney U test. *** p<0.001 (c) Error bar represents mean with SD and statistics were plotted using Mann-Whitney U test. **p<0.01.

Western blotting analysis of the 6 selected clones revealed 2 that showed no RIF1 expression (Fig 12a). On sequencing the targeted region of *Rif1*, 1 of them contained homozygous in-frame deletions that led to PTC. The second clone had a single nucleotide insertion and deletion of nucleotides that also led to an in-frame PTC in both alleles (Fig. 12b). This indicated that no protein expression is presumably through nonsense mediated decay.

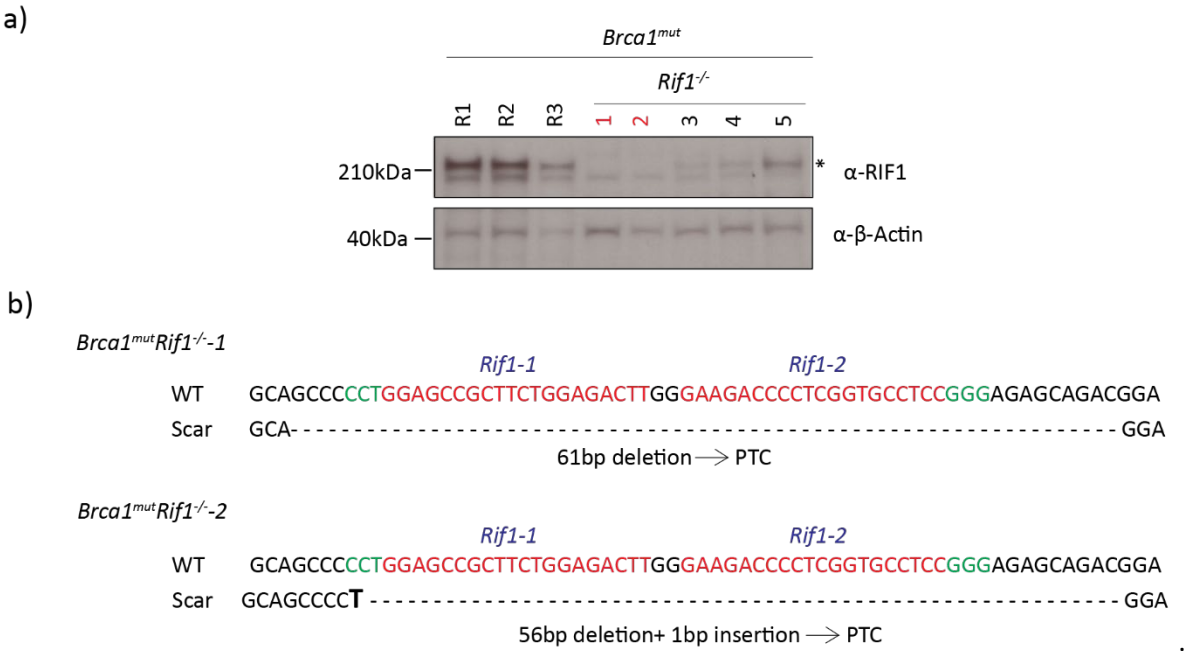

Figure 12. Western blot and Sanger sequencing confirms RIF1 deletion in *Brca1^{mut}* CH12. a) Western blot from whole cell extracts from the indicated genotype. * indicates RIF1 band. Samples marked in red do not show RIF1 protein. *Brca1^{mut}Rif1$^{-/-}$*R1-R3 are *Brca1^{mut}* targeted with random gRNA that does not target anywhere in the mouse genome. b) Genomic scar of the samples marked in red in a). Sequence marked in red are gRNA *Rif1-1,2* and green indicates the PAM. PTC-Premature Termination Codon.

Next, I assessed whether the viability rescue following RIF1 ablation was caused by restoration of HR defect which would lead to less accumulation of genomic instability. Therefore, I performed chromosomal aberration analysis on the selected *Brca1^{mut}Rif1$^{-/-}$* clonal lines, and found that chromatid breaks and radials were dramatically reduced in both cases as in agreement with previous research[46] (Fig. 13). I concluded that RIF1 deletion in BRCA1-deficient CH12 cells confers resistance to PARPi treatment, and validated the use of *Brca1^{mut}* CH12 cell lines for our screen.

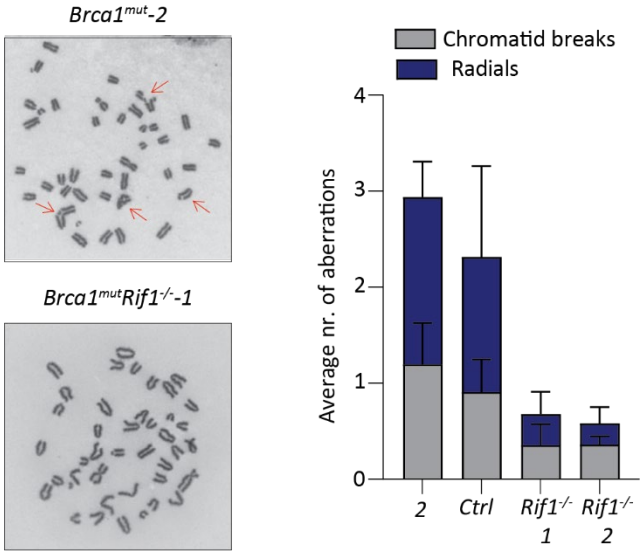

Figure 13. Chromosomal aberration analysis in *Brca1^{mut}Rif1$^{-/-}$* CH12 cell lines. Representative metaphase spreads of the indicated genotypes following 1µM PARPi treatment for 24h. Red arrows indicate chromatid breaks and radials. 100 metaphase were quantified. (Right) Bar graph quantifies average number of aberrations in the indicated genotype. Line indicates mean with SD. Ctrl refers to a *Brca1^{mut}* cell line targeted with random gRNA that does not target anywhere in the mouse genome.

4.1.3. A gain-of-viability screen for the identification of components of RIF1 end protection machinery

In order to define the pool of candidates to be tested in our screen, I took advantage of a proteomic approach we recently performed in our laboratory to define RIF1 interacting proteins in irradiated, highly proliferative B lymphocytes[144]. Briefly, a SILAC-based mass spectrometric analysis was performed on RIF1-immuno-precipitates from splenocytes isolated from mice expressing endogenous RIF1 tagged with 1x Flag and 2X HA. The heavy (H) and light (L) medium treated cells were mixed at 1:1 ratio, cryolysed to extract the proteins and a FLAG based immunoisolation was performed to identify effectors potentially interacting with RIF1. A high SILAC ratio H/(H+L) indicates a specific interactor since splenocytes from *Rif1$^{FH/FH}$* mouse were grown in heavy media (Fig. 14). Peptides from several proteins were identified with

the *bona fide* RIF1 interactor 53BP1 identified with very high SILAC ratio which increased our confidence in this list (Fig. 14).

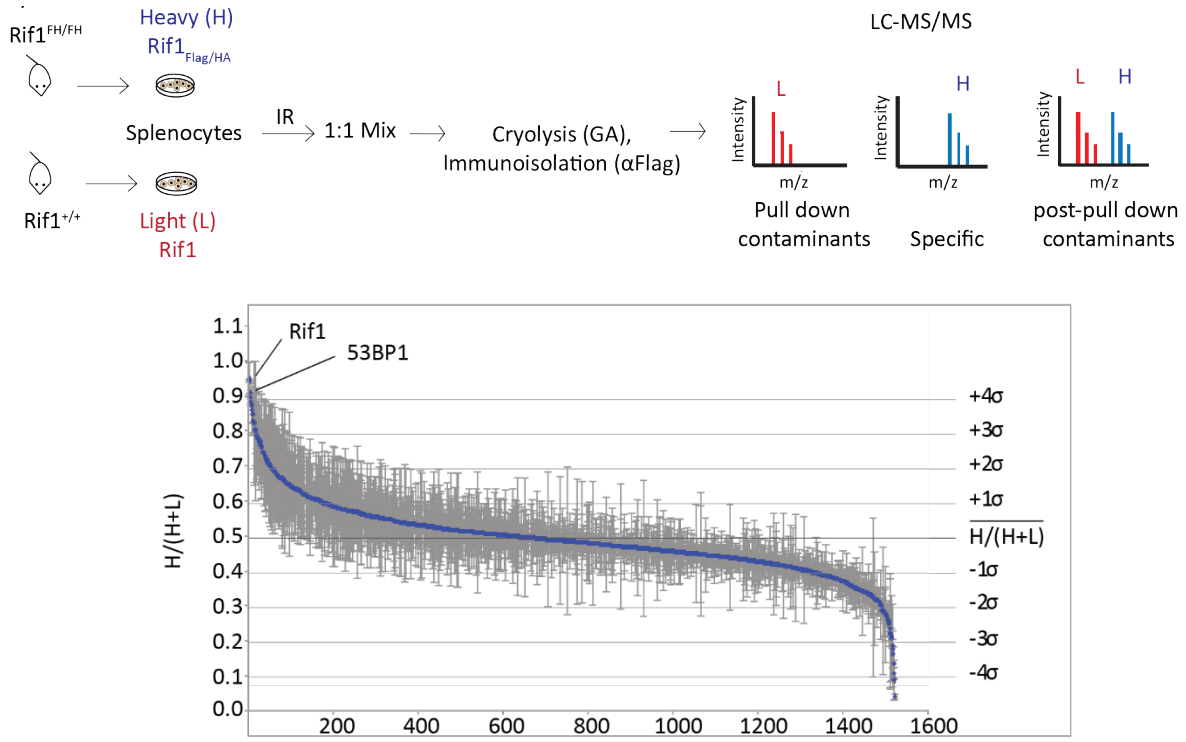

Figure 14. Identification of RIF1 interactors by I-DIRT. (Top) Workflow of I-DIRT. Splenocytes from Wild type and *Rif1*$^{FH/FH}$ mice were treated with Heavy (H) and Light(L) media respectively. They were irradiated and mixed in a 1:1 ratio, after which proteins were extracted and a FLAG-based immunoprecipitation was carried out to identify specific interactors of RIF1. (bottom) Graph shows distribution of SILAC ratio (H/H(H+L)) of all the candidates identified in I-DIRT.

To functionally identify the RIF1 effectors in end protection, I optimized the gain-of-viability assay in *Brca1*^{mut} CH12. Candidates whose ablation rescues the survival defect would represent putative RIF1 effectors in DNA end protection and DSB repair pathway choice. CRISPR-Cas9 genome editing was used to efficiently target each individual candidate in bulk *Brca1*^{mut} CH12 cultures. 3 guide RNAs against each candidate were individually cloned into a GFP containing mammalian expression vector with wild type Cas9. After electroporation in *Brca1*^{mut} CH12 cells, GFP^{+} cells were sorted and allowed to recover for 72 hours to allow sufficient reduction in protein expression and then treated with DMSO and PARPi and the viability was assessed by flow cytometry (Fig. 15).

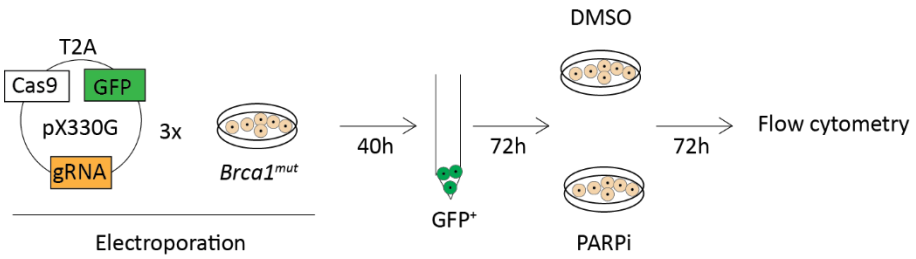

Figure 15. Scheme of gain-of-viability of assay to functionally identify RIF1 effectors in end protection. 3 plasmids expressing individual gRNAs against the selected candidate was electroporated into *Brca1*^{mut} CH12 and sorted for GFP^{+} cells 40 hours later and allowed to recover for 72 hours. The cells were seeded in replica plates and treated either with DMSO or 1µM PARPi for 72 hours and the viability was assessed by flow cytometry.

As a first step and proof of principle, I tested control samples electroporated with gRNAs against RIF1, its *bona fide* interactor 53BP1 and downstream effector REV7. 53BP1, RIF1 and REV7 are key components of the DSB end protection pathway with REV7 recruited by RIF1 in a yet unidentified mechanism[46,75,145] (Fig. 16). Deletion of any of these factors in a BRCA1-deficient background rescues the HR defect and increases viability upon treatment with PARPi[46,73,146].

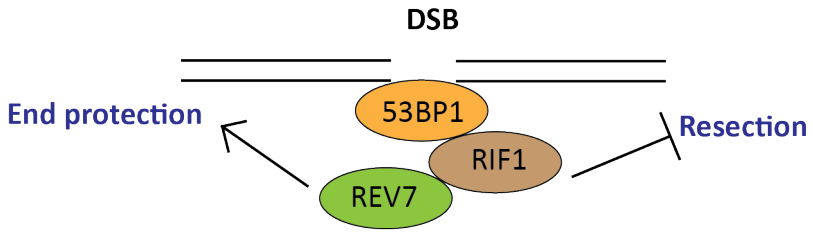

Figure 16. Simplified representation of DSB end protection mediated by 53BP1-RIF1-REV7 axis. 53BP1 is recruited to the DSB following which it recruits RIF1 in a phosphorylation dependent manner. RIF1 recruits further downstream effector REV7 through a yet unidentified mechanism. These 3 factors promote end protection and inhibit resection of DSB.

Cas9-mediated targeting of all 3 factors led to a significant rescue of viability, which validated our in-bulk screening strategy in *Brca1*^{mut} CH12 (Fig. 17). Using 3 positive controls as opposed to one increased the robustness of this assay. In agreement with literature, the survival levels 53BP1>RIF1>MAD2L2 confirmed their epistatic relationship[146]. With this I concluded that the functional rescue-of-viability assay can be used to rapidly screen for RIF1 effectors involved in DSB pathway choice.

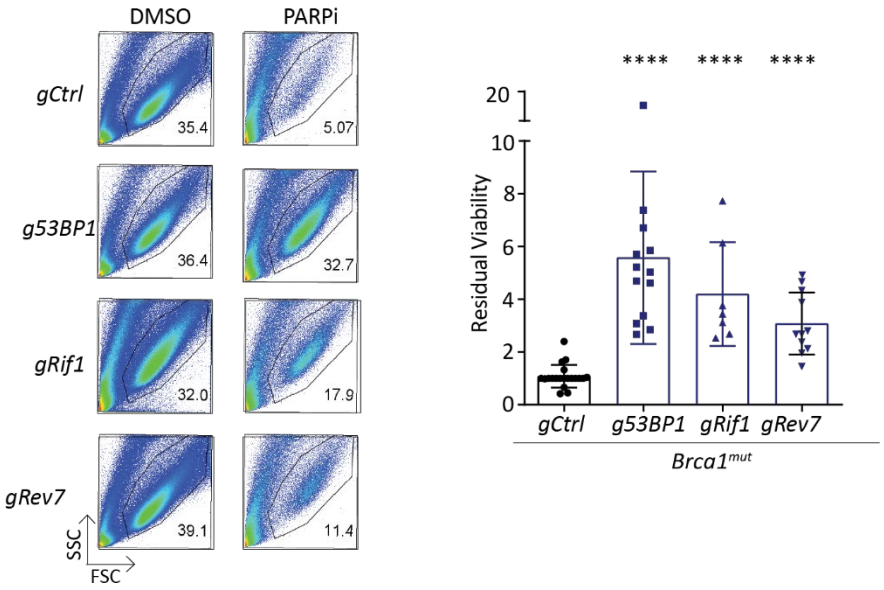

Figure 17. Deletion of 53BP1, RIF1 and REV7 in bulk cultures rescues viability of *Brca1^{mut}* CH12. (left) representative FACS plots showing percentage live cells of the indicated genotype following DMSO or 1µM PARPi for 72h. (Right) Bar graph indicating fold change increase in residual viability in the indicated genotypes. Graph is representative of at least 8 experiments. Error bars indicate SD. *p<0.05, ***p<0.001, ****p<0.0001.

Out of the many hits identified in the I-DIRT screen, I selected 40 candidates using the following criteria: 1) H/(H+L) ratio higher than 2 standard deviations above the mean for the distribution; 2) peptide count >= 2; and 3) Posterior Error Probability (PEP) ≤1x10-4. I ablated the selected candidates in *Brca1^{mut}* CH12 using the workflow described before (Fig. 15). Although most candidates upon deletion behaved similar to the *Brca1^{mut}* CH12, the initial screen revealed that deletion of ZRANB2 which was identified with a SILAC ratio of 0.8 showed an approximately 2-fold increase in survival when targeted with a pool of gRNAs (Fig. 18).

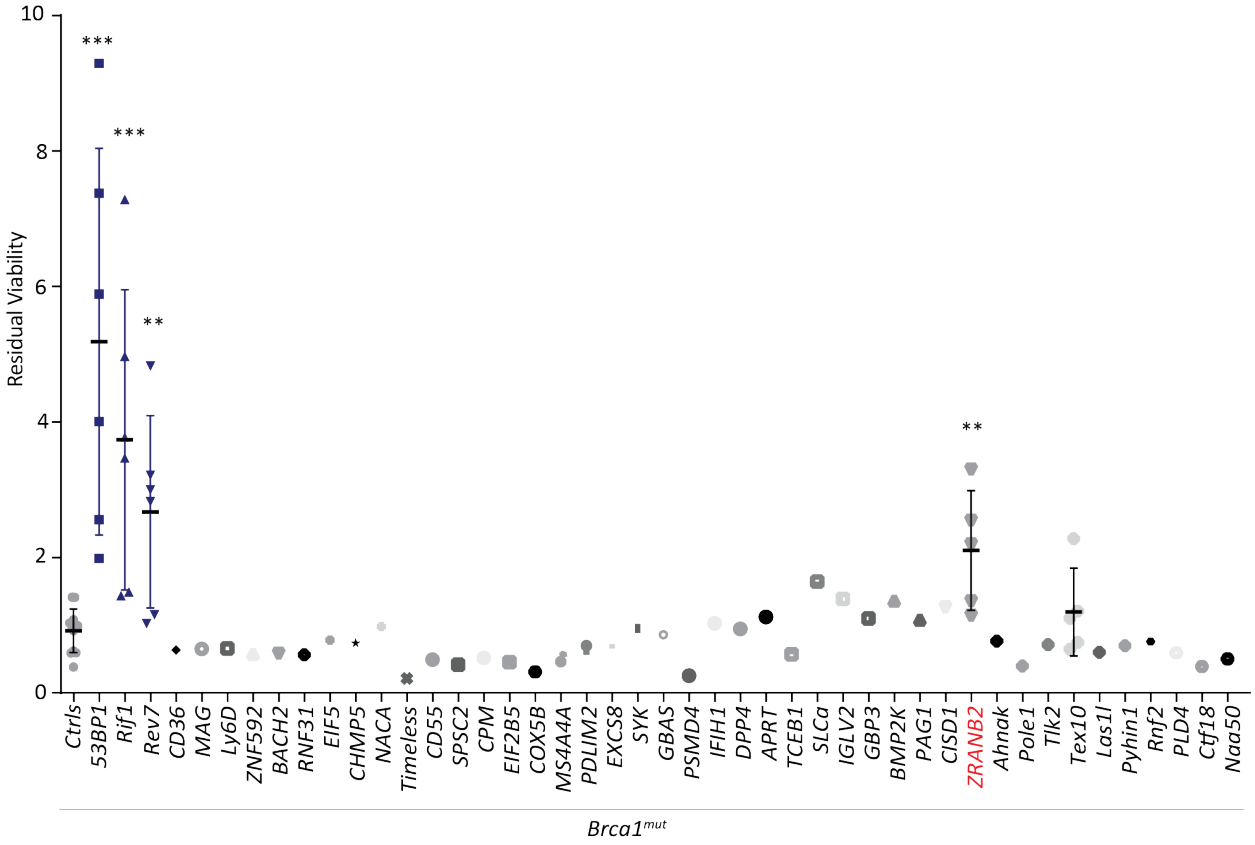

Figure 18. Summary of rescue-of-viability screen of the selected RIF1 effectors identified by I-DIRT. Graph shows fold change in residual viability after targeting the indicated genes in bulk cultures of *Brca1*^{mut} CH12. *Ctrls* refer to *Brca1*^{mut} CH12 targeted with random gRNAs that do not target anywhere in the mouse genome. Samples marked in blue indicate the positive controls and ZRANB2 is indicated in red. Error bars indicate SD and statistics was calculated using Mann-Whitney U-test. **p<0.01, ***p<0.001.

4.1.4 Deletion of ZRANB2 in *Brca1*^{mut} CH12 cell lines modestly rescues the lethality phenotype

ZRANB2 (Zinc finger Ran-Binding domain-containing protein 2) is a ubiquitous RNA-Binding protein involved in alternative splicing of pre-mRNA transcripts[86]. Few of its targets have been identified however none so far in DSB repair. A genome wide siRNA screen revealed deletion of ZRANB2 resulted in enrichment of γH2AX signal in human cells, however nothing further was discovered[147].

The rescue of viability following ZRANB2 deletion in bulk CH12 cells was not as dramatic as for RIF1/REV7. To assess whether the limited rescue reflected technical aspects of the screen strategy (i.e. low percentage of ZRANB2 targeting in the cell culture) or an actual modest effect of ZRANB2 in DSB pathway choice, I targeted exon 1 of the *Zranb2* gene in *Brca1*^{mut} CH12 cells by CRISPR-Cas9 system and generated

clonal derivatives (*Brca1*^{mut} *Zranb2*$^{-/-}$) (Fig. 19a). I selected 3 clones that showed no protein expression by western blotting analysis, and had frameshift mutations leading to premature termination codon (PTC) in both alleles (Fig. 19b,c).

a)

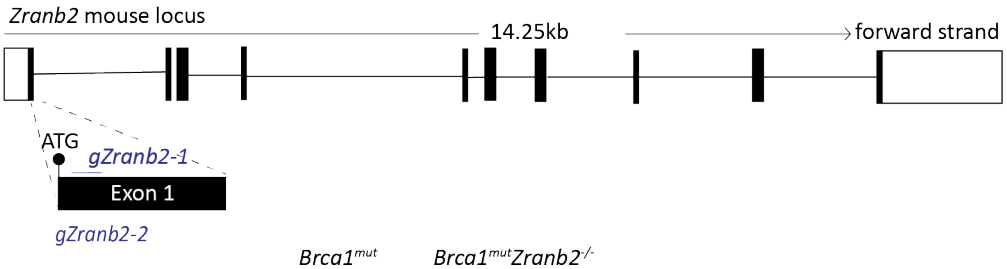

b)

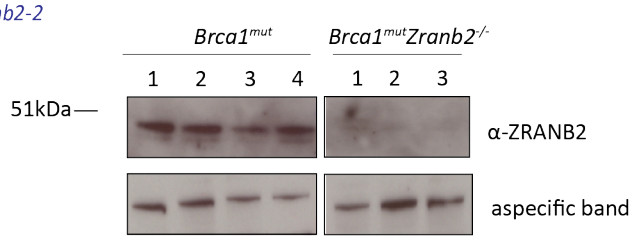

c)

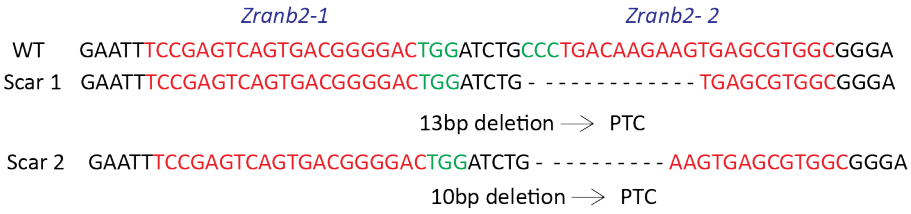

Clone	Scar 1	Scar 2
2	4bp deletion leads to PTC	2bp deletion leads to PTC
3	196bp deletion leads to PTC	31bp deletion leads to PTC

Figure 19. Generation and characterization of *Brca1*^{mut} *Zranb2*$^{-/-}$ CH12. a) Scheme showing murine *Zranb2* genomic locus and the location of gRNAs used. b) Western blot analysis from whole cell extracts probed with anti-ZRANB2 antibody. c) Genomic scar of the samples from a). Sequence marked in red are gRNA *Zrnab2-1,2* and green indicates the PAM. PTC-Premature Termination Codon.

To determine if complete abrogation of ZRANB2 led to a further increase in viability, I treated *Brca1*^{mut} *Zranb2*$^{-/-}$ with PARPi for 72 hours. Survival was increased by two-fold more than *Brca1*^{mut} CH12. With this result I concluded that ZRANB2$^{-/-}$ only modestly rescues viability in *Brca1*^{mut} cells following PARPi treatment (Fig. 20).

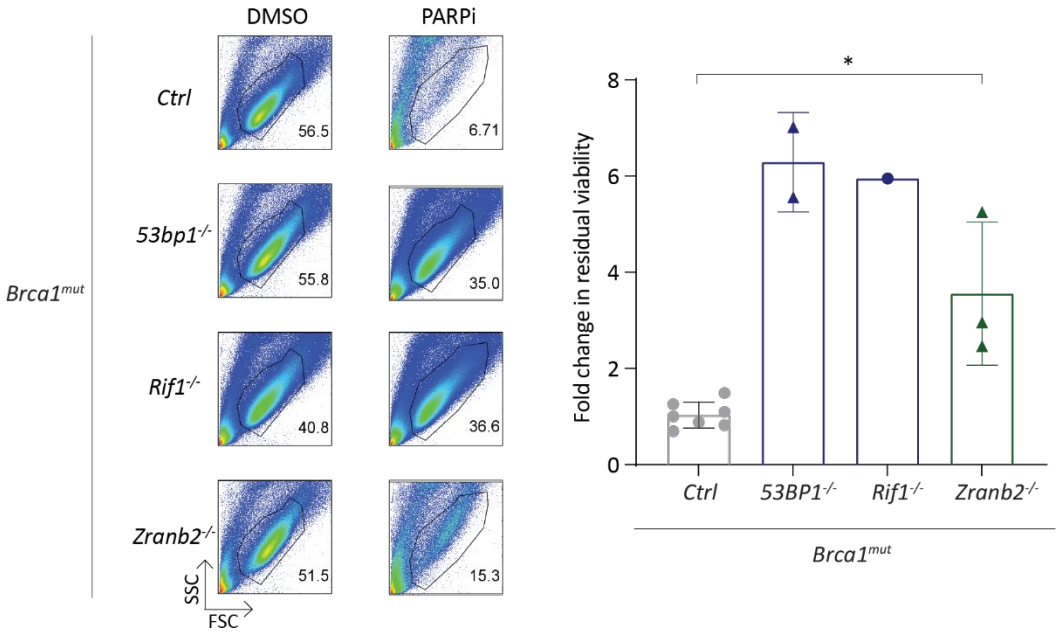

Figure 20. *Brca1*^{mut} *Zranb2*$^{-/-}$ modestly rescues viability following PARPi treatment. (Left) representative FACS plots showing percentage live cells of the indicated genotype following DMSO or 1μM PARPi for 72h. (Right) summary bar graph indicating fold change increase in residual viability of the indicated genotype following PARPi treatment. Error bars indicate SD and statistics was calculated using Mann-Whitney U-test. *p<0.05.

RIF1 and 53BP1 function exclusively in the early step of DSB repair by protecting the ends from resection. Due to their critical roles in promoting genome instability in BRCA1-defciient cells, deletion of 53BP1/RIF1 consistently leads to 4-5 fold rescue of viability in BRCA1-deficient cells in both bulk gene editing approaches and clonal derivative model systems. However, factors playing a dual role in DSB repair, at the level of DNA end protection as well as in later stages of HR would theoretically lead to only a modest rescue of viability upon deletion in BRCA1-deficient cells since the HR pathway would still be defective (Fig. 21a). For example, tumor suppressor BRCA2 is required for strand invasion of the sister chromatid to mediate efficient repair of replication-associated DSB by HR (Fig 3). Due to this function, BRCA2-deficient tumors are extremely sensitive to PARPi since DSBs in S phase are still repaired by toxic NHEJ reactions[77]. Since BRCA2 functions exclusively in late-stage HR and has no known functions in DSB end protection, deletion of 53BP1/RIF1 does not mediate PARPi resistance in BRCA2-deficient tumors. However, due to critical functions in late-stage HR, BRCA2 is still sensitive to PARPi. Similarly, it is possible that the modest levels of viability rescue in *Brca1*^{mut} *Zranb2*$^{-/-}$ are due to additional functions of ZRANB2 in HR.

To test this hypothesis, I generated *Zranb2*$^{-/-}$ clonal derivatives in a wild type CH12 background, and assessed viability following PARPi treatment, which is a well-established read-out for HR proficiency. Defects in survival would indicate a potential role of ZRANB2 in late-stage HR. I selected 3 *Zranb2*$^{-/-}$ clones that showed no protein expression upon western blotting (Fig. 21b). The viability of all *Zranb2*$^{-/-}$ clones following PARPi treatment was indistinguishable from wild-type clones (Fig. 21c). Therefore, I concluded that ZRANB2 does not play a role in late stage HR.

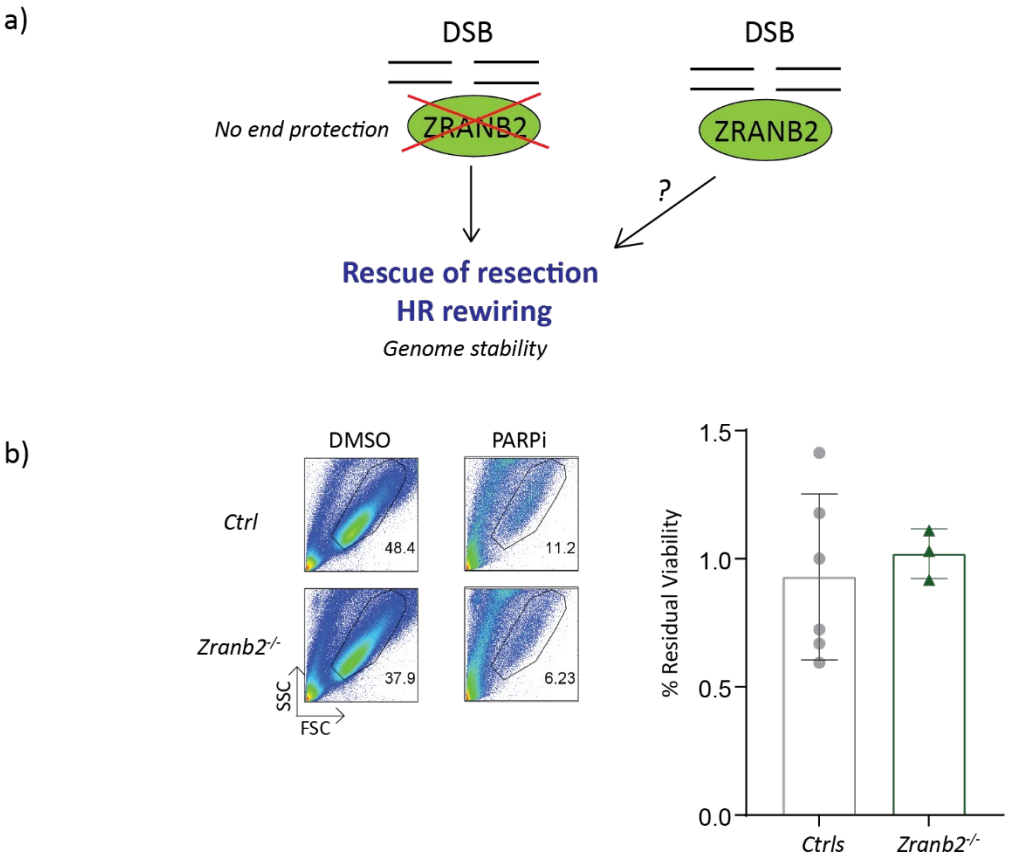

Figure 21. *Zranb2*$^{-/-}$ have a proficient HR pathway following PARPi treatment a) Schematic showing the possible scenarios of ZRANB2 role in the DSB repair. b) Western blot showing ZRANB2 levels from whole cell extracts. Red indicates the clones without ZRANB2. c) (Top) representative FACS plots of showing live cells of the indicated genotype following PARPi treatment for 72 hours (bottom) summary bar graph indicating fold change in viability of the indicated genotype. Error bars represents SD.

Altogether, our data indicates that ZRANB2 ablation only modestly rescues the lethality phenotype of BRCA1-deficient cells, which suggests that its potential contribution to the regulation of DNA end protection is marginal. Furthermore, the very limited dynamic range would also pose considerable

technical challenges to an in-depth investigation. For this reason, and because of exciting positive results obtained in the parallel project (Part II), I decided to not pursue this line of investigation further.

4.2. Phosphorylation of a conserved SQ cluster in RIF1 is dispensable for DSB end protection but required for nascent fork protection during replication stress

Phosphorylation is the key PTM mediating the two main effector functions in DDR, which are DNA damage repair and cell cycle arrest. ATM and ATR kinase are recruited following DSB induction and replication stress respectively, phosphorylate several key substrates involved in repair, replication fork stabilization and cell cycle arrest[33]. As explained in section 1.3.3. and 1.5.2., 53BP1 is one such protein that is phosphorylated in several sites by ATM to mediate DNA DSB end protection. Phosphorylated 53BP1 recruits several key downstream effectors including RIF1 to protect DNA ends thereby promoting NHEJ[72]. Rewiring pathway choice by depleting RIF1 in BRCA1-deficient cells renders them resistant to PARPi.

As explained in section 1.4.3, RIF1 also mediates replication fork stabilization by preventing newly replicated DNA from degradation by nucleases. This function is critical to promote fork restart and avoid the accumulation of under replicated DNA which is a source of genomic instability[42,121]. RIF1-deficient MEFs also survived less upon treatment with replication stress inducing reagents HU and aphidicolin (APH). A crucial point to note here is that RIF1 functions at the replication fork are independent of its roles in DSB repair.

Mammalian RIF1 has several SQ/TQ sites that are ATM/ATR consensus motifs. It is still undiscovered how phosphorylation regulates RIF1 function to maintain genome stability. Therefore, I set to investigate if phosphorylation of RIF1 in the ATM/ATR consensus motifs mediates its functions in DNA DSB end protection and nascent replication fork protection.

4.2.1. Three conserved SQ sites in mouse RIF1 are phosphorylated in primary cultures of B lymphocytes

In order to understand this, I once again interrogated the I-DIRT dataset (Fig. 14) for phosphopetides of RIF1. The I-DIRT was performed in primary B lymphocytes that were irradiated to induce DSB formation. Additionally, B lymphocytes are one of the fastest proliferating cells in the body. This makes the dataset a powerful resource not only to identify events in DSB repair pathway choice but also in replication (Fig. 22a). Immunoprecipitation of RIF1 allowed for its high coverage making this dataset identify both RIF1 phosphopeptides and its effectors (Fig 22b).

a)

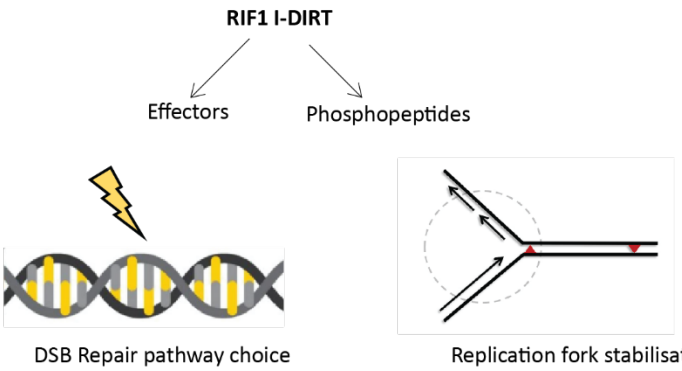

b)

Figure 22. I-DIRT identifies effectors and phoshphopetides of RIF1. a) I-DIRT identifies effectors and phosphopetides of RIF1 which can mediate RIF1 function in DSB repair pathway choice and replication fork stabilization. b) Scheme representing MS analysis coverage relative to RIF1 isoform 2 (XP_011237438.1). Max Quant analysis performed by W. Zhang (Chait Lab, Rockefeller University, NY).

Analysis of bait phospho-peptides revealed that several residues in RIF1 were modified by phosphorylation in irradiated culture of highly proliferating B cells. Several identified residues were consensus sequences for CDK kinases which are involved in cell cycle control while a cluster of three SQ/TQ motifs (S1387, S1416 and S1528), were identified which are consensus motifs for ATM/ATR kinases (Fig. 23).

Identified consensus residues	Phoshphorylating kinase
S376, S387, S391, T1205, S1231,S1233, S1439, S1457, S1683, S1828,S1868,S2297	CDK
S1387, S1416, S1528	ATM/ATR

Figure 23. RIF1 I-DIRT identifies phosphorylated residues that are consensus motifs for CDK and ATM/ATR kinases. Table depicting the 12 S/T-P sites that are consensus motifs for CDK kinase and 3 SQ sites that are consensus motifs for ATM/ATR kinase.

Murine RIF1 contains 17 S/T-Q sites spread throughout the length of the protein, with 3 clusters in the intrinsically disordered region. The sites S1387, S1416 and S1528 belonging to cluster II (SQ-CII) were identified as phosphorylated with high confidence in the RIF1 I-DIRT (Fig. 24a) and are present in a region with high probability of disorder (Fig. 24b). Phosphorylation in disordered regions of proteins is often associated with predicted or observed binding sites for partners[148]. Furthermore, the sites are highly conserved among eukaryotes (Fig 24c). Finally, the human ortholog of S1528 was found to be phosphorylated following IR by Matsouka. *et al*[139]. All of these considerations raised the interesting possibility that phosphorylation at these sites might regulate RIF1 function in DSB repair.

a)

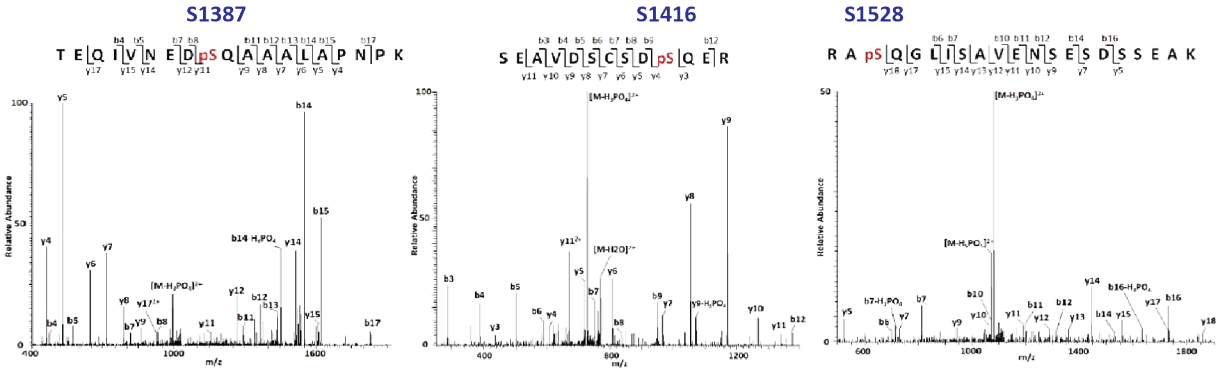

b)

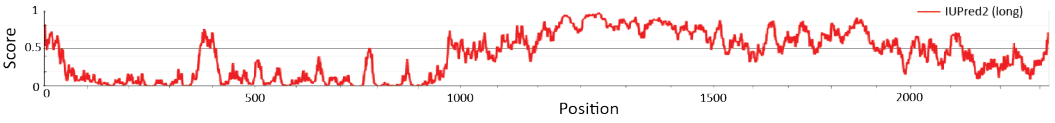

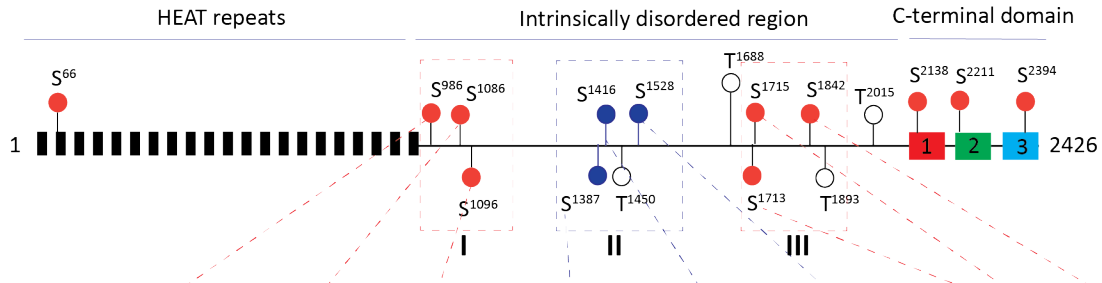

c)

Mouse	TEN**SQ**LNV	LDA**SQ**DTL	QF**SQ**EES	NED**SQ**AAA	CSD**SQ**ERES	RRA**SQ**GL	GEK**SQ**S**Q**E	DI**SQ**KQ
Rat	QEN**SQ**LNV	LMRHQGTL	QLVVSMK	NEG**SQ**AAA	CSD**SQ**ERES	RRA**SQ**GL	GEK**SQ**S**Q**E	DI**SQ**KY
Naked mole rat	TEN**SQ**LNM	LDV**SQ**DTL	HY**SQ**EES	NEE**SQ**V--Q	IGDNQDKEN	RRA**SQ**GL	GEK**SQ**LQE	DISEEY
Human	TEN**SQ**LNV	LDV**SQ**DTL	QY**SQ**EEP	NED**SQ**V--Q	TTE**SQ**DKEN	RRA**SQ**GL	GEK**SQ**PQE	NV**SQ**E-
Bonobo	TEN**SQ**LNV	LDV**SQ**DTL	QY**SQ**EEP	NED**SQ**V--Q	TTE**SQ**DKEN	RRA**SQ**GL	GEK**SQ**PQE	NV**SQ**E-
Chimpanzee	TEN**SQ**LNV	LDV**SQ**DTL	QY**SQ**EEP	NED**SQ**V--Q	TTE**SQ**DKEN	RRA**SQ**GL	GEK**SQ**PQE	NV**SQ**E
Cat	TEN**SQ**LNM	LDV**SQ**DTL	QYTHEES	DEDSTI--Q	TTD**SQ**EKEN	RRA**SQ**GL	GEK**SQ**PQE	NV**SQ**E
Lion	TEN**SQ**LNM	LDV**SQ**DTL	QYTHEES	DEDSTI--Q	TTD**SQ**EKEN	RRA**SQ**GL	GEK**SQ**PQE	RDNSLEY
Whale	TEN**SQ**LNM	LDV**SQ**DTL	QYGQEES	NEDSHV--Q	TTD**SQ**EKEN	RRA**SQ**GL	GEK**SQ**PQE	RDNSLEY
Horse	REN**SQ**LNM	LDV**SQ**DAL	QYGQEES	NEDSHV--Q	TTD**SQ**EKEN	RRA**SQ**GL	GEK**SQ**PQE	KDISLEC

Figure 24. Identification of phosphorylated conserved SQ cluster in RIF1 I-DIRT. a) MS/MS spectra of the identified mRIF1 peptides encompassing residues S1387, S1416, and S1528. b) (top) prediction of RIF1 disorder using IUPred2A web interface (bottom) Structure of murine RIF1 containing 21 HEAT repeats in the N-terminal followed by an intrinsically disordered region followed by the C-terminal domain divided into 3 regions. RIF1 has 17 predicted S/T-Q sites. The sites marked in red are moderately conserved, sites marked blue are highly conserved and white sites are not conserved. The sites marked blue are identified in RIF1 I-DIRT. The dashed lines indicate the S/T-Q sites present in a cluster I, II and III. (c) Multiple sequence alignment performed using ClustalOmega depicting the conservation of the three clusters in mammals.

Generation and characterization of RIF1 SQ-CII phosphomutant cell lines in CH12. To study the function of the SQ-CII cluster in RIF1 role in end protection, in collaboration with a former PhD student in the lab, Matteo Andreani, I generated *Brca1*^{mut} CH12 clonal cell lines harbouring serine to alanine and serine to aspartic acid mutations in all 3 phosphosites to obtain phosphodeficient *(Rif1*$^{S\rightarrow A}$*)* and potential phospho-mimetic cell lines *(Rif1*$^{S\rightarrow D}$*)*, respectively. We used the CRISPR-Cas9 genome editing system to introduce site-directed mutations in the genomic locus of *Rif1* through HDR repair. Briefly, 2 gRNAs targeting exon 30 of *Rif1* were cloned into a single plasmid system also expressing wild type Cas9-T2A-GFP. The gRNAs were electroporated into the *Brca1*^{mut} CH12, together with a donor plasmid containing the desired mutations flanked on either side by 1000bp homology arms (Fig. 25a). The donor sequence introduced: (i) non-synonymous mutations to convert serine to alanine or serine to glutamic acid to make phosphodeficient and potential phospho-mimetic clones respectively; (ii) a unique Nhe1 restriction enzyme site through silent mutation to differentiate and efficiently select targeted clones from wild type; and (iii) mutations in the PAM and the protospacer sequences to avoid repeated targeting by Cas9 in the desired clones (Fig. 25a). Following electroporation and single cell sorting of GFP positive cells, the clones were allowed to recover, and genomic DNA was extracted. In order to avoid any off-target amplifications of the donor sequence, the targeted region was amplified with at least one primer annealing to outside the homology arm. Digestion with Nhe1 revealed how many clones had homozygous insertions. This allowed for unbiased selected of targeted clones (Fig. 25b).

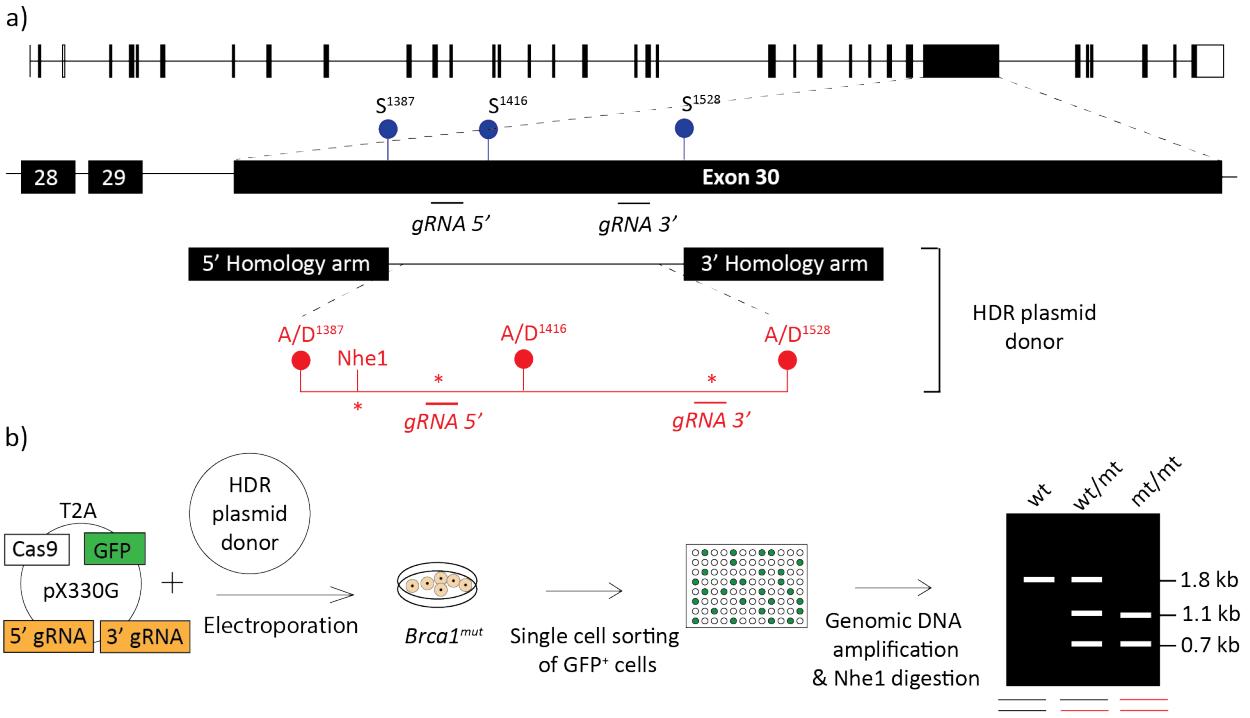

Figure 25. Methodology and workflow for generation of *Rif1*$^{S\rightarrow A}$ and *Rif1*$^{S\rightarrow D}$ cell lines in *Brca1*^{mut} CH12. a) Schematic showing the position of the SQ-CII cluster in exon 30 and the location of the gRNAs used. Donor plasmid contains the desired Ser→Ala and Ser→Asp mutations, along with a Nhe1 site and mutations in the PAM and protospacer. It contains a 1000bp homology arms on either side to enable efficient HR repair. b) Workflows starts with electroporation of pX330G plasmid containing 5' and 3' gRNA and HDR donor into *Brca1*^{mut} CH12. GFP^{+} cells are single cell sorted and allowed to recover after which their genomic DNA is extracted. Targeted region is amplified and digested with Nhe1 with untargeted or wildtype (*wt*) clones showing a 1.8kb band, heterozygous (*wt/mt*) showing 1.8kb+1.1kb and 0.7kb and homozygous clones (*mt/mt*) having 1.1kb+0.7kb bands.

Screening of 80 clones revealed a homozygous KI efficiency of 21% for *Brca1*^{mut} *Rif1*$^{S\rightarrow A}$ and 19% for *Brca1*^{mut}*Rif1*$^{S\rightarrow D}$. Heterozygous clones with 1 allele containing the desired mutations was obtained at an efficiency of 11.25% of *Brca1*^{mut} *Rif1*$^{S\rightarrow A}$ and 12.5% of *Brca1*^{mut}*Rif1*$^{S\rightarrow D}$ (data not shown). CRISPR-Cas9 KI strategies exploit the HR pathway to repair the DSBs introduced by Cas9. In the process, the donor sequence provided will be used as template for repair using which the desired mutations will accurately introduced. Considering that BRCA1 is critical for HR repair, it was intriguing that we could obtain the *Rif1*$^{S\rightarrow A}$ and *Rif1*$^{S\rightarrow D}$ in a *Brca1*^{mut} background through CRISPR-Cas9 KI. Three clones per genotype were selected based on the correct digestion pattern for homozygous clones (1.1kb + 0.7kb), equal levels of

RIF1 by western blotting, and the presence of the desired Ser→Ala and Ser→Asp mutations through Sanger sequencing. (Fig. 26a,b).

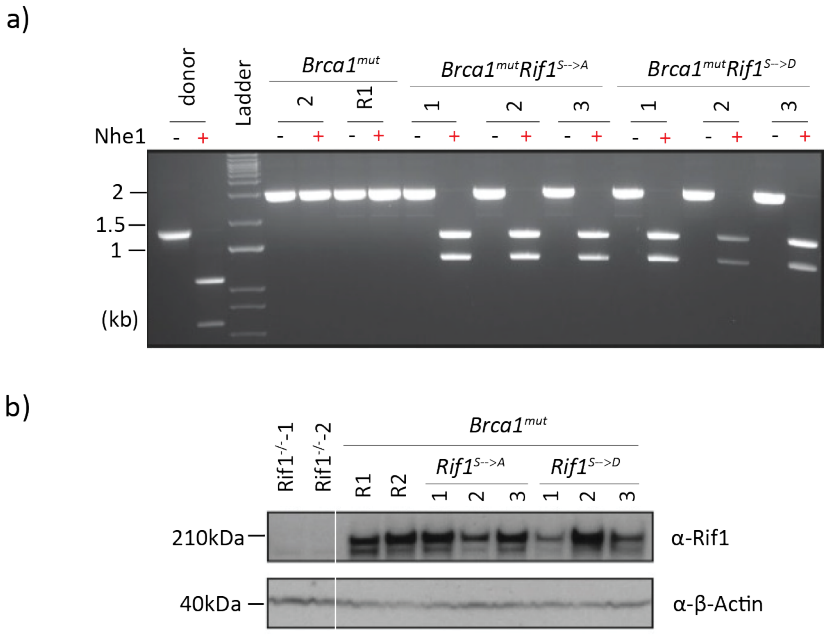

Figure 26. Characterization of *Brca1*^{mut} *Rif1*$^{S→A}$ and *Brca1*^{mut} *Rif1*$^{S→D}$. a) Nhe1 digestion of amplified region from *Rif1* exon 30. Digestion of the HDR donor plasmid gives 0.6kb+0.4kb . Homozygous *Brca1*^{mut} *Rif1*$^{S→A}$ and *Brca1*^{mut} *Rif1*$^{S→D}$ clones show a band pattern of 1.1kb+0.7kb. Controls used here are the parental *Brca1*^{mut} and *Brca1*^{mut} targeted with random gRNA that does not target anywhere in the genome, (R1) + indicates samples in which Nhe1 was added. b) Western blot analysis showing RIF1 levels in whole cell extracts from the indicated genotype. β-actin is used as loading control.

4.2.2. RIF1 harboring Ser to Ala/Asp substitutions of the SQ-CII cluster can still promote PARPi-induced genome instability and lethality

BRCA1-deficient cells are impaired for resection due to which replication-associated DSB are repaired by toxic end protection events mediated by RIF1. Radials and chromatid breaks are hallmarks of HR deficiency and deletion of *Rif1* in *Brca1*^{mut} background rescues the defect. To understand the function of RIF1 phosphorylation at SQ-CII in DSB repair, chromosome aberration analysis on metaphase spreads was performed to quantify the levels of radials and chromatid breaks in *Brca1*^{mut} *Rif1*$^{S→A}$ and *Brca1*^{mut} *Rif1*$^{S→D}$ after treatment with PARPi.

Control samples namely *Brca1*^{mut} and *Brca1*^{mut} treated with random gRNA behaved identically showing high average number of chromatid breaks and radials. The *Brca1*^{mut}*Rif1*$^{-/-}$ showed a complete rescue in chromosomal aberrations. All the 3 characterized *Brca1*^{mut} *Rif1*$^{S\rightarrow A}$ clones showed high average number of radials and chromatid breaks similar to the parental controls indicating that resection in *Brca1*^{mut} background is not rescued upon abrogation of RIF1 phosphorylation in the SQ-CII cluster. *Brca1*^{mut} *Rif1*$^{S\rightarrow D}$ clones showed a slight reduction in radials although this reduction is not statistically significant (Fig. 27).

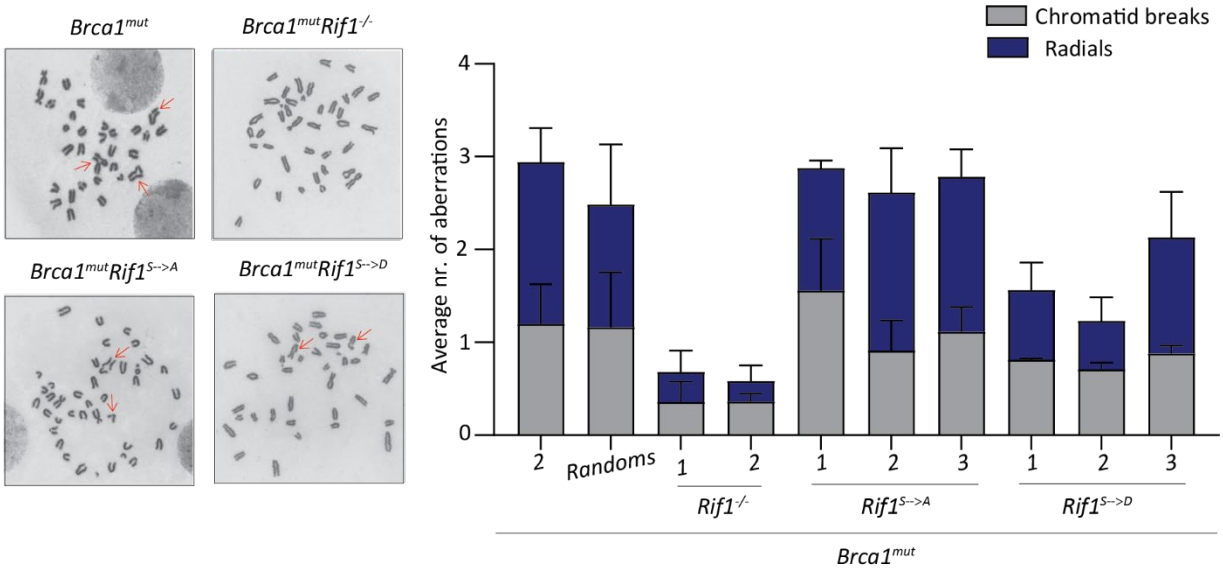

Figure 27. RIF1 harboring Ser to Ala/Asp substitutions of the SQ-CII cluster promotes PARPi-induced genome instability. (left) representative images of metaphase spreads of the indicated genotype. Red arrows indicate radials and chromatid breaks (left) summary bar graph indicates the average number of chromatid breaks and radials in the indicated genotype following 1µM PARPi treatment for 24 hours. 100 metaphases were analysed and error bars indicates SD.

High levels of genomic instability trigger cell death. Accordingly, PARPi-treated *Brca1*^{mut} *Rif1*$^{S\rightarrow A}$ and *Brca1*^{mut} *Rif1*$^{S\rightarrow D}$ cell lines exhibited high levels of lethality due to the chromosomal aberrations accumulated (Fig. 28). With these results, I concluded that RIF1 harboring Ser to Ala/Asp substitutions of the SQ-CII cluster can still promote PARPi-induced genome instability and lethality.

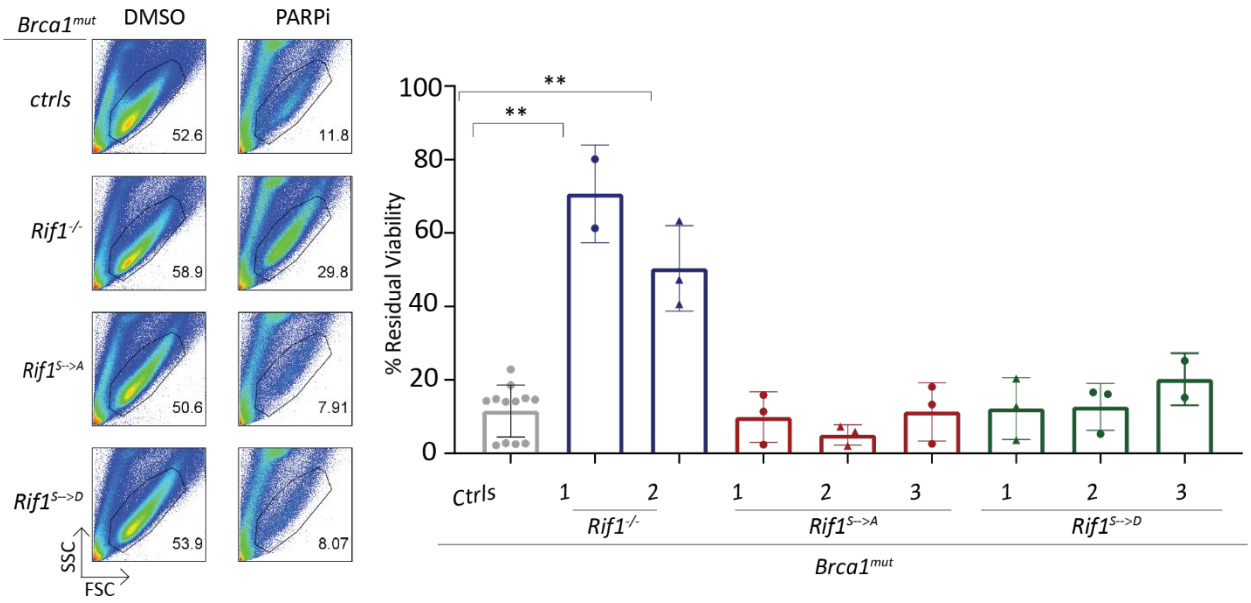

Figure 28. RIF1 harboring Ser to Ala/Asp substitutions of the SQ-CII cluster promotes PARPi-induced genome instability. (Left) Representative FACS plots showing percentage live cells of the indicated genotype (right) summary bar graph showing levels of residual viability following treatment with 1µM PARPi for 72 hours. Graph represents experiments performed at least twice. Error bars represent SD and statistics were plotted using Mann-Whitney U test. **p<0.01.

4.2.3. RIF1 harboring Ser to Ala/Asp substitutions of the SQ-CII cluster is dispensable for DSB end protection during G1 phase of the cell cycle

As I have described in the above paragraphs, DSBs are extremly toxic lesions which need to be accurately repaired using the correct pathway to prevent genomic loss. However, in some cases DSBs are also programmed to occur in the case of antibody diversification reaction during CSR in mature B lymphocytes. As explained in paragraph 1.3.5., B lymphocytes upon encounter with an antigen or cytokines recombine their immunoglobulin heavy chain locus to generate antibodies with different effector functions. CSR reaction occurs in the G1 phase of the cell cycle with programmed DSBs initiated in the highly repetitive switch regions of the donor and acceptor (Fig. 29a). These programmed breaks are repaired by NHEJ which leads to productive antibody diversification reactions[82]. 53BP1/RIF1 play crucial roles in in this reaction by protecting the DSB ends from resection. Depletion of either of the factors completely abrogates CSR in mammals[46,53,75].

CH12 is the only cell line that can perform CSR *in vitro* and this makes it a powerful model system to study repair events in G1 phase. Additionally, BRCA1 does not mediate CSR[89,90]. Data from our lab (generated by Tannishtha Saha) showed that *Brca1*^{mut} CH12 upon activation with cytokines displayed the same levels of CSR as seen in the wild type (Fig. 29b). As a result, *Brca1*^{mut} CH12 can be used to identify RIF1 functions in end protection during both G1 and S phase of the cell cycle.

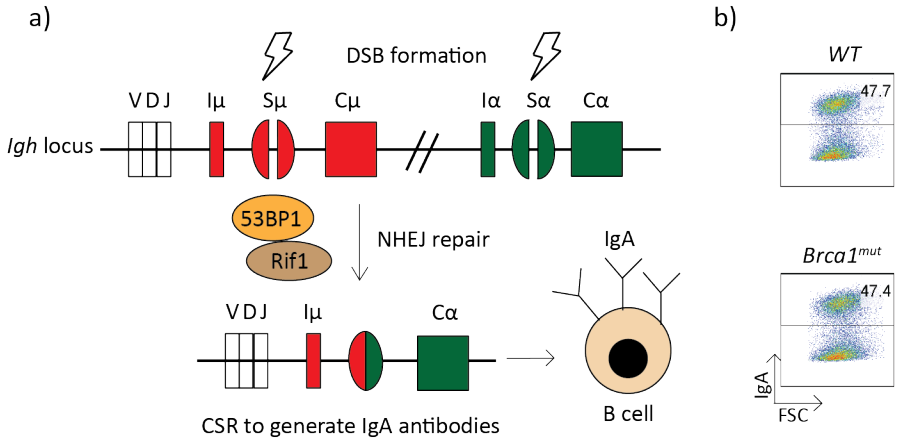

Figure 29. CSR reaction in B lymphocytes. Simplified schematic of CSR reaction in mature B cells. Following encounter with an antigen or cytokines, programmed DSB occur in the switch region Sμ and in one of the downstream acceptor regions here Sα. These breaks are repaired by NHEJ with 53BP1 and RIF1 as the critical mediators of this reaction. This leads to productive CSR reaction resulting in the formation of IgA antibodies that are expressed on the surface of mature B cells. (Bottom) representative FACS plot showing percentage IgA positive cells in CH12 of the indicated genotype following stimulation with cytokines IL-4, TGF-β and CD40L for 48 hours (b) Representative FACS plots of the indicated genotype in CH12 showing percentage IgA positive cells.

In order to investigate if phoshphoregulation of RIF1 in SQ-CII cluster mediates end protection during G1, *Brca1*^{mut} *Rif1*$^{S\rightarrow A}$ and *Brca1*^{mut} *Rif1*$^{S\rightarrow D}$ CH12 were activated to undergo CSR using cytokines IL-4, TGF-β and CD40L to stimulate switching to IgA. While the wild type controls showed high percentage of IgA positive cells, as expected *Rif1*$^{-/-}$ showed dramatic loss in IgA levels. Both the phospho-mimetic and the phosphodeficient clones behaved similarly to the controls. I concluded that phosphorylation of RIF1 at the conserved SQ-CII cluster is dispensable to protect DSB in *Igh* locus during the G1 reaction CSR (Fig 30).

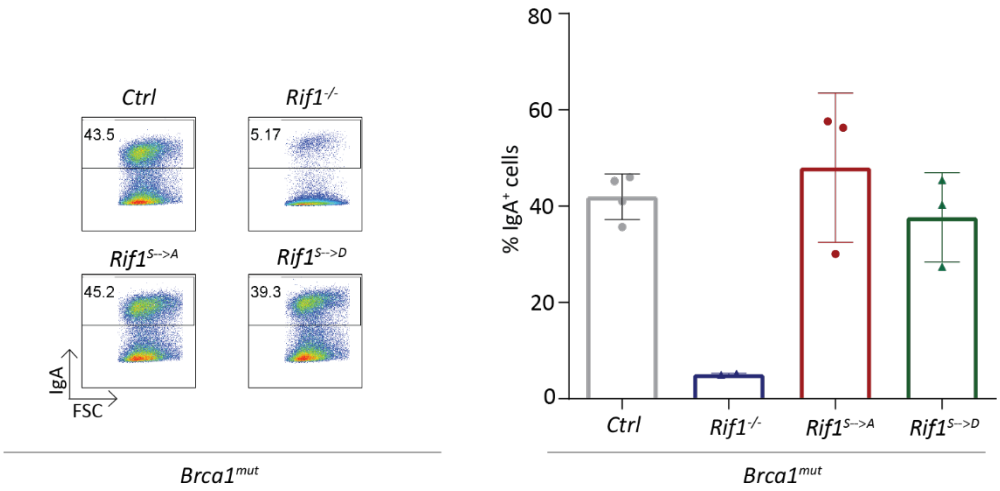

Figure 30. RIF1 harboring Ser to Ala/Asp substitutions of the SQ-CII cluster is dispensable for CSR in activated B lymphocytes. (left) representative flow cytometry plots showing percentage of IgA positive cells (right) Summary bar graph showing percentage IgA positive cells of the indicated genotype following activation using IL-4, TGF-β and CD40L for 48 hours.

DSB end protection by RIF1 is critical to repair programmed DSB that arise during CSR in G1 phase and for stochastic DSB that arise during replication in S phase. In the first case, DSB end protection leads to genome diversification, whereas in the second repair of DSB in *Brca1*^{mut} cells can lead to toxic repair and give rise to genome instability. I have so far concluded that murine RIF1 harboring mutations to Ala/Asp in the conserved SQ-CII is dispensable for end protection of both programmed DSB during CSR in G1 phase and replication-associated DSB during S phase. Furthermore, it does not contribute to PARPi resistance in BRCA1-deficient background.

4.2.4. RIF1-deficient CH12 show aberrant degradation of nascent DNA at stalled replication forks

Apart from its function in DSB end protection, mammalian RIF1 maintains genome stability during DNA replication by protecting nascent replication forks from degradation by nucleases following replication stress. Recently two research groups identified that loss of RIF1 in mouse and human cell lines promotes fork degradation by DNA2 nuclease[120,121]. This resulted in delayed replication fork restart which in turn caused significant genome instability and reduced survival following replication stress[120]. However, the mechanism by which RIF1 modulates fork protection has not been completely elucidated yet. The I-DIRT dataset from which the RIF1 phosphopetides were identified was performed in highly proliferating primary B cells (Fig. 24a). This implies that results from this dataset could give insights on RIF1 function in replication (Fig. 22b). In addition, several potential RIF1 effectors identified in this list were recruited to stalled replication forks following replication stress. This raised the exciting possibility that the cluster of phosphosites we identified regulates RIF1 function in the maintenance of genome stability following replication stress.

To assess whether CH12 cells are a suitable model system to study RIF1 function in fork protection, I first optimized the DNA fiber assay using *wt* and *Rif1*$^{-/-}$ CH12. This assay quantified fork degradation by measuring the tract lengths of DNA following replication stress. Replicating CH12 cells were sequentially labelled with different analogues of thymidine (IdU then CldU) to allow for incorporation in newly-replicating DNA and then treated with HU to promote replication stress. The tract length of IdU and CldU was measured and the ratio CldU/IdU being less than 1 signifies fork degradation of the newly replicated strands following HU treatment (Fig. 31).

To test if RIF1-deficient CH12 also show fork degradation upon replication stress, I quantified the CldU/IdU ratio. Since BRCA1 is also implicated in nascent fork protection[101], I used *Brca1*^{mut} CH12 as a positive control for increased fork degradation. The ratio of CldU to IdU was close to 1 in the negative controls indicating robust fork protection as expected. In agreement with previous research, *Brca1*^{mut} displayed dramatic fork degradation. *Rif1*$^{-/-}$ CH12 also showed highly significant levels of nascent fork degradation similar to that of *Brca1*^{mut}. With this, I concluded that CH12 is an appropriate model system to study nascent fork degradation where both *Brca1*^{mut} and *Rif1*$^{-/-}$ promotes stalled fork degradation in agreement with what is known in the field[120,121].

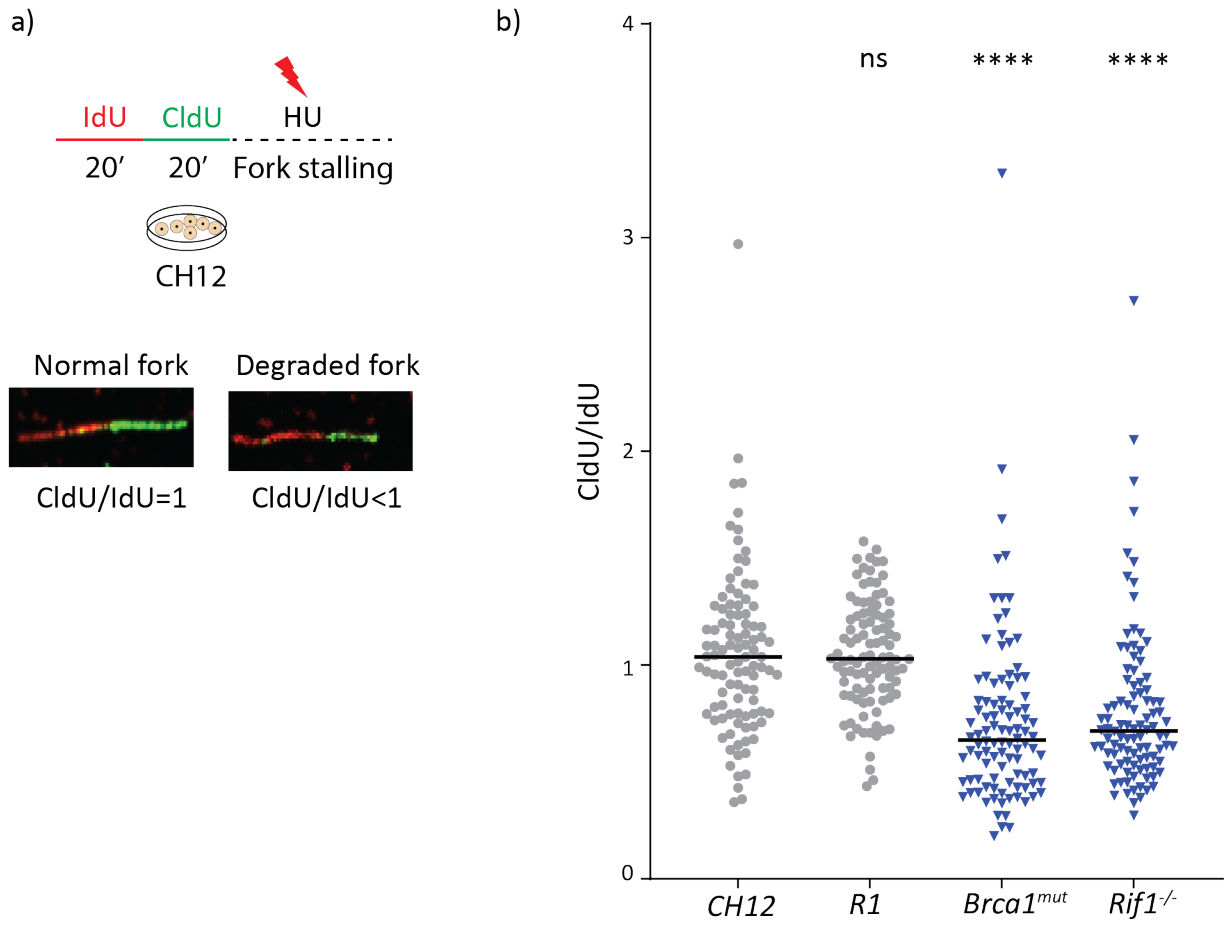

Figure 31. RIF1 mediates nascent fork protection in CH12 following replication stress. a) Schematic representation of DNA fiber assay. CH12 cells are treated with IdU and CldU for 20 minutes following which 4mM HU is added for 3h to induce fork stalling. Representative IF images of DNA fibers are shown below. Ratio of CldU to IdU tract length is considered the readout for fork degradation. b) Graph showing distribution of CldU to IdU ratio in 100 DNA fibers from the indicated genotype following HU treatment. R1 refers to CH12 cell line targeted with random gRNA that does not target anywhere in the mouse genome. Line indicates median. ns-non significant, ****p<0.0001.

4.2.5. Abrogation of RIF1 phosphorylation in the conserved SQ-CII cluster promotes DNA replication fork degradation

Since BRCA1 contributes to replication fork protection *via* a mechanism independent from RIF1, I could not use the *Brca1*^{mut} *Rif1* phosphomutant cell lines that I previously generated. To assess if phosphorylation events in SQ-CII of RIF1 could mediate its function in fork stabilisation, I took advantage of *Rif1* phosphomutant cell lines generated by Matteo Andreani. These cell lines *Rif1*$^{S\rightarrow A}$ and *Rif1*$^{S\rightarrow D}$ harbored mutations from Ser to Ala and Ser to Asp in the SQ-CII cluster on a BRCA1-proficient (WT) background and were generated using the same gene editing approach described for the *Brca1*^{mut} *Rif1* phosphomutants (Fig. 25).

Upon testing the different RIF1 phosphomutants following HU, I discovered that both the phosphodeficient and the potential phospho-mimetic cell lines showed significant reduction in CldU/IdU ratio, implicating substantial degradation of stalled forks following replication stress (Fig. 32). Intriguingly mutation of RIF1 phosphorylation at just the three SQ motifs promoted fork degradation effect comparable to that of a complete knockout. Both the negative control samples showed fork protection and *Brca1*^{mut} displayed substantial degradation of stalled forks. Based on these results, I concluded that abrogation of RIF1 phosphorylation in the conserved SQ-CII cluster is critical to protect stalled forks following replication stress.

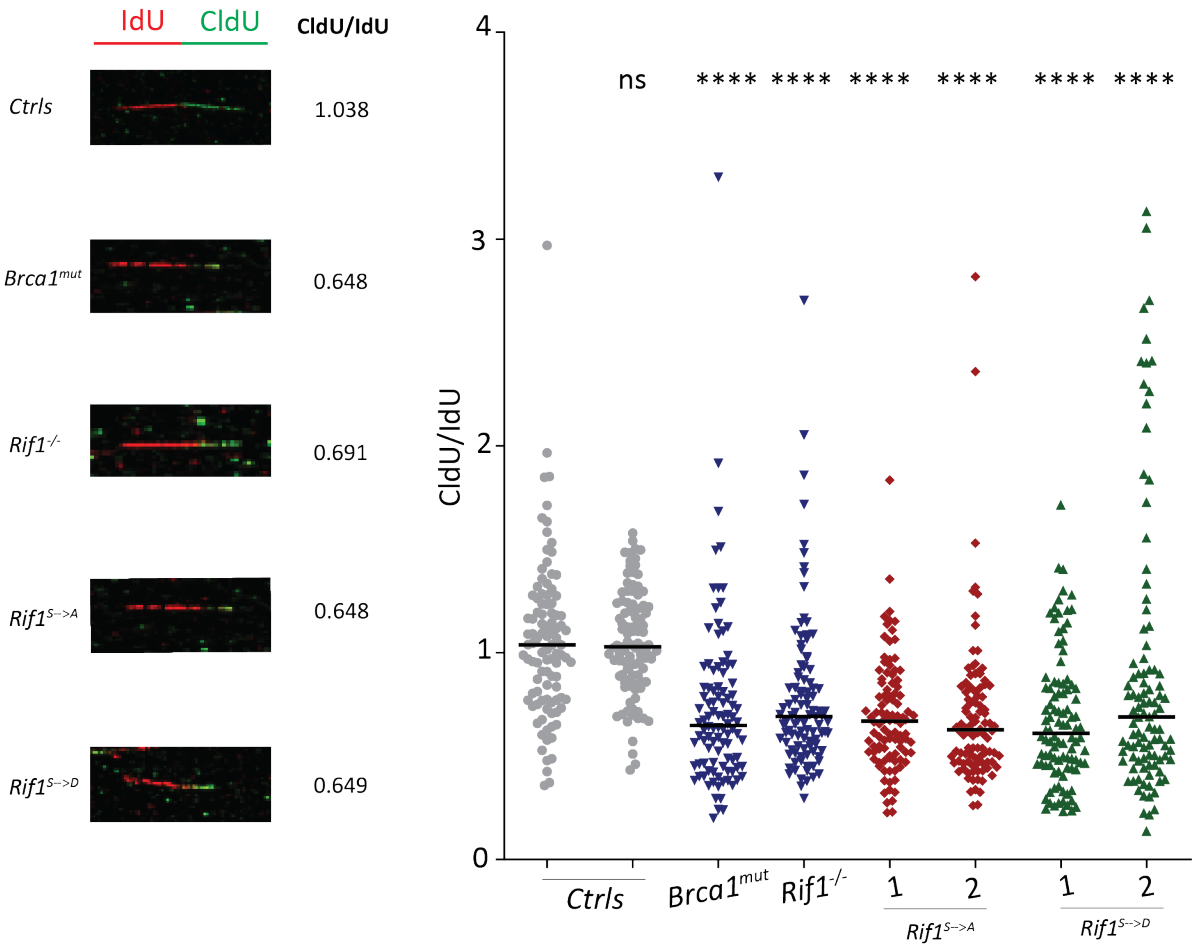

Figure 32. RIF1 harboring Ser→ Asp mutation in the SQ-CII cluster promotes nascent fork degradation following replication stress. (Left) representative IF images of DNA fiber following treatment with 3mM HU for 4 hours. IdU is marked in red and CldU marked using green fluorophore respectively. CldU/IdU indicate median fork degradation ratio of the indicated genotype. (Right) Graph showing distribution of CldU/IdU ratio of 100 fibers of the indicated genotype. *Ctrls* refer to wild type CH12 and CH12 targeted with random gRNA that does not target anywhere in the genome. Line indicates median. ns- non significant. ****p<0.0001.

5. Discussion

Maintaining genome stability during replication is essential for cell survival. However, the progressing replication fork can slow or stall due to various obstacles like SSBs, ICLs, difficult to replicate sequences. Stabilization of stalled fork is essential to complete replication and avoid under replicated DNA leading to genome instability. When stabilization is impaired, stalled forks collapse leading to the formation of poisonous DSBs which needs to be repaired to avoid toxic genomic rearrangements. Mammalian RIF1 plays a crucial role in maintaining genome stability by mediating both fork stabilization and DSB repair albeit through independent mechanisms. In order to understand the molecular mechanism of how RIF1 mediates its crucial functions, I screened for novel effectors of RIF1 using a robust rescue-of-viability assay in *Brca1*^{mut} CH12. This screen led to the discovery of ZRANB2 which upon deletion in *Brca1*^{mut} CH12 modestly rescues viability following treatment with PARPi. Furthermore, I also investigated the post translational regulation of RIF1 to further dissect its molecular mechanisms. I discovered that the conserved SQ cluster II of RIF1 consisting of 3 serine sites (S1387, S1416 and S1528) is phosphorylated in highly proliferating primary B lymphocytes. Abrogation of phosphorylation in this cluster is dispensable for RIF1 function in DSB end protection and is essential for stabilization of stalled replication forks in CH12.

5.1. Applications of *Brca1*^{mut} CH12 and insights on RIF1 interactome

CH12 is the only cell line that can undergo efficient CSR *in vitro*[149]. CSR occurs in the G1 phase of the cell cycle with the introduction of programmed DSBs in the switch regions of the specialized *Igh* locus[150]. These breaks are protected by 53BP1/RIF1 to promote repair by NHEJ that ensures productive antibody switching reactions. As a result, deletion of 53BP1/RIF1 completely abolishes CSR (Section 1.3.5).

Antibody switching events rely exclusively on NHEJ for repair of programmed DSBs. Recombination mediated by HR is deleterious to the cells and BRCA1 does not function during CSR that takes place during G1 phase of the cell cycle[89,90]. However, during S phase deletion of BRCA1 leads to aberrant end joining reactions by 53BP1/RIF1 which leads to gross chromosomal changes[43,49,53]. As a result, the *Brca1*^{mut} CH12 have the unique advantage of being a model system in which repair events at both S phase and G1 can be studied (Fig. 27, 30).

Deletion of RIF1 completely abolishes CSR while increasing the viability of *Brca1*^{mut} upon PARPi (Fig. 28,30). Hence this system can be used to screen novel effectors of RIF1 in the context of both CSR and aberrant

repair during S phase. Additionally, CH12 being a suspension cell line can be used efficiently and robustly for flow cytometry-based CSR and residual viability assays.

Apart from DSB end protection, CSR also relies on chromatin reorganization, transcription and programmed DNA damage and the effectors involved in these processes are not completely identified yet[151]. Hence, *Brca1*^{mut} CH12 can also used identify effectors of CSR that function not just in end protection but in many other cellular processes[144]. Hence creating *Brca1*^{mut} in CH12 gives the dual advantage to study DSB end protection during both G1 and S phase of the cell cycle and to identify novel effectors in CSR.

5.1.1. Applications of rescue-of-viability assay

The gain-of-viability assay enabled the rapid identification of novel effectors of RIF1 that mediate DSB repair choice *via* a functional read-out (Fig. 18). Since, deletion or mutations in end protection factors is one of the mechanisms of PARPi resistance, effectors identified in this screen also sheds on light on how RIF1 promotes PARPi resistance. The use of several different positive controls like deletion of 53BP1, RIF1 and REV7 consistently produced increased the survival of *Brca1*^{mut} CH12 (3-7 fold) (Fig. 17). The rescue of viability assay represents a robust functional readout for DNA end protection and PARPi resistance.

5.1.2. Insights on RIF1 interactome

Screening for novel RIF1 effectors in DSB repair pathway choice revealed that only deletion of ZRANB2 showed a consistent yet modest 2-fold increase in viability of *Brca1*^{mut} CH12 hinting its role in DSB pathway choice/end protection (Fig. 18, 20).

ZRANB2 is an RNA-binding protein with no function identified in DSB repair so far. ZRANB2 is a part of the supraspliceosome: a macromolecular machine active in alternate splicing in which the entire repertoire of nuclear pre-mRNAs are individually packaged [86,152]. A few targets of ZRANB2 have been identified but none of them are directly implicated in DSB repair[86,153]. However, emerging evidence suggests that alternate splicing plays a bigger role in DNA DSB repair than thought before.

A genome-wide siRNA screen in human cells identified genes that mediated γH2AX formation which is a bona fide DSB mark[147]. This study revealed the surprise enrichment of several mRNA processing factors involved in alternate splicing. One of the many candidates identified in this screen was ZRANB2 which upon knockdown showed significant enrichment in γH2AX levels[147]. It would be interesting to know if the *Brca1*^{mut} *Zranb2*$^{-/-}$ have reduced level of γH2AX following IR. This could be a possible explanation for the

modest rescue in viability I observed since reduction in the DSB mark indicates a more stable genome. However further experiments are needed to clarify if this hypothesis is true.

Another study revealed inhibiting the spliceosome formation in human U2OS cell line significantly reduced the focal accumulation of several DSB repair factors including 53BP1, BRCA1 and RAD51 following irradiation to introduce DSB. By inhibiting splicing, RNF8 protein levels were reduced and its ubiquitin ligase activity is crucial to recruit BRCA1 and 53BP1 to chromatin surrounding DSB to begin repair. In fact, upon inhibiting splicing HR repair frequency was reduced by 60%[154]. However, the components of the spliceosome that mediated this key function have not been identified. Since ZRANB2 is also part of the spliceosome it would be worth investigating if *Brca1*^{mut} *Zranb2*$^{-/-}$ CH12 displays reduced focal accumulation of 53BP1/RIF1 following IR. This would hint if the higher viability I observed upon PARPi treatment is due to reduced recruitment of 53BP1/RIF1 that would inhibit toxic DNA end-joining reaction. Although the above hints point to a possible role of ZRANB2 in DSB repair, more studies need to be performed to understand if ZRANB2 mediates DSB repair pathway choice through RIF1.

5.1.3. Additional applications of *Brca1*^{mut} CH12

This assay robustly determined if new effectors mediate DSB pathway choice. For example, chromatin reader ZMYND8 was identified as a potential RIF1 interactor in the I-DIRT list[144]. To investigate if its function in DNA DSB pathway choice, I performed the rescue-of-viability assay and observed that ZMYND8 knockdown did not increase survival of bulk cultures of *Brca1*^{mut} CH12 (Fig. 18). This hinted that ZMYND8 does not function in repair of replication-associated breaks. In confirmation of this result, *ZMYND8*$^{-/-}$ MEFs showed no defect in focal accumulation of DSB repair factors like y-H2AX, 53BP1 and RIF1 indicating a proficient DSB repair pathway. *ZMYND8*$^{-/-}$ MEFs also did not have survival defects following IR and PARPi confirming that ZMYND8 is dispensable for DSB repair.

Additionally, our lab recently identified RIF1 truncation mutants in the CTD and to study their role in DSB pathway choice both residual viability and CSR was used as a functional readout. Preliminary studies identified that the truncation mutants consistently show normal CSR, but failed to rescue viability of *Brca1*^{mut} CH12, thus hinting at an exciting separation-of- function of RIF1 in CSR and repair of replication-associated DSB (data not shown). Thus, *Brca1*^{mut} CH12 can be used as a tool to dissect the mechanisms of how RIF1 and other possible effectors function independently in the repair of programmed breaks in the *Igh* locus and replication-associated DSBs during S phase.

5.1.4. Caveats of the screen

Despite having stringent conditions for selection of candidates from the RIF1 I-DIRT list (including the SILAC ratio, the number of peptides identified and the low PEP value) to avoid false positives, we were surprised to find that only deletion of ZRANB2 showed a modest rescue whereas none of the other 39 factors did (Fig 18). This could be due to several technical reasons. First, the gRNAs used were designed using robust software tools that predicted off-target effects and generated gene/sequence-specific gRNAs (CRISPRDesign and CrispRGold)[155,156]. However, these gRNAs were not experimentally tested for their targeting efficiency or off-target effects. To increase the chances of causing indels at the desired locus, 3-6 gRNAs per candidate were designed and electroporated together as a pool in equal ratio. Nevertheless, this does not exclude the option that a negative result in the screen could be due to inefficient gRNA targeting. Second, factors involved in cell fitness would not be identified as hits in our screen because, the deletion of these genes would automatically lead to cell death, which would result in no effects on viability rescue. Third, different proteins have different turnover rates, which could lead to incomplete removal of target protein in the 72 hours following sorting of Cas9 positive cells despite successful gene targeting.

Apart from technical issues, certain biological aspects could also explain the results from the residual viability screen. The RIF1 I-DIRT was performed on primary splenocytes that were activated to undergo CSR and were irradiated to introduce stochastic DSBs in addition to programmed CSR damage (Fig. 15)[144]. Furthermore, splenocytes are also one of the most proliferative cell types in the body. Hence, the candidates obtained from the I-DIRT could modulate RIF1 functions in one or many of its functions including DSB repair, CSR, B cell homeostasis, or replication fork stability (Fig. 22a). In support of this possibility, among the 40 hits several like Timeless, Pol ε and CTF18 are recruited to both elongating and stalled replication forks[104]. BACH2, CD36, CHMP5 and IGLV2 mediate immunological recognition, inflammation and B cell development[144,157,158]. In addition, ZMYND8 identified in this screen is dispensable for DNA DSB repair but regulates CSR by binding to promoters and super enhancers in the *Igh* locus[144]. In conclusion, due to the model system where the RIF1 I-DIRT was performed (primary B cells) and the employed experimental conditions, it is possible that the negative hits from the viability-rescue assay represent RIF1 effectors involved in DNA replication stress, CSR as well as other aspects of B cell physiology rather than DSB repair.

5.2. Phosphoregulation of RIF1

Phosphorylation is one of the most abundant PTM in the DDR as it mediates several functions like protein-protein interactions, protein-DNA interactions, and activation of signaling pathways. ATM/ATR are critical kinases that mediate functions in DSB repair and replication stress, respectively[33]. RIF1 has several S/T Q sites that are consensus sequences for both ATM and ATR, some of which are highly conserved in mammals (Fig. 24c).

In this study, we have identified RIF1 to be in phosphorylated on a conserved group of SQ motifs in highly proliferating mouse primary B lymphocytes (Fig. 24b). The sites S1387, S1416 and S1528 (SQ-CII) form a cluster in the IDR of mouse which are hotspots for post-translational modifications and frequently mediate protein-protein interactions through binding and coupled folding reactions[137,138]. Abrogation of phosphorylation in the conserved SQ-CII cluster by mutagenesis revealed that these PTMs are dispensable for RIF1 role in DSB end protection but are essential for nascent fork protection following replication stress.

To study the function of these phosphorylation events, I created phospho-mimetic and phosphodeficient clones in the RIF1-SQCII cluster in *wt* and *Brca1*^{mut} CH12 backgrounds through CRISPR-Cas9 mediated KI. Surprisingly, despite the putative HR-deficiency of BRCA1-mutated CH12 cells, the efficiency of KI was comparable in both the wild type and *Brca1*^{mut} CH12 backgrounds. This observation could be due to potential residual BRCA1 function in the *Brca1*^{mut} clones since the indels in the *Brca1* locus of all selected clonal derivatives caused internal amino acid deletions rather than PTC, which could be hinting at the expression of hypomorphic mutant proteins. In agreement with this possibility, it has been reported that not all BRCA1 variants lead to loss of HR[159].

Both the phosphodeficient and the phospho-mimetic clones were dispensable for RIF1 role in DSB end protection as observed by the accumulation of chromosomal aberrations and the subsequent loss of viability in *Brca1*^{mut} cell lines following PARPi (Fig. 27,28). Furthermore, they did not affect CSR (Fig. 29). The I-DIRT dataset from which the SQ-CII phosphopetide were observed was originally performed to identify effectors of RIF1 following IR and during CSR reaction. Hence, the samples included irradiated and activated splenocytes from both *RIF1*$^{FH/FH}$ and *wt* mice and did not use untreated samples (Fig. 14). The addition of the irradiated *wt* mice allows differentiating between real and spurious interactors of RIF1 following DNA damage induction. While this experimental setup is sufficient to identify specific RIF1

effectors due to the lack of untreated sample, it leaves the possibility open that the phosphorylation events detected are constitutive or they are not required for DNA DSB end protection.

Since RIF1 does not have any catalytic activity, we hypothesized that the phosphorylation in the conserved SQ-CII cluster is likely to serve as a bridging protein to bring together the components of the end protection machinery. Recently, the Durocher lab discovered that RIF1 is required for Shieldin recruitment in human cells[160]. They observed that following siRNA knockdown of RIF1, Shieldin recruitment to the DSBs is abolished. SHLD2 binds to shortly resected ssDNA and the Shieldin complex recruits CST which thanks to its polymerase activity can fill in the resected DNA, thereby making the ends compatible for ligation by Ligase IV. Therefore, recruitment of the shieldin complex is essential for end protection. Since both the phospho-mimetic and the phosphodeficient mutants of RIF1 SQ-CII cluster can still protect the DSBs occurring in both G1 and S phase, it is highly likely that phosphorylation of the serine sites S1387,S1416 and S1528 do not mediate RIF1 recruitment of the Shieldin complex to DSB.

This study discovered that abrogation of phosphorylation in RIF1 SQ-CII cluster resulted in significant nascent fork degradation following replication stress (Fig. 32). Intriguingly, the SQ-CII cluster is not present in the CTD of RIF1 which is required for RIF1-PP1 binding to mediate fork protection. Instead it is present in the IDR of RIF1 which is a hotspot for PTMs and protein-protein interaction (Fig. 24b)[137]. Although only 3 sites were mutated (Fig. 25a), the phosphodeficient clones showed nascent fork degradation levels comparable to what was observed upon complete RIF1 deletion (Fig. 32). Surprisingly the phospho-mimetic mutants of RIF1 SQ-CII cluster also showed a similar defect in fork protection (Fig 32). This observation can be explained by considering how the cell lines were generated. Phospho-mimetic mutations are obtained by conversion of serine to aspartic acid (Fig. 25a). Aspartic acid is negatively charged and hence it should mimic the negative charge of a protein following its phosphorylation. However, the conformational changes induced following this PTM may not be necessarily phenocopied by replacing the phospho-residues with negatively charged amino acids. In line with this conclusion, phosphodeficient and phospho-mimetic mutants of several proteins have been reported to exhibit the same phenotypes in different cellular contexts[72].

In support of our result that phosphoregulation of RIF1 modulates its role in replication fork protection, Timeless, Pol ε and CTF18 were found in the I-DIRT with high confidence. These candidates are recruited to both stalled and unperturbed forks[104]. Timeless belongs to the fork protection complex which travels with the replisome and is one of the first responders to replication stress by activating ATR upon fork stalling[161]. Pol ε is the leading strand polymerase required for fork progression[162] and CTF18 is recruited

to stalled forks and is required for ATR activation[163,164]. Due to their critical functions, deletion of any of these effectors severely compromises genome integrity during replication.

Chirantani *et al.* also reported that RIF1 was recruited to the stalled replication fork[120]. However, how this is mediated remains an open question. It is possible that abrogation of phosphorylation at RIF1 SQ-CII cluster prevents RIF1 recruitment to the stalled fork. This would explain why even if the SQ-CII cluster is not in CTD of RIF1 that recruits PP1, it showed nascent fork degradation comparable to levels of *Rif1*$^{-/-}$. This hypothesis is supported by studies in yeast Rif1. Abrogation of phosphorylation in a cluster of 7 S/T Q sites abolished replication fork protection following HU to levels comparable to Rif1Δ[140]. Similar to mammals, Rif1-Glc7/PP1 was required for this function. The nuclease responsible is still unclear, although Dna2 is a possible candidate. The sites in yeast Rif1 are also consensus motifs for Mec1/Tel1 kinases (ATM/ATR in mammals). Intriguingly, this cluster is present in an unstructured region of the protein. Yeast Rif1 is also recruited to the stalled fork however the mechanism has not been identified yet. It is hypothesized that phosphorylation at the 7 S/TQ sites by Mec1/Tel1 mediate Rif1 recruitment to the stalled fork. This is supported by the result that a truncation mutant of Rif1 missing most of these sites was not recruited to stalled fork[165]. In conclusion, based on the studies from yeast it is highly likely abrogation of phosphorylation at mouse RIF-SQCII inhibits its recruitment to the stalled fork which is essential for nascent fork protection following replication stress. Considering that post translational modifications in IDRs mediates protein-protein interactions, it would be interesting to know if RIF1 recruitment to the fork is mediated by other effectors.

Many factors involved in the DNA damage response, like BRCA1, BRCA2, and RAD51, play an independent role in DSB repair and fork protection following replication stress during S phase. BRCA1/2 mainly function in HR by inhibiting DNA DSB end protection and promoting recruitment of RAD51 respectively[49]. Independently of this HR function, BRCA1/2 also protect stalled replication forks from degradation by MRE11[113]. Similarly, RAD51 is recruited by BRCA2 during HR repair to promote strand invasion into the sister chromatid which is required for successful HR[117]. Independently of this function, RAD51 also mediates fork reversal of stalled replication forks[116].

RIF1 originally identified in mammals as a DSB repair factor also mediates replication fork stabilization following mild replication stress. RIF1 is recruited by phosphorylated 53BP1 following DSB induction to protect the ends and this recruitment is essential to prevent resection by nucleases[46,75]. In a 53BP1-independent role, RIF1 recruits PP1 at stalled replication forks to dephosphorylate DNA2 nuclease and

prevent degradation of newly replicated DNA[120,121]. This function of RIF1 is independent of its role in DNA DSB end protection.

Stabilization of stalled forks is critical to prevent under replicated DNA and ensure fork restart so that the genome can be duplicated accurately. Hence, RIF1 maintains genome stability in S phase by mediating fork protection. When DSBs are formed due to collapsed replication forks during chronic stress, RIF1 protects the break ends from nucleolytic digestion and promotes NHEJ. It is imperative that replication-associated breaks are not repaired by NHEJ as this leads to aberrant repair reactions causing gross chromosomal rearrangement and translocations leading to genome instability. However, in BRCA1-deficient cells impaired for HR, DSBs in S-phase can only be repaired by toxic NHEJ mediated by RIF1 (Fig. 13,27). Subsequently, deletion of RIF1 rescues the viability of BRCA1-deficient cells contributing to PARPi resistance. Thus, RIF1 functions in 2 stages during replication to maintain genome stability. First, in stabilization of stalled replication forks and in the repair of collapsed replication forks.

ATM/ATR substrates often contain several closely spaced SQ/TQ motifs in regions that have been termed SQ/TQ cluster domains (SCDs). SCDs are now considered a structural hallmark of DNA -damage -response proteins. Mutational analyses of several SCD-containing proteins indicate that multisite phosphorylation of SQ/TQ motifs is required for normal DNA damage responses, most commonly by mediating protein-protein interactions in the formation of DNA damage-induced complexes[137,138]. Structural disorder of SCDs could be advantageous for efficient phosphorylation by ATM/ATR kinases and enable them to be molded into distinct conformations to facilitate flexible interactions with multiple binding partners[138]. Several DNA damage response proteins are phosphorylated in clusters. For instance, abrogation of phosphorylation in of 7 serine sites of 53BP1 completely abolishes the recruitment of mouse RIF1 and this impairs DNA end protection of DSBs[144]. Also, 53BP1 engages in protein-protein interactions that are mediated by independent phosphorylation events by recruiting PTIP through phosphorylation in one site, whereas RIF1 is recruited by phosphorylation in 7 different sites. Similarly, CHK2 phosphorylation switches BRCA1 function from HR to error prone NHEJ reactions[166,112].

Phosphorylation of RIF1 at the conserved SQ-CII cluster could function as a molecular switch such that this phosphorylation is required for stalled fork protection but dispensable for DNA DSB repair. This way RIF1 could mediate independent functions at the replication fork to maintain genome stability.

6. REFERENCES

1. Aguilera, A. & García-Muse, T. Causes of genome instability. *Annu. Rev. Genet.* **47**, 1–32 (2013).
2. Leonard, A. C. & Mechali, M. DNA replication origins. *Cold Spring Harb. Perspect. Med.* **3**, 1–18 (2013).
3. Bleichert, F. Mechanisms of replication origin licensing: a structural perspective. *Curr. Opin. Struct. Biol.* **59**, 195–204 (2019).
4. Bleichert, F. Mechanisms of replication origin licensing: a structural perspective. *Curr. Opin. Struct. Biol.* **59**, 195–204 (2019).
5. Mott, M. L. & Berger, J. M. DNA replication initiation: Mechanisms and regulation in bacteria. *Nat. Rev. Microbiol.* **5**, 343–354 (2007).
6. Shibata, E. *et al.* Two subunits of human ORC are dispensable for DNA replication and proliferation. *Elife* **5**, 5–7 (2016).
7. Moldovan, G. L., Pfander, B. & Jentsch, S. PCNA, the Maestro of the Replication Fork. *Cell* **129**, 665–679 (2007).
8. Zeman, M. K. & Cimprich, K. A. Causes and consequences of replication stress. *Nat. Cell Biol.* **16**, 2–9 (2014).
9. Dalgaard, J. Z. Causes and consequences of ribonucleotide incorporation into nuclear DNA. *Trends Genet.* **28**, 592–597 (2012).
10. Helmrich, A., Ballarino, M., Nudler, E. & Tora, L. Transcription-replication encounters, consequences and genomic instability. *Nat. Struct. Mol. Biol.* **20**, 412–418 (2013).
11. Bermejo, R., Lai, M. S. & Foiani, M. Preventing Replication Stress to Maintain Genome Stability: Resolving Conflicts between Replication and Transcription. *Mol. Cell* **45**, 710–718 (2012).
12. Anglana, M., Apiou, F., Bensimon, A. & Debatisse, M. Dynamics of DNA replication in mammalian somatic cells: Nucleotide pool modulates origin choice and interorigin spacing. *Cell* **114**, 385–394 (2003).
13. Poli, J. *et al.* dNTP pools determine fork progression and origin usage under replication stress. *EMBO J.* **31**, 883–894 (2012).
14. Beck, H. *et al.* Cyclin-Dependent Kinase Suppression by WEE1 Kinase Protects the Genome through Control of Replication Initiation and Nucleotide Consumption. *Mol. Cell. Biol.* **32**, 4226–4236 (2012).
15. Saldivar, J. C. *et al.* Initiation of Genome Instability and Preneoplastic Processes through Loss of Fhit Expression. *PLoS Genet.* **8**, (2012).
16. Shima, N. *et al.* A viable allele of Mcm4 causes chromosome instability and mammary adenocarcinomas in mice. *Nat. Genet.* **39**, 93–98 (2007).
17. Debatisse, M., Le Tallec, B., Letessier, A., Dutrillaux, B. & Brison, O. Common fragile sites: Mechanisms of instability revisited. *Trends Genet.* **28**, 22–32 (2012).

18. Besnard, E. *et al.* Unraveling cell type-specific and reprogrammable human replication origin signatures associated with G-quadruplex consensus motifs. *Nat. Struct. Mol. Biol.* **19**, 837–844 (2012).

19. Maizels, N. & Gray, L. T. The G4 Genome. *PLoS Genet.* **9**, 1–10 (2013).

20. Halazonetis, T. D., Gorgoulis, V. G. & Bartek, J. An oncogene-induced DNA damage model for cancer development. *Science (80-.).* **319**, 1352–1355 (2008).

21. Jones, R. M. *et al.* Increased replication initiation and conflicts with transcription underlie Cyclin E-induced replication stress. *Oncogene* **32**, 3744–3753 (2013).

22. Byun, T. S., Pacek, M., Yee, M. C., Walter, J. C. & Cimprich, K. A. Functional uncoupling of MCM helicase and DNA polymerase activities activates the ATR-dependent checkpoint. *Genes Dev.* **19**, 1040–1052 (2005).

23. Mourón, S. *et al.* Repriming of DNA synthesis at stalled replication forks by human PrimPol. *Nat. Struct. Mol. Biol.* **20**, 1383–1389 (2013).

24. Blair, R. HHS Public Access. *Physiol. Behav.* **176**, 139–148 (2017).

25. Iyer, D. R. & Rhind, N. The intra-S checkpoint responses to DNA damage. *Genes (Basel).* **8**, (2017).

26. Alexander, J. L. & Orr-Weaver, T. L. Replication fork instability and the consequences of fork collisions from rereplication. *Genes Dev.* **30**, 2241–2252 (2016).

27. Räschle, M. *et al.* repair. **134**, 969–980 (2009).

28. Neelsen, K. J. *et al.* Deregulated origin licensing leads to chromosomal breaks by rereplication of a gapped DNA template. *Genes Dev.* **27**, 2537–2542 (2013).

29. Scully, R., Panday, A., Elango, R. & Willis, N. A. DNA double-strand break repair-pathway choice in somatic mammalian cells. *Nat. Rev. Mol. Cell Biol.* **20**, 698–714 (2019).

30. Katsuki, Y., Jeggo, P. A., Uchihara, Y., Takata, M. & Shibata, A. DNA double-strand break end resection: a critical relay point for determining the pathway of repair and signaling. *Genome Instab. Dis.* **1**, 155–171 (2020).

31. Ciccia, A. & Elledge, S. J. The DNA Damage Response: Making It Safe to Play with Knives. *Mol. Cell* **40**, 179–204 (2010).

32. Grabarz, A., Barascu, A., Guirouilh-Barbat, J. & Lopez, B. S. Initiation of DNA double strand break repair: signaling and single-stranded resection dictate the choice between homologous recombination, non-homologous end-joining and alternative end-joining. *Am. J. Cancer Res.* **2**, 249–68 (2012).

33. Blackford, A. N. & Jackson, S. P. ATM, ATR, and DNA-PK: The Trinity at the Heart of the DNA Damage Response. *Mol. Cell* **66**, 801–817 (2017).

34. Jackson, S. P. Sensing and repairing DNA double-strand breaks. *Carcinogenesis* **23**, 687–696 (2002).

35. Haince, J. F. *et al.* PARP1-dependent kinetics of recruitment of MRE11 and NBS1 proteins to multiple DNA damage sites. *J. Biol. Chem.* **283**, 1197–1208 (2008).

36. Zhu, M., Zhao, H., Limbo, O. & Russell, P. Mre11 complex links sister chromatids to promote repair

of a collapsed replication fork. *Proc. Natl. Acad. Sci. U. S. A.* **115**, 8793–8798 (2018).

37. Lee, K. J. *et al.* Phosphorylation of Ku dictates DNA double-strand break (DSB) repair pathway choice in S phase. *Nucleic Acids Res.* **44**, 1732–1745 (2015).

38. Weterings, E. & Chen, D. J. The endless tale of non-homologous end-joining. *Cell Res.* **18**, 114–124 (2008).

39. Shrivastav, M., De Haro, L. P. & Nickoloff, J. A. Regulation of DNA double-strand break repair pathway choice. *Cell Res.* **18**, 134–147 (2008).

40. Burma, S., Chen, B. P., Murphy, M., Kurimasa, A. & Chen, D. J. ATM Phosphorylates Histone H2AX in Response to DNA Double-strand Breaks. *J. Biol. Chem.* **276**, 42462–42467 (2001).

41. Lamarche, B. J., Orazio, N. I. & Weitzman, M. D. The MRN complex in double-strand break repair and telomere maintenance. *FEBS Lett.* **584**, 3682–3695 (2010).

42. Chaudhuri, A. R. *et al.* Replication fork stability confers chemoresistance in BRCA-deficient cells. *Nature* **535**, 382–387 (2016).

43. Jasin, M. & Rothstein, R. Repair of strand breaks by homologous recombination. *Cold Spring Harb. Perspect. Biol.* **5**, (2013).

44. Zhao, F., Kim, W., Kloeber, J. A. & Lou, Z. DNA end resection and its role in DNA replication and DSB repair choice in mammalian cells. *Exp. Mol. Med.* **52**, 1705–1714 (2020).

45. Greenberg, R. A. *et al.* Multifactorial contributions to an acute DNA damage response by BRCA1/BARD1-containing complexes. *Genes Dev.* **20**, 34–46 (2006).

46. Chapman, J. R. *et al.* RIF1 Is Essential for 53BP1-Dependent Nonhomologous End Joining and Suppression of DNA Double-Strand Break Resection. *Mol. Cell* **49**, 858–871 (2013).

47. Thorslund, T. *et al.* The breast cancer tumor suppressor BRCA2 promotes the specific targeting of RAD51 to single-stranded DNA. *Nat. Struct. Mol. Biol.* **17**, 1263–1265 (2010).

48. Jensen, R. B., Carreira, A. & Kowalczykowski, S. C. Purified human BRCA2 stimulates RAD51-mediated recombination. *Nature* **467**, 678–683 (2010).

49. Prakash, R., Zhang, Y., Feng, W. & Jasin, M. Homologous Recombination and Human Health. *Perspect. Biol.* 1–29 (2015).

50. Hiom, K. Recombination: Homologous recombination branches out. *Curr. Biol.* **11**, 278–280 (2001).

51. Krejci, L., Altmannova, V., Spirek, M. & Zhao, X. Homologous recombination and its regulation. *Nucleic Acids Res.* **40**, 5795–5818 (2012).

52. Zhao, W. *et al.* BRCA1-BARD1 promotes RAD51-mediated homologous DNA pairing. *Nature* **550**, 360–365 (2017).

53. Bothmer, A. *et al.* Regulation of DNA End Joining, Resection, and Immunoglobulin Class Switch Recombination by 53BP1. *Mol. Cell* **42**, 319–329 (2011).

54. Ahnesorg, P., Smith, P. & Jackson, S. P. XLF interacts with the XRCC4-DNA Ligase IV complex to promote DNA nonhomologous end-joining. *Cell* **124**, 301–313 (2006).

55. Lieber, M. R. The mechanism of human nonhomologous DNA End joining. *J. Biol. Chem.* **283**, 1–5 (2008).

56. Gottlieb, T. M. & Jackson, P. The DNA-Dependent Protein Ki for DNA Ends and AssocWbn with Ku Antigen. *Cell* **72**, 131–142 (1993).

57. Shibata, A. *et al.* DNA Double-Strand Break Resection Occurs during Non-homologous End Joining in G1 but Is Distinct from Resection during Homologous Recombination. *Mol. Cell* **65**, 671-684.e5 (2017).

58. Chapman, J. R., Taylor, M. R. G. & Boulton, S. J. Playing the End Game: DNA Double-Strand Break Repair Pathway Choice. *Mol. Cell* **47**, 497–510 (2012).

59. Zimmermann, M. & De Lange, T. 53BP1: Pro choice in DNA repair. *Trends Cell Biol.* **24**, 108–117 (2014).

60. Chen, L., Nievera, C. J., Lee, A. Y. L. & Wu, X. Cell cycle-dependent complex formation of BRCA1·CtIP·MRN is important for DNA double-strand break repair. *J. Biol. Chem.* **283**, 7713–7720 (2008).

61. Mimitou, E. P. & Symington, L. S. Sae2, Exo1 and Sgs1 collaborate in DNA double-strand break processing. *Nature* **455**, 770–774 (2008).

62. Wang, H. *et al.* The Interaction of CtIP and Nbs1 Connects CDK and ATM to Regulate HR-Mediated Double-Strand Break Repair. *PLoS Genet.* **9**, 25–27 (2013).

63. Mimitou, E. P. & Symington, L. S. Ku prevents Exo1 and Sgs1-dependent resection of DNA ends in the absence of a functional MRX complex or Sae2. *EMBO J.* **29**, 3358–3369 (2010).

64. Venkitaraman, A. R. Cancer susceptibility and the functions of BRCA1 and BRCA2. *Cell* **108**, 171–182 (2002).

65. Escribano-Díaz, C. *et al.* A Cell Cycle-Dependent Regulatory Circuit Composed of 53BP1-RIF1 and BRCA1-CtIP Controls DNA Repair Pathway Choice. *Mol. Cell* **49**, 872–883 (2013).

66. Mirman, Z. & de Lange, T. 53BP1: a DSB escort. *Genes Dev.* **34**, 7–23 (2020).

67. Setiaputra, D. & Durocher, D. Shieldin – the protector of DNA ends . *EMBO Rep.* **20**, 1–11 (2019).

68. Mirman, Z. *et al.* 53BP1–RIF1–shieldin counteracts DSB resection through CST- and Polα-dependent fill-in. *Nature* **560**, 112–116 (2018).

69. Dev, H. *et al.* Shieldin complex promotes DNA end-joining and counters homologous recombination in BRCA1-null cells. *Nat. Cell Biol.* **20**, 954–965 (2018).

70. Lukas, J., Lukas, C. & Bartek, J. More than just a focus: The chromatin response to DNA damage and its role in genome integrity maintenance. *Nat. Cell Biol.* **13**, 1161–1169 (2011).

71. Harding, S. M. & Bristow, R. G. Discordance between phosphorylation and recruitment of 53BP1 in response to DNA double-strand breaks. *Cell Cycle* **11**, 1432–1444 (2012).

72. Callen, E. *et al.* 53BP1 mediates productive and mutagenic DNA repair through distinct phosphoprotein interactions. *Cell* **153**, 1266–1280 (2013).

73. Bunting, S. F. *et al.* 53BP1 inhibits homologous recombination in brca1-deficient cells by blocking

resection of DNA breaks. *Cell* **141**, 243–254 (2010).

74. Evers, B. & Jonkers, J. Mouse models of BRCA1 and BRCA2 deficiency: Past lessons, current understanding and future prospects. *Oncogene* **25**, 5885–5897 (2006).

75. Di Virgilio, M. *et al.* Rif1 prevents resection of DNA breaks and promotes immunoglobulin class switching. *Science (80-.).* **339**, 711–715 (2013).

76. Helleday, T. The underlying mechanism for the PARP and BRCA synthetic lethality: Clearing up the misunderstandings. *Mol. Oncol.* **5**, 387–393 (2011).

77. Benafif, S. & Hall, M. An update on PARP inhibitors for the treatment of cancer. *Onco. Targets. Ther.* **8**, 519–528 (2015).

78. Sonnenblick, A., De Azambuja, E., Azim, H. A. & Piccart, M. An update on PARP inhibitors - Moving to the adjuvant setting. *Nat. Rev. Clin. Oncol.* **12**, 27–41 (2015).

79. Fojo, T. & Bates, S. Mechanisms of resistance to PARP inhibitors-three and counting. *Cancer Discov.* **3**, 20–23 (2013).

80. Gogola, E., Rottenberg, S. & Jonkers, J. Resistance to PARP Inhibitors: Lessons from preclinical models of BRCA-Associated Cancer. *Annu. Rev. Cancer Biol.* **3**, 235–254 (2019).

81. Lord, C. J. & Ashworth, A. Mechanisms of resistance to therapies targeting BRCA-mutant cancers. *Nat. Med.* **19**, 1381–1388 (2013).

82. Stavnezer, J., Guikema, J. E. J. & Schrader, C. E. Mechanism and regulation of class switch recombination. *Annu. Rev. Immunol.* **26**, 261–292 (2008).

83. Chaudhuri, J. & Alt, F. W. Class-switch recombination: Interplay of transcription, DNA deamination and DNA repair. *Nat. Rev. Immunol.* **4**, 541–552 (2004).

84. Barnes, D. E. & Lindahl, T. Repair and genetic consequences of endogenous DNA base damage in mammalian cells. *Annu. Rev. Genet.* **38**, 445–476 (2004).

85. Sun, J., Lee, K. J., Davis, A. J. & Chen, D. J. Human Ku70/80 protein blocks exonuclease 1-mediated DNA resection in the presence of human Mre11 or Mre11/Rad50 protein complex. *J. Biol. Chem.* **287**, 4936–4945 (2012).

86. Yang, Y. H. J. *et al.* ZRANB2 localizes to supraspliceosomes and influences the alternative splicing of multiple genes in the transcriptome. *Mol. Biol. Rep.* **40**, 5381–5395 (2013).

87. Aparicio, T., Baer, R. & Gautier, J. DNA double-strand break repair pathway choice and cancer. *DNA Repair (Amst).* **19**, 169–175 (2014).

88. Ward, I. M. *et al.* 53BP1 is required for class switch recombination. *J. Cell Biol.* **165**, 459–464 (2004).

89. Cell-cycle regulation of brca1 inhibits homologous recombination in g1. *Cancer Discov.* **6**, 119 (2016).

90. Saha, J. & Davis, A. J. Unsolved mystery: The role of BRCA1 in DNA end-joining. *J. Radiat. Res.* **57**, i18–i24 (2016).

91. Rickman, K. & Smogorzewska, A. Advances in understanding DNA processing and protection at stalled replication forks. *J. Cell Biol.* **218**, 1096–1107 (2019).

92. Maréchal, A. & Zou, L. DNA damage sensing by the ATM and ATR kinases. *Cold Spring Harb. Perspect. Biol.* **5**, 1–17 (2013).

93. Syljuåsen, R. G. *et al.* Inhibition of Human Chk1 Causes Increased Initiation of DNA Replication, Phosphorylation of ATR Targets, and DNA Breakage. *Mol. Cell. Biol.* **25**, 3553–3562 (2005).

94. Toledo, L. I. *et al.* XATR prohibits replication catastrophe by preventing global exhaustion of RPA. *Cell* **155**, 1088 (2013).

95. Vassin, V. M., Anantha, R. W., Sokolova, E., Kanner, S. & Borowiec, J. A. Human RPA phosphorylation by ATR stimulates DNA synthesis and prevents ssDNA accumulation during DNA-replication stress. *J. Cell Sci.* **122**, 4070–4080 (2009).

96. Mason, J. M., Chan, Y. L., Weichselbaum, R. W. & Bishop, D. K. Non-enzymatic roles of human RAD51 at stalled replication forks. *Nat. Commun.* **10**, (2019).

97. Sidorova, J. A game of substrates: replication fork remodeling and its roles in genome stability and chemo-resistance. *Cell Stress* **1**, 115–133 (2017).

98. Sogo, J. M., Lopes, M. & Foiani, M. Fork reversal and ssDNA accumulation at stalled replication forks owing to checkpoint defects. *Science (80-.).* **297**, 599–602 (2002).

99. Manosas, M., Perumal, S. K., Croquette, V. & Benkovic, S. J. Direct observation of stalled fork restart via fork regression in the T4 replication system. *Science (80-.).* **338**, 1217–1220 (2012).

100. Atkinson, J. & McGlynn, P. Replication fork reversal and the maintenance of genome stability. *Nucleic Acids Res.* **37**, 3475–3492 (2009).

101. Lemaçon, D. *et al.* MRE11 and EXO1 nucleases degrade reversed forks and elicit MUS81-dependent fork rescue in BRCA2-deficient cells. *Nat. Commun.* **8**, (2017).

102. Rooks, M.G and Garrett, W.S, 2016. 乳鼠心肌提取 HHS Public Access. *Physiol. Behav.* **176**, 139–148 (2017).

103. Vujanovic, M. *et al.* Replication Fork Slowing and Reversal upon DNA Damage Require PCNA Polyubiquitination and ZRANB3 DNA Translocase Activity. *Mol. Cell* **67**, 882-890.e5 (2017).

104. Sirbu, B. M. *et al.* Analysis of protein dynamics at active, stalled, and collapsed replication forks. *Genes Dev.* **25**, 1320–1327 (2011).

105. Bhat, K. P. *et al.* RADX Modulates RAD51 Activity to Control Replication Fork Protection. *Cell Rep.* **24**, 538–545 (2018).

106. Bugreev, D. V., Rossi, M. J. & Mazin, A. V. Cooperation of RAD51 and RAD54 in regression of a model replication fork. *Nucleic Acids Res.* **39**, 2153–2164 (2011).

107. McGrail, D. J. *et al.* Defective Replication Stress Response Is Inherently Linked to the Cancer Stem Cell Phenotype. *Cell Rep.* **23**, 2095–2106 (2018).

108. Hanada, K. *et al.* The structure-specific endonuclease Mus81 contributes to replication restart by generating double-strand DNA breaks. *Nat. Struct. Mol. Biol.* **14**, 1096–1104 (2007).

109. Taglialatela, A. *et al.* HHS Public Access. **68**, 414–430 (2018).

110. Thangavel, S. *et al.* DNA2 drives processing and restart of reversed replication forks in human cells.

J. Cell Biol. **208**, 545–562 (2015).

111. Pathania, S. *et al.* BRCA1 haploinsufficiency for replication stress suppression in primary cells. *Nat. Commun.* **5**, (2014).

112. Min, W. *et al.* Poly(ADP-ribose) binding to Chk1 at stalled replication forks is required for S-phase checkpoint activation. *Nat. Commun.* **4**, (2013).

113. Schlacher, K. *et al.* Double-strand break repair-independent role for BRCA2 in blocking stalled replication fork degradation by MRE11. *Cell* **145**, 529–542 (2011).

114. Feng, W. & Jasin, M. Homologous Recombination and Replication Fork Protection: BRCA2 and More! *Cold Spring Harb. Symp. Quant. Biol.* **82**, 329–338 (2017).

115. Barlow, J. H. *et al.* Identification of early replicating fragile sites that contribute to genome instability. *Cell* **152**, 620–632 (2013).

116. Feng, Z. & Zhang, J. A dual role of BRCA1 in two distinct homologous recombination mediated repair in response to replication arrest. *Nucleic Acids Res.* **40**, 726–738 (2012).

117. Bhat, K. P. & Cortez, D. RPA and RAD51: Fork reversal, fork protection, and genome stability. *Nat. Struct. Mol. Biol.* **25**, 446–453 (2018).

118. Okamoto, Y. *et al.* Replication stress induces accumulation of FANCD2 at central region of large fragile genes. *Nucleic Acids Res.* **46**, 2932–2944 (2018).

119. D Isaacson, J L Mueller, J. C. N. and S. S. 基因的改变NIH Public Access. *Bone* **23**, 1–7 (2006).

120. Mukherjee, C. *et al.* Ef Fi Cient Restart To Maintain Genome Stability. *Nat. Commun.* 1–16 doi:10.1038/s41467-019-11246-1.

121. Garzón, J., Ursich, S., Lopes, M., Hiraga, S. ichiro & Donaldson, A. D. Human RIF1-Protein Phosphatase 1 Prevents Degradation and Breakage of Nascent DNA on Replication Stalling. *Cell Rep.* **27**, 2558-2566.e4 (2019).

122. Eckelmann, B. J. *et al.* XRCC1 promotes replication restart, nascent fork degradation and mutagenic DNA repair in BRCA2-deficient cells. *NAR Cancer* **2**, 1–15 (2020).

123. Bennett, L. G. *et al.* MRNIP is a replication fork protection factor. *Sci. Adv.* **6**, (2020).

124. Lyu, X. *et al.* Human CST complex protects stalled replication forks by directly blocking MRE11 degradation of nascent-strand DNA. *EMBO J.* **40**, 1–20 (2021).

125. Calzada, A., Hodgson, B., Kanemaki, M., Bueno, A. & Labib, K. Molecular anatomy and regulation of a stable replisome at a paused eukaryotic DNA replication fork. *Genes Dev.* **19**, 1905–1919 (2005).

126. Ge, X. Q., Jackson, D. A. & Blow, J. J. Dormant origins licensed by excess Mcm2-7 are required for human cells to survive replicative stress. *Genes Dev.* **21**, 3331–3341 (2007).

127. Petermann, E. & Helleday, T. Pathways of mammalian replication fork restart. *Nat. Rev. Mol. Cell Biol.* **11**, 683–687 (2010).

128. Petermann, E., Orta, M. L., Issaeva, N., Schultz, N. & Helleday, T. Hydroxyurea-Stalled Replication Forks Become Progressively Inactivated and Require Two Different RAD51-Mediated Pathways for

Restart and Repair. *Mol. Cell* **37**, 492–502 (2010).

129. Llorente, B., Smith, C. E. & Symington, L. S. Break-induced replication: What is it and what is it for? *Cell Cycle* **7**, 859–864 (2008).

130. Elango, R. *et al.* Break-induced replication promotes formation of lethal joint molecules dissolved by Srs2. *Nat. Commun.* **8**, (2017).

131. Silverman, J., Takai, H., Buonomo, S. B. C., Eisenhaber, F. & De Lange, T. Human Rif1, ortholog of a yeast telomeric protein, is regulated by ATM and 53BP1 and functions in the S-phase checkpoint. *Genes Dev.* **18**, 2108–2119 (2004).

132. Saito, Y., Kobayashi, J., Kanemaki, M. T. & Komatsu, K. RIF1 controls replication initiation and homologous recombination repair in a radiation dose-dependent manner. *J. Cell Sci.* **133**, (2020).

133. Yamazaki, S. *et al.* Rif1 regulates the replication timing domains on the human genome. *EMBO J.* **31**, 3667–3677 (2012).

134. Daley, J. M. & Sung, P. RIF1 in DNA Break Repair Pathway Choice. *Mol. Cell* **49**, 840–841 (2013).

135. Hayano, M. *et al.* Rif1 is a global regulator of timing of replication origin firing in fission yeast. *Genes Dev.* **26**, 137–150 (2012).

136. Feng, L., Fong, K. W., Wang, J., Wang, W. & Chen, J. RIF1 counteracts BRCA1-mediated end resection during DNA repair. *J. Biol. Chem.* **288**, 11135–11143 (2013).

137. Wright, P. E. & Dyson, H. J. Intrinsically disordered proteins in cellular signalling and regulation. *Nat. Rev. Mol. Cell Biol.* **16**, 18–29 (2015).

138. Iakoucheva, L. M. *et al.* The importance of intrinsic disorder for protein phosphorylation. *Nucleic Acids Res.* **32**, 1037–1049 (2004).

139. Matsuoka, S. *et al.* ATM and ATR substrate analysis reveals extensive protein networks responsive to DNA damage. *Science (80-.).* **316**, 1160–1166 (2007).

140. 徐家壮 1， 梁瑗瑛 1， 李忠明 1,* 1. *37th Eur. Photovolt. Sol. Energy Conf.* 610065 (2020).

141. Wang, J. *et al.* Rif1 phosphorylation site analysis in telomere length regulation and the response to damaged telomeres. *DNA Repair (Amst).* **65**, 26–33 (2018).

142. Noordermeer, S. M. & van Attikum, H. PARP Inhibitor Resistance: A Tug-of-War in BRCA-Mutated Cells. *Trends Cell Biol.* **29**, 820–834 (2019).

143. Bakr, A. *et al.* Impaired 53BP1/RIF1 DSB mediated end-protection stimulates CtIP-dependent end resection and switches the repair to PARP1- dependent end joining in G1. *Oncotarget* **7**, 57679–57693 (2016).

144. Delgado-Benito, V. *et al.* The Chromatin Reader ZMYND8 Regulates Igh Enhancers to Promote Immunoglobulin Class Switch Recombination. *Mol. Cell* **72**, 636-649.e8 (2018).

145. Boersma, V. *et al.* MAD2L2 controls DNA repair at telomeres and DNA breaks by inhibiting 5′ end resection. *Nature* **521**, 537–540 (2015).

146. Xu, G. *et al.* REV7 counteracts DNA double-strand break resection and affects PARP inhibition. *Nature* **521**, 541–544 (2015).

147. Paulsen, R. D. *et al.* A Genome-wide siRNA Screen Reveals Diverse Cellular Processes and Pathways that Mediate Genome Stability. *Mol. Cell* **35**, 228–239 (2009).

148. Nieminuszczy, J., Schwab, R. A. & Niedzwiedz, W. The DNA fibre technique – tracking helicases at work. *Methods* **108**, 92–98 (2016).

149. Nakamura, M. *et al.* High frequency class switching of an IgM+ B lymphoma clone CH12F3 to IgA+ cells. *Int. Immunol.* **8**, 193–201 (1996).

150. Li, Z., Woo, C. J., Iglesias-Ussel, M. D., Ronai, D. & Scharff, M. D. The generation of antibody diversity through somatic hypermutation and class switch recombination. *Genes Dev.* **18**, 1–11 (2004).

151. Sundaravinayagam, D. *et al.* 53BP1 Supports Immunoglobulin Class Switch Recombination Independently of Its DNA Double-Strand Break End Protection Function. *Cell Rep.* **28**, 1389-1399.e6 (2019).

152. Loughlin, F. E. *et al.* The zinc fingers of the SR-like protein ZRANB2 are single-stranded RNA-binding domains that recognize 5' splice site-like sequences. *Proc. Natl. Acad. Sci. U. S. A.* **106**, 5581–5586 (2009).

153. Tanaka, I. *et al.* ZRANB2 and SYF2-mediated splicing programs converging on ECT2 are involved in breast cancer cell resistance to doxorubicin. *Nucleic Acids Res.* **48**, 2676–2693 (2020).

154. Pederiva, C., Böhm, S., Julner, A. & Farnebo, M. Splicing controls the ubiquitin response during DNA double-strand break repair. *Cell Death Differ.* **23**, 1648–1657 (2016).

155. Chu, V. T. *et al.* Efficient CRISPR-mediated mutagenesis in primary immune cells using CrispRGold and a C57BL/6 Cas9 transgenic mouse line. *Proc. Natl. Acad. Sci. U. S. A.* **113**, 12514–12519 (2016).

156. Hsu, P. D. *et al.* DNA targeting specificity of RNA-guided Cas9 nucleases. *Nat. Biotechnol.* **31**, 827–832 (2013).

157. Afzali, B. *et al.* BACH2 immunodeficiency illustrates an association between super-enhancers and haploinsufficiency. *Nat. Immunol.* **18**, 813–823 (2017).

158. Howard, W. A., Bible, J. M., Finlay-Dijsselbloem, E., Openshaw, S. & Dunn-Walters, D. K. Immunoglobulin light-chain genes in the rhesus macaque II: Lambda light-chain germline sequences for subgroups IGLV1, IGLV2, IGLV3, IGLV4 and IGLV5. *Immunogenetics* **57**, 655–664 (2005).

159. Ludwig, T., Fisher, P., Ganesan, S. & Efstratiadis, A. Tumorigenesis in mice carrying a truncating Brca1 mutation. *Genes Dev.* **15**, 1188–1193 (2001).

160. Setiaputra, D. *et al.* RIF1 acts in DNA repair through phosphopeptide recognition of 53BP1. *bioRxiv* 2021.04.26.441429 (2021).

161. Leman, A. R., Noguchi, C., Lee, C. Y. & Noguchi, E. Human Timeless and Tipin stabilize replication forks and facilitate sister-chromatid cohesion. *J. Cell Sci.* **123**, 660–670 (2010).

162. Takeda, D. Y. & Dutta, A. DNA replication and progression through S phase. *Oncogene* **24**, 2827–2843 (2005).

163. Srivastava, M. *et al.* Replisome Dynamics and Their Functional Relevance upon DNA Damage through the PCNA Interactome. *Cell Rep.* **25**, 3869-3883.e4 (2018).

164. Kaneko, Y., Daitoku, H., Komeno, C. & Fukamizu, A. CTF18 interacts with replication protein A in response to replication stress. *Mol. Med. Rep.* **14**, 367–372 (2016).

165. Hiraga, S. I. *et al.* Rif1 controls DNA replication by directing Protein Phosphatase 1 to reverse Cdc7-mediated phosphorylation of the MCM complex. *Genes Dev.* **28**, 372–383 (2014).

166. Zhuang, J. *et al.* Checkpoint kinase 2-mediated phosphorylation of BRCA1 regulates the fidelity of nonhomologous end-joining. *Cancer Res.* **66**, 1401–1408 (2006).

167. Figure 1-5 were created with BioRender.com

7. Appendix

7.1 Selbstständigkeitserklärung

Hiermit erkläre ich, dass ich die vorliegende Arbeit mit dem Titel " Dissecting the molecular mechanisms of RIF1 in maintaining DNA replication-associated genome stability" selbstständig und ohne Hilfe Dritter angefertigt habe (sofern nicht anders angegeben). Sämtliche Hilfsmittel, Hilfen sowie Literaturquellen sind als solche kenntlich gemacht. Außerdem erkläre ich hiermit, dass ich mich nicht anderweitig um einen entsprechenden Doktorgrad beworben habe. Die Promotionsordnung des Fachbereichs Biologie, Chemie und Pharmazie der Freien Universität Berlin habe ich gelesen und akzeptiert.

7.2 Abbreviations

ATM	ataxia telangiectasia mutated
BARD1	BRCA1-associated ring domain protein 1
BLM	Bloom syndrome RECQ like helicase
Bp	base pair
BRCA1/BRCA2	breast cancer type 1/2 susceptibility protein
BSA	bovine serum albumin
Cas9D10A	nickase Cas9
Cas9D10A	Cas9 nickase mutant
CDK	cyclin-dependent kinase
CH	immunoglobulin heavy chain constant region
CHK	checkpoint kinase 1
CRISPR	clustered regularly interspaced short palindromic repeats
CSR	class-switch recombination
CTC1	conserved telomere maintenance component 1
CtIP	CTBP-interacting protein
Ctrl	control
DDK	DBF4-dependent kinase
DDR	DNA damage response
dHJ	double Holliday junction
DMSO	dimethyl sulfoxide
DNA	deoxyribonucleic acid
DNA2	DNA replication helicase/nuclease 2
DNA-PKcs	DNA-dependent protein kinase catalytic subunit
DSB	double-strand break
dsDNA	double-stranded DNA
EDTA	ethylenediaminetetraacetic acid
EXO1	exonuclease 1
FH	FLAG-2xHA
gDNA	genomic DNA
GFP	green fluorescent protein
gRNA	guide RNA
H/H+L	SILAC ratio

H2A.X	H2A histone family member X
HEAT	Huntingtin, elongation factor 3, protein phosphatase 2A, TOR1)-like repeats domain
HEPES	4-(2-hydroxylethyl)-1-piperazineethanesulfonic acid
HR	homologous recombination
HRP	horseradish peroxidase
HTS	high-throughput samples
I-DIRT	isotopic differentiation of interactions as random or targeted
IDR	intrinsically disordered region
IgH	immunoglobulin heavy chain
IRIF	ionizing radiation-induced foci
KI	knock-in
KO	knock-out
LIG4	DNA ligase 4
MDC1	mediator of DNA damage checkpoint 1
MEF	mouse embryonic fibroblast
min	minute(s)
MRE11	meiotic recombination 11 homolog 1
MS/MS	tandem mass spectrometry
NBS1	Nijmegen breakage syndrome 1
NHEJ	non-homologous end joining
PAPRi	PARP inhibitor
PAR	poly-ADP ribose
PARP1	poly(ADP-ribose) polymerase-1
PBS	phosphate-buffered saline
PCR	polymerase-chain reaction
PEP	posterior error probability
PP1	protein phosphatase 1
PTIP	PAX transcription activation domain interacting protein
PTM	post-translational modification
RIF1	Rap1-interacting factor 1
RNF8/RNF138/ RNF168	ring finger protein 4/8/11/20/40/138/168
	reactive oxygen species
RPA	replication protein A
RT	room temperature
S → A	serine to alanine mutation
S → D	serine to aspartate
SD	standard deviation
SDS	sodium dodecyl sulfate
sec	second(s)
SEM	standard error of the mean

SSB	single-strand break
SHLD1/2/3	Shieldin 1/2/3
ssDNA	single-stranded DNA
STN1	suppressor of CDC thirteen homolog
TEN1	telomere length regulation protein TEN1 homolog
TGFβ	transforming growth factor β
UDR	ubiquitylation-dependent recruitment
UFB	anaphase ultrafine bridge
V(D)J	variable, diversity and joining genes
WB	western blot
WT	wild-type
XLF	XRCC4-like factor
XRCC4	x-ray repair cross complementing 4
ZMYND8	zinc finger MYND-type containing 8
γH2AX	phosphorylated histone H2AX

7.3 List of publications

53BP1 supports Immunoglobulin Class Switch Recombination independently of its DNA Double Strand Break End Protection function.

Sundaravinayagam D., Rahjouei A., Andreani M., Tupina D., **Balasubramanian S.**, Saha T., Delgado-Benito V., Coralluzzo V., Daumke O., and Di Virgilio M. Cell Rep., 28, pp. 1389-1399 (2019). Paper was previewed by J. Chaudhuri (MSKCC, NY)

PDGFA-associated protein 1 protects mature B lymphocytes from stress-induced cell death and promotes antibody gene diversification

Delgado-Benito V., Berruezo-Llacuna M., Altwasser R, Winkler W., Sundaravinayagam D., **Balasubramanian S.**, Caganova M., Graf R., Rahjouei M., Henke M., Driesner M., Keller L., Prigione A., Janz M., Akalin A., Di Virgilio M. . J. Exp. Med. 217, (2020).

7.4 Acknowledgements

The PhD has been the single most challenging task I could have ever dared to ask for. As I started this journey, I was simply not prepared for all the joy, excitement, sorrow, anxieties, pressure, fun, anticipation, and the endless adrenaline that came along. I remember starting as a young, idealistic and innocent student and 5 years later this PhD has made me tough, resistant, and ever ready for all the challenges: not just I my career but in every aspect of life. Its never just a PhD! What a ride it has been! And I owe this to all the people I was surrounded with who have inspired me endlessly and have pushed me to go far beyond what I ever thought I was capable of.

First and foremost, I would like to thank Michela for accepting me as her student and always believing in me even during the times that I was unable to. I would also like to thank you for providing such a challenging, collaborative and nurturing environment in the lab. I have come to love this so much that I am afraid to not have the same in my next job! And most importantly, your never-ever-give up persona is truly inspiring and has always pushed me to give my best.

I would like to thank Prof. Dr. Oliver Daumke for kindly agreeing to be my reviewer. I would also like to thank Prof. Dr. Blankenstein for his support.

I would like to thank my committee members: Dr. Claus Scheidereit, Dr. Ralf Kuhn, and Dr. Jana Wolf for their valuable comments and insights.

Thank you to the PhD office: Michaela and Annette for your constant support and encouragement. I would also like to thank the PhD office from FU namely Mrs. Reinsberg for her support.

Sylvia and Andrea from the Welcome office: Thank you for your constant support and for making me feel welcome right from the time I came to MDC.

I would like to thank all the members of the lab for their contributions: Ali, Dev, Lisa, Maria, Tanu, Julia, Jenisha, Robert. Every person has been really helpful and accommodating and I really enjoyed interacting with all of you!

MA and VD: without you two this journey would have been impossible! Thank you for the discussions, your bullying, your company and for sticking with me through thick and thin. I love you both!

Thank you Tanu and Sophiya for adopting me into your household! I loved every movie/sleepover/morning breakfast sessions we have had! And you both have made me almost forget

my filter coffee and look for chai instead! Thank you also to Rishabh, Sumeet, Kumar and Shikha who have made life in Berlin even more memorable.

Thank you to the lovely 2.0 group! I never thought I would get to know and love so many people from different backgrounds and find something common with all of you! You have all made my experience here so exciting and it is going to be tough to get something similar again!

Thank you Leon and Basti for your support and for making me feel home always!

Thank you to Sowmya, Poorni, Durgu, Snegu, Vivek and Saishini for the endless conversations, your support, your empathy and your love. Distance and time will never make us grow apart! I love you all!

Thank you Amma and Appa for your constant encouragement, your unshakable belief in me and your unconditional love. I would have never been able to finish what I started if it had not been for you both. I love you both so much! Thanks da Cheeku for always entertaining me and being my technical support system during my innumerable clueless times!

Last but not the least, thank you Vishnu. I have no words to express how grateful I am that we met and I am truly sorry it has to end this way. Thank you da for your love, your kindness, and your generosity and I wish you only the best for the years to come. Thank you for everything Balos..